

TRANSCRIPTIONAL REGULATION OF *DROSOPHILA*
NEURAL DEVELOPMENT

Stephanie Beth Stagg

A dissertation submitted to the faculty of the University of North Carolina at Chapel Hill
in partial fulfillment of the requirements for the degree of Doctor of Philosophy in the
Curriculum of Neurobiology.

Chapel Hill
2010

Approved by:

Stephen T. Crews, Ph.D.

Manzoor A. Bhat, Ph.D.

Frank L. Conlon, Ph.D.

Robert J. Duronio, Ph.D.

Larysa H. Pevny, Ph.D.

ABSTRACT

STEPHANIE STAGG: Transcriptional Regulation of *Drosophila* Neural Development

(Under the Direction of Dr. Stephen T. Crews)

The CNS consists of a diverse array of motorneurons, interneurons, and glia. We are interested in how transcription factors and signaling pathways interact in regulatory circuits to control cell fate and differentiation during development. The *Drosophila* CNS midline cells consist of 22 cells per segment including glia, interneurons, motorneurons, and neurosecretory cells. We identified and analyzed the expression of 286 genes expressed in midline cells, and are now utilizing this information to understand how midline neurons acquire their distinct identities. Despite the small number of embryonic midline cells, the origins of midline neurons and glia remained relatively unknown. We used a combination of single-cell gene expression mapping and time-lapse imaging to identify individual midline precursor (MP) cells, their locations, movements, and stereotyped patterns of division. This information was then utilized to reveal multiple roles of *lethal of scute* [*l(1)sc*] in midline neuronal cell development.

Midline precursors (MPs) divide once to generate 2 neurons, and MP3 divides asymmetrically to yield two different neurons, H-cell and H-cell sib. *Notch* signaling directs the fates of the glutamatergic H-cell sib. We demonstrated that *l(1)sc* plays an essential role in the development of the dopaminergic H-cell. *l(1)sc* is expressed in MP3, and both daughter neurons (H-cell and H-cell sib) after birth. However, L(1)sc protein

soon becomes asymmetrically localized in H-cell. Mutant and misexpression studies indicated that *l(1)sc* is required for expression of genes involved in dopamine biosynthesis and transport, and neurotransmitter receptor genes. There are 4 additional transcription factors (BarH1, Scute, SoxNeuro, and Tailup) that are expressed in H-cell, and genetic experiments indicated that these control subsets of H-cell-expressed genes. Thus, *l(1)sc* is required for most H-cell-specific gene expression, and additional transcription factors function combinatorially to carry-out this regulatory program. Using a combination of genetics and genomics we have defined a series of molecular events that describe neuronal differentiation from precursor division to acquisition of differentiated properties.

ACKNOWLEDGEMENTS

I am grateful for the privilege to have been able to pursue my graduate career in the Crews Lab. I would like to thank Steve for all of his guidance, support and knowledge. I have been fortunate enough to work with highly talented post docs in the lab. Thank you to the original midline crew: Scott Wheeler, Joe Kearney, and Amaris Guardiola. Under Steve's leadership, you raised me and taught me how to do science. Thanks to Scott for his advice and skill that he shared with me every day across the bench. Thank you to all Crews Lab members for making this work possible. The completion of this dissertation would not have been possible without the expertise and direction from my committee members: Dr. Bhat, Dr. Conlon, Dr. Duronio and Dr. Pevny. Thanks to all my friends and family for their moral support. Thanks to Kristen for being a wonderful sister and friend. Finally, I would like to thank my parents for their endless and boundless love, support, and encouragement.

Table of Contents

LIST OF TABLES	x
LIST OF FIGURES	xi
LIST OF ABBREVIATIONS.....	xiii
CHAPTER ONE: GENERAL INTRODUCTION.....	1
Neurogenesis: generating diversity in the CNS	2
<i>Drosophila</i> proneural genes	3
<i>AS-C</i> genes: roles in neuroblast formation and precursor specification	4
Asymmetric cell division: generation of two cell fates	5
Dopamine regulation in <i>Drosophila</i>	5
Overview of CNS midline development	6
Gene expression changes during midline development	8
<i>AS-C</i> genes at the midline	9
References	12

CHAPTER TWO: MULTIPLE <i>NOTCH</i> SIGNALING EVENTS CONTROL <i>DROSOPHILA</i> CNS MIDLINE NEUROGENESIS, GLIOGENESIS, AND NEURONAL IDENTITY	15
Summary	16
Introduction	17
Materials and methods	18
<i>Drosophila</i> strains and genetics	18
In situ hybridization and immunostaining	19
Microscopy and image analysis	19
Live imaging of midline cells	20
Results	20
Identification of MPs and their pattern of division	20
<i>Notch</i> signaling promotes midline glia, MNB, and MP5,6 formation and inhibits MP1,3,4 formation	23
<i>Notch</i> activation converts MPs to midline glia	27
<i>numb</i> and <i>spdo</i> direct sibling neuronal fates in MP asymmetric divisions	29
Numb and Spdo are localized asymmetrically during MP3-6 divisions	34
Discussion	36
Patterns of stages 10-11 midline cell divisions and gene expression.....	36

<i>Notch</i> signaling directs the formation of midline glia and inhibits neurogenesis	36
<i>Notch</i> signaling promotes MNB and MP5,6 formation	39
<i>Notch</i> signaling and <i>numb</i> generate asymmetric midline neuronal cell fates.....	40
Towards a molecular basis for neuronal and glial cell fate determination.....	41
Acknowledgements.....	42
Supplemental Figures.....	43
Supplemental Movie Legends	52
References	53
CHAPTER THREE: THE <i>DROSOPHILA</i> H-CELL DOPAMINERGIC NEURON: GENETIC REGULATION OF CELL-TYPE SPECIFIC GENE EXPRESSION.....	58
Summary	59
Introduction	60
Materials and Methods.....	63
<i>Drosophila</i> Strains	63
L(1)sc and Sc Antisera	64
In Situ Hybridization and Immunostaining	64
Microscopy and Image Analysis.....	65
Results	65

Expression of H-Cell Neural Function and Regulatory Genes	65
<i>AS-C</i> Genes are Expressed in Midline Precursors and their Neuronal Progeny	67
<i>L(1)Sc</i> Misexpression Activates H-Cell Gene Expression	71
<i>L(1)Sc</i> is Required for H-Cell Gene Expression	73
<i>l(1)Sc</i> is Required for Formation of a Subset of Midline Neuronal Precursors	78
<i>Tup</i> And <i>SoxN</i> Regulate Different Components of H-Cell Gene Expression	81
Discussion	84
<i>L(1)sc</i> and <i>Tup</i> are Preferentially Localized to H-cell and Control Neural Differentiation	84
Negative Regulation of <i>L(1)Sc</i> and <i>Tup</i> in H-cell sib and H-cell	86
<i>L(1)sc</i> Selectively Controls Midline Precursor Formation	87
Defining H-Cell Gene Expression	89
Evolutionary Aspects of <i>Drosophila</i> Dopaminergic Neuron Regulation	90
Acknowledgements	92
Supplemental Figures	93
References	95
CHAPTER FOUR: MidExDB: A DATABASE OF <i>DROSOPHILA</i> CNS MIDLINE CELL GENE EXPRESSION	99
Abstract	100

Background	101
Construction and content	104
Utility and discussion.....	112
Conclusions	116
Availability and requirements	116
Acknowledgements.....	117
References	118
CHAPTER FIVE: GENERAL DISCUSSION.....	119
Model of early midline development: identification of MPs and their divisions	119
<i>AS-C</i> genes are expressed in midline precursors and their neuronal progeny	122
<i>l(1)sc</i> regulates gene expression in the Notch-independent cell.....	123
<i>l(1)sc</i> controls MNB formation and posterior MP formation	127
Evolutionary Aspects of <i>Drosophila</i> Dopaminergic Cell Fate Specification.....	129
Conclusion.....	130
References	132

LIST OF TABLES

Table S2.1 Midline genes	51
Table 3.1 Quantitative summary of H-cell genetic data	76
Table 4.1 Midline-expressed genes newly added to MidExDB.	106

LIST OF FIGURES

Figure 1.1. Model of midline cell development.....	7
Figure 2.1. Formation of MPs and MP neurons.....	22
Figure 2.2. Time-lapse imaging of sequential MP division.....	22
Figure 2.3. Notch signaling influences midline cell fate.....	24
Figure 2.4. MP number increases in the absence of Notch signaling	25
Figure 2.5. numb and spdo control MP3 neuronal cell fate.....	30
Figure 2.6. numb and spdo control VUM neuronal cell fate	32
Figure 2.7. Numb and Spdo localization during MP divisions.....	35
Figure 2.8. Model of Notch regulation of midline cell fate.....	37
Figure S2.1. Midline precursor divisions occur during stage 11	43
Figure S2.2. Notch signaling is active in midline glia, MPs, and neurons.....	45
Figure S2.3. sim-Gal4/UAS-Su(H).VP16 females have reduced fertility.....	47
Figure S2.4. numb and spdo regulate axonal trajectory	49
Figure S2.5. numb and spdo are not required for MP1 neuronal fate	50
Figure 3.1. H-Cell gene expression.....	66
Figure 3.2. Tup and AS-C Genes are expressed in precursors and neurons.....	68
Figure 3.3. l(1)Sc activates H-Cell gene expression	72
Figure 3.4. Mutants of l(1)sc affect H-Cell gene expression.....	75
Figure 3.5. l(1)sc controls VUM neuron and MNB formation.....	79
Figure 3.6. SoxN and Tup control aspects of H-Cell gene expression	83
Figure S3.1. ac, sc, and ase do not affect H-cell gene expression	93
Figure S3.2. l(1)sc affects mVUM, but not iVUM, gene expression.....	94

Figure 4.1. CNS midline gene expression	103
Figure 4.2. MidExDB search modes	105
Figure 4.3. Gene expression during midline cell development	108
Figure 4.4. Movies of confocal data.....	110
Figure 4.5. Descriptions of midline cell types and development.....	115

LIST OF ABBREVIATIONS

CNS	central nervous system
VNC	ventral nerve cord
MNB	median neuroblast
vnd	ventral nervous system defective
ind	intermediate neuroblasts defective
msh	muscle specific homeobox
NB	neuroblast
GMC	ganglion mother cell
ac	achaete
sc	scute
l(1)sc	lethal of scute
ase	asense
AS-C	achaete-scute complex
PNS	peripheral nervous system
tup	tailup

TH	tyrosine hydroxylase
ple	pale
AMG	anterior midline glia
PMG	posterior midline glia
MG	midline glia
MP	midline precursor
iVUM	interneuronal ventral unpaired medial neuron
mVUM	motorneuronal ventral unpaired medial neuron
en	engrailed
spdo	sanpodo
Su(H)	Suppressor of Hairless
GFP	green fluorescent protein
DI	Delta
N	Notch
mira	Miranda
odd	odd-skipped
wor	worniu

SoxN	SoxNeuro
Ddc	dopa decarboxylase
Vmat	vesicular monoamine transporter
DAT	dopamine membrane transporter
5-HT1A	serotonin receptor
NPFR1	neuropeptide F receptor
DA	dopamine
sim	single-minded
nub	nubbin
pmd2	POU domain protein 2
Tbh	Tyramine β hydroxylase
cas	castor
E(spl)	Enhancer of split
Ngn2	Neurogenin 2
Mash1	Mouse achaete-scute homolog
BrdU	Bromodeoxyuridine
AP	alkaline phosphatase

hh hedgehog

wg wingless

CHAPTER I

GENERAL INTRODUCTION

One of the fundamental questions in developmental biology is how different cell types are generated. The generation of diversity is particularly important in the central nervous system (CNS). Within this tissue, a small number of precursor cells give rise to different cell classes such as motoneurons, interneurons, and glia and within each of these classes there are different cell types. All of these different cell types are required to work together in order to have a functional nervous system. Defects in neurogenesis could result in not having the correct total number of cells, or in missing specific cell types, or in cell types that are incorrectly specified, i.e. cells that do not express the correct complement of genes. All of these phenotypes can lead to functional abnormalities and diseases. Autism is believed to be a developmental disorder and many genes that are found to be mutated in individuals with autism are those that function early in development during neurogenesis (Polleux and Lauder, 2004).

Understanding how different cell types are generated is also important for the treatment of diseases. Parkinson's disease is caused by the loss and degeneration of dopaminergic neurons in the midbrain (Iversen and Iversen, 2007). One proposed treatment of Parkinson's disease is the replacement of dopaminergic neurons generated

by stem cells. This treatment requires knowing how dopaminergic neurons are generated from precursors. The replacement cells must not only produce dopamine, but the cells may also have to express the correct combination of transporters, receptors, and may need to make functional connections. Many of the gene regulatory events that control this level of cell type specific gene expression are unknown.

In order to determine the gene regulatory networks responsible for generating cell type-specific gene expression, it is useful to analyze development at the single cell level. The *Drosophila* embryonic CNS consists of the brain and ventral nerve cord (VNC). The *Drosophila* CNS midline cells lie along the ventral midline of the embryo within the VNC. The midline cells are functionally similar to vertebrate floorplate cells because they both lie along the ventral midline of the embryo and they are both the source of guidance cues (Dickson, 2002; Ruiz i Altaba et al., 2003). The midline cells are an ideal system to study neurogenesis because they consist of a small number of diverse cell types including neurons of 8 identifiable types, 2 types of glia and a median neuroblast (MNB) (Wheeler et al., 2006). Each of these cells can be studied at the single cell level to determine how these cells establish cell type specific gene expression.

Neurogenesis: generating diversity in the CNS

Drosophila CNS development consists of a series of well-defined steps (Skeath and Thor, 2003). The VNC arises from ventral ectodermal cells. The combination of the three columnar genes, *ventral nervous system defective* (*vnd*), *intermediate neuroblasts defective* (*ind*) and *muscle specific homeobox* (*msh*) and anterior-posterior patterning genes subdivide the ventral ectoderm into a regular pattern of proneural clusters (Skeath,

1999). Each cell in a proneural cluster expresses proneural genes and is equivalent in its ability to become a neuroblast (NB). One cell expresses proneural genes at a higher level and delaminates to become the neuroblast. The remaining cells of the cluster extinguish proneural expression and take on an epidermal fate via a process termed lateral inhibition that is mediated by *Notch* signaling (for review see Skeath and Thor, 2003). The neuroblast then asymmetrically divides in a stem cell-like manner to give rise to smaller ganglion mother cells (GMCs). Each GMC then divides to give rise to two post-mitotic neurons and or glia. Each neuroblast generates a stereotyped pattern of neurons and glia (Schmid et al., 1999). While the process of neuroblast formation is well understood, the genetic regulatory cascades that are initiated by proneural genes that result in neuronal fate are unknown. While whole-genome microarray analysis has identified genes that are upregulated in proneural clusters, direct targets of proneural genes that act to control cell fate are lacking (Reeves and Posakony, 2005).

***Drosophila* proneural genes**

The AS-C genes are conserved neural regulators that are required for neuroblast formation and subsequently to specify their fate (Villares and Cabrera, 1987). The AS-C consists of 3 proneural genes, *achaete* (*ac*), *scute* (*sc*) and *lethal of scute* (*l(1)sc*) and the neural precursor gene *asense* (Garcia-Bellido, 1978). *asense* is considered a neural precursor gene because it is expressed in every neuroblast and not in proneural clusters (Brand et al., 1993). The AS-C genes are bHLH transcription factors that are required for neuroblast formation. In a *l(1)sc* mutant, 50% of the neuroblasts do not form (Jimenez and Campos-Ortega, 1990). In a *sc* mutant there is a loss of sensory bristles, but in an *ac*

mutant, bristle formation is normal and there are no abnormalities in the PNS (Marcellini et al., 2005). This suggests that *ac* may have as yet, an unknown function.

AS-C genes: roles in neuroblast formation and precursor specification

There is evidence that not only do the AS-C genes promote neuroblast formation, but also specify neuroblast fate and identity. In an AS-C mutant, the MP2 neuroblast does not form and neuroblast formation can be rescued by *l(1)sc*, *ac*, and *sc* (Parras et al., 1996; Skeath and Doe, 1996). Expression of *ac*, *sc*, or *l(1)sc* resulted in rescue of a neuroblast in the MP2 position. But only *ac* and *sc*, the proneural genes normally expressed in the MP2 neuroblast, could rescue MP2 specific gene expression. This suggests that *ac*, *sc* and *l(1)sc* are equivalent in their ability to form a neuroblast in the MP2 position. But that only *ac* and *sc* have the ability to control MP2 cell fate specification. Since *ac*, *sc*, and *l(1)sc* all have similar functions in neural precursor formation, *l(1)sc* could have a similar function as *ac* and *sc* in regulating cell fate specification in other cell types.

AS-C genes are transiently expressed in the CNS; expression is extinguished before each neuroblast divides to generate a GMC (Cubas et al., 1991; Skeath and Carroll, 1991). So AS-C genes must activate other transcription factors to control neuronal differentiation, but there is a lack of known direct targets of AS-C genes that control cell specification. *asense* is expressed in every neuroblast and it is a direct target of *ac* and *sc* (Brand et al., 1993; Jarman et al., 1993). Despite its widespread expression pattern, the mutant phenotype of *asense* is not severe; there is only abnormal formation in

mechanosensory bristles on the wing (Jarman et al., 1993). This suggests that direct target genes of the *AS-C* genes still remain to be identified.

Asymmetric cell division: generation of two cell fates

Asymmetric cell division is one way to generate diversity and the *Notch* signaling pathway is one way to generate two different cell fates during asymmetric cell divisions. *Notch* signaling is well-characterized regarding the asymmetric division of GMCs in the lateral CNS (Spana et al., 1995; Wai et al., 1999). The first GMC from NB4-2 generates the RP2 and RP2 sib neurons. In a *numb* mutant both daughter cells take on the RP2 sib fate, while in a *Notch* mutant both daughter cells take on the RP2 fate (Wai et al., 1999). *Notch* signaling is required for the RP2 fate, but it is unknown what controls gene expression in the other, *Notch*-independent cell.

Dopamine regulation in *Drosophila*

In the *Drosophila* embryonic CNS, there are dopaminergic neurons in the brain and 3 dopaminergic neurons in the VNC; 2 dorsal lateral dopamine neurons in the lateral CNS and one dopaminergic neuron in the midline (Lundell and Hirsh, 1994). H-cell is the midline dopaminergic neuron (Wheeler et al., 2006). There have been insights into how dopamine is regulated in H-cell, but there are questions that remain unanswered. The LIM homeo-domain transcription factor *tailup* (*tup*), a homologue of the mouse *islet-1* and *islet-2* genes has been shown to regulate tyrosine hydroxylase (TH) (Thor and Thomas, 1997). TH is a biosynthetic enzyme required for dopamine synthesis and is encoded by the *pale* (*ple*) gene in *Drosophila* (Neckameyer and White, 1993). The *ple* gene is expressed in the midline beginning at stage 13 (Lundell and Hirsh, 1994). In

mutants deficient for *tup*, *ple* expression is lost in the midline. The functions of *tup* are cell type-dependent. *tup* is required for *ple* expression in the midline, but *tup* regulates serotonin expression in neurons in the lateral CNS. Misexpression of *tup* does not expand *ple* expression in all cells, but only in a subset (Thor and Thomas, 1997). So, the function of *tup* must be dependent on other cell-type specific factors.

Also, *tup* is not required for all embryonic CNS *ple* expression. There are dopaminergic neurons in the brain that do not express *tup* and loss of *tup* has no effect on *ple* expression in these neurons. This indicates there must be other transcription factors that regulate *ple* expression and dopaminergic cell fate. Other genes such as the biosynthetic enzyme, *Dopa decarboxylase (Ddc)* and *dopamine transporter (DAT)* are required for dopaminergic cell fate. It is unknown if *tup* regulates these genes. The *tup* gene functions in post-mitotic neurons, since *tup* expression does not begin until stage 11. Since midline cell fate is established before stage 11, there must be cell type-specific genes that regulate *tup* expression, but these are unknown.

Overview of CNS midline development

The *Drosophila* CNS midline cells arise in the blastoderm embryo as two cellular stripes on either side of the embryo. Early during the mesectoderm anlage stage, gastrulation brings the stripes together at the midline, so there are 8 cells per segment (Fig. 1.1). Then midline precursors simultaneously divide to give rise to 16 cells per segment late during the mesectoderm anlage stage (stages 7-8). The midline cells then divide, differentiate, and migrate during the midline primordium stages (stages 9-12).

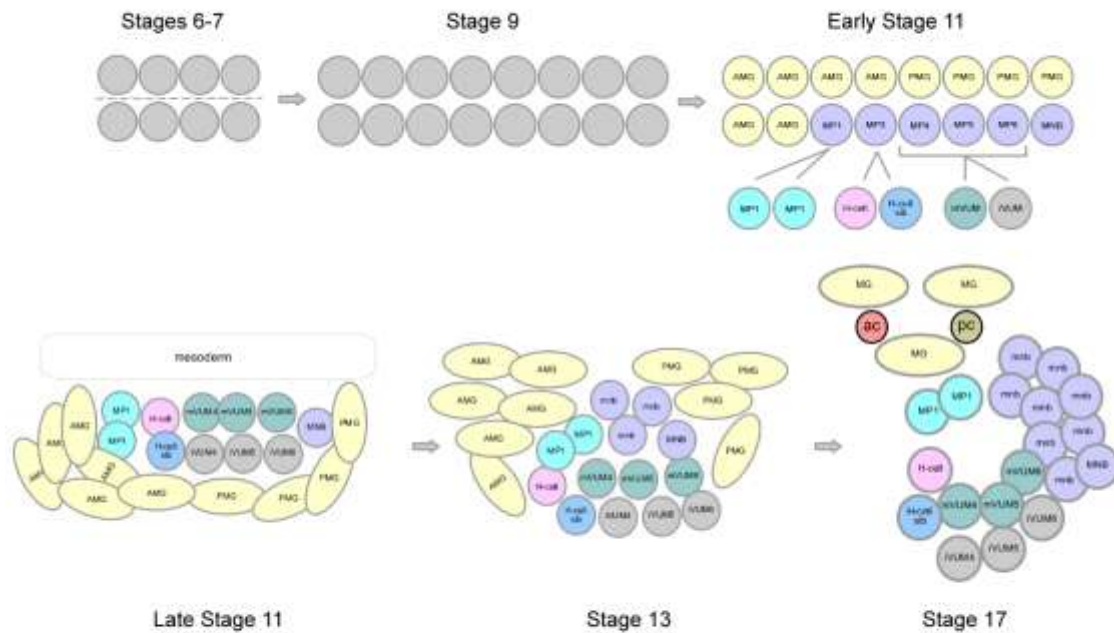


Figure 1.1. Model of midline cell development. Schematic of the CNS midline cells at 6 stages in development shown in horizontal view (stages 6, 9, early 11, and late 11) and sagittal view (stages 13 and 17). Each circle or oval corresponds to a single midline cell. Abbreviations are as follows: MG (midline glia), MP1 (MP1 neurons), MNB (median neuroblast), mnb (median neuroblast progeny), H-sib (H-cell sibling neuron), H-cell (H-cell neuron), mVUM (VUM motorneuron), iVUM (VUM interneuron). At stage 6: midline cells form two rows of 4 cells each at the ventral midline and then undergo a synchronous cell division at stage 8. The resulting 16 cells give rise to 10 midline glia (MG) and 6 neural precursors: 5 midline precursors (MPs) numbered 1,3-6 and the median neuroblast (MNB). At stage 11, neural precursors then divide: MP1 divides to generate 2 identical MP1 neurons, MP3 divides to give yield H-cell and H-cell sib and MP4-6 each divide to yield a VUM motorneuron (mVUM) and a VUM interneuron (iVUM). At stage 13: anterior midline glia (AMG) and posterior midline glia (PMG) migrate internally and the AMG further migrate towards the posterior. Midline neurons begin to express peptide neurotransmitter and neurotransmitter biosynthetic enzyme genes. At stage 16: PMG have undergone apoptosis and 3 AMG remain. Midline neurons have migrated to their final positions.

During the mature midline stages (stages 13-17), cells differentiate and undergo apoptosis to consist of 18 neurons and 3 midline glia. There are two types of glia at the midline, the anterior midline glia (AMG) and the posterior midline glia (PMG) (Dong and Jacobs, 1997). The AMG consist of 6 cells at stage 11, but half of the AMG die by apoptosis, so their number decreases to 3 cells by stage 17. The PMG consists of 4 cells at stage 11, but all PMG undergo by apoptosis by stage 16 and are not present at stage 17 (Dong and Jacobs, 1997).

Midline neurons are generated by two mechanisms: a midline precursor (MP) divides once to give rise to two daughter neurons or the median neuroblast divides in a stem cell-like manner to give rise to 8 embryonic neuronal progeny. There are 10 MP derived neurons: 2 identical peptidergic MP1 neurons, 2 MP3-derived neurons: the dopaminergic H-cell and glutamatergic H-cell sib, and 3 GABAergic ventral unpaired medial interneurons (iVUM) and 3 glutamatergic and octopamatergic ventral unpaired medial motoneurons (mVUM). There are 3 VUM precursors that each divide once to generate 1 mVUM and 1 iVUM. Prior to this dissertation, the origin of two pairs of VUM neurons, was unclear because clonal analysis studies have shown that one or two pairs of VUM neurons share lineage with the MNB (Bossing and Technau, 1992; Schimid et al.,1999).

Gene expression changes during midline development

Early patterning genes control gene expression changes at the midline early in development and also act to control cell fate specification (Bossing and Brand, 2006). In order to determine the regulatory events occurring in each cell early in development, each

immature cell must be identifiable and linked to its terminal fate. Prior to this dissertation, midline cells could not be identified early in development. Late in development, midline cells were identifiable based on their morphology, axon trajectories, and composite gene expression (Wheeler et al., 2006). The glia reside dorsally while the neurons reside more ventrally. The midline cells are positioned differently at late stage 11; the two types of midline glia reside on either side of the neurons. Cell types could be identified at this stage because gene expression can be followed from late stage 11 to stage 17. Cell types were not distinguishable based on their composite gene expression at stage 9 because there is a lack of continuity of gene expression between stages 9 and 11. Many of the genes expressed at stage 9 are extinguished by stage 11 and genes expressed at stage 11 are not expressed earlier at stage 9.

In addition to the lack of continuity of gene expression at the midline between stages 9 and 11, there is also a fundamental reorganization of the midline at stage 10. At stage 9, the midline cells exist as two columns of cells, but by stage 11 neurons and glia have distinct locations. These dynamic cell movements made it difficult to link mature midline cells with midline cells at earlier stages in development. Cell divisions also occur at stage 10, but the exact number and timing of these divisions is unclear. Therefore, further analysis of these early stages was required to link individual midline precursor cells with terminal differentiated fates and to understand how these cells become specified.

AS-C genes at the midline

All 4 *AS-C* genes are expressed at the midline in overlapping and non-overlapping patterns in both neurons and glia (Kearney et al., 2004). Recent work suggested that the *AS-C* genes also regulate gene expression changes in midline cells. In mutants deficient for *ac*, *sc*, and *l(1)sc*, the number of *engrailed* (*en*) positive cells is reduced (Bossing and Brand, 2006). The authors concluded that *AS-C* genes regulate *en* expression. This is uncertain, however, since it was not determined if the *en* expressing cells were present in the mutant embryos. *AS-C* mutant phenotypes must be carefully analyzed because the *AS-C* genes have been shown to have roles both in precursor formation and in regulating cell fate. So, the lack of cell type-specific gene expression in the *AS-C* mutant could indicate that *AS-C* genes are required for *en* expression or that the precursor does not form and generate its neuronal progeny or both. Similar to their roles in the lateral CNS, *AS-C* genes could control both neural precursor formation and cell fate specification at the midline. The midline is an ideal model system to determine both the function of each *AS-C* proneural gene and to identify targets of the *AS-C* genes since gene expression can be mapped at the single cell level.

The focus of this dissertation was to determine the gene regulatory network that controls midline dopaminergic cell fate. Before the hierarchy of gene expression could be identified, it first had to be determined how a dopaminergic cell is generated. MPs had to be identified and the timing of divisions determined. This work is described in Chapter 2, which addresses the identification of genes that are expressed during early midline development and how these genes fit into the genetic pathways that control midline cell fate. The molecular maps for stage 10 and 11 developed in Chapter 2 were used as diagnostic tools in analyzing mutant phenotypes in Chapter 3. Chapter 3 addresses the

role of proneural genes in determining dopaminergic neural cell fate. Chapter 4 details the identification and cataloguing of midline-expressed genes. In Chapter 5, these results and potential future directions are discussed.

References

- Bossing, T. and Brand, A. H.** (2006). Determination of cell fate along the anteroposterior axis of the drosophila ventral midline. *Development* **133**, 1001-1012.
- Bossing, T. and Technau, G. M.** (1994). The fate of the CNS midline progenitors in *drosophila* as revealed by a new method for single cell labelling. *Development* **120**, 1895-1906.
- Bossing, T., Udolph, G., Doe, C. Q. and Technau, G. M.** (1996). The embryonic central nervous system lineages of drosophila melanogaster. I. neuroblast lineages derived from the ventral half of the neuroectoderm. *Dev. Biol.* **179**, 41-64.
- Brand, M., Jarman, A. P., Jan, L. Y. and Jan, Y. N.** (1993). Asense is a drosophila neural precursor gene and is capable of initiating sense organ formation. *Development* **119**, 1-17.
- Cabrera, C. V. and Alonso, M. C.** (1991). Transcriptional activation by heterodimers of the achaete-scute and daughterless gene products of drosophila. *EMBO J.* **10**, 2965-2973.
- Campuzano, S., Carramolino, L., Cabrera, C. V., Ruiz-Gomez, M., Villares, R., Boronat, A. and Modolell, J.** (1985). Molecular genetics of the achaete-scute gene complex of *D. melanogaster*. *Cell* **40**, 327-338.
- Cubas, P., de Celis, J. F., Campuzano, S. and Modolell, J.** (1991). Proneural clusters of achaete-scute expression and the generation of sensory organs in the drosophila imaginal wing disc. *Genes Dev.* **5**, 996-1008.
- Dickson, B. J.** (2002). Molecular mechanisms of axon guidance. *Science* **298**, 1959-1964.
- Dong, R. and Jacobs, J. R.** (1997). Origin and differentiation of supernumerary midline glia in *drosophila* embryos deficient for apoptosis. *Dev. Biol.* **190**, 165-177.
- Garcia-Bellido, A.** (1979). Genetic analysis of the achaete-scute system of DROSOPHILA MELANOGASTER. *Genetics* **91**, 491-520.
- Garcia-Bellido, A. and Santamaria, P.** (1978). Developmental analysis of the achaete-scute system of DROSOPHILA MELANOGASTER. *Genetics* **88**, 469-486.
- Iversen, S. D. and Iversen, L. L.** (2007). Dopamine: 50 years in perspective. *Trends Neurosci.* **30**, 188-193.

- Jarman, A. P., Brand, M., Jan, L. Y. and Jan, Y. N.** (1993). The regulation and function of the helix-loop-helix gene, *asense*, in drosophila neural precursors. *Development* **119**, 19-29.
- Jimenez, F. and Campos-Ortega, J. A.** (1990). Defective neuroblast commitment in mutants of the achaete-scute complex and adjacent genes of *D. melanogaster*. *Neuron* **5**, 81-89.
- Kearney, J. B., Wheeler, S. R., Estes, P., Parente, B. and Crews, S. T.** (2004). Gene expression profiling of the developing drosophila CNS midline cells. *Dev. Biol.* **275**, 473-92.
- Lundell, M. J. and Hirsh, J.** (1994). Temporal and spatial development of serotonin and dopamine neurons in the drosophila CNS. *Dev. Biol.* **165**, 385-396.
- Marcellini, S., Gibert, J. M. and Simpson, P.** (2005). Achaete, but not scute, is dispensable for the peripheral nervous system of drosophila. *Dev. Biol.* **285**, 545-553.
- Neckameyer, W. S. and White, K.** (1993). Drosophila tyrosine hydroxylase is encoded by the pale locus. *J. Neurogenet.* **8**, 189-199.
- Parras, C., Garcia-Alonso, L. A., Rodriguez, I. and Jimenez, F.** (1996). Control of neural precursor specification by proneural proteins in the CNS of drosophila. *EMBO J.* **15**, 6394-6399.
- Reeves, N. and Posakony, J. W.** (2005). Genetic programs activated by proneural proteins in the developing drosophila PNS. *Dev. Cell.* **8**, 413-425.
- Ruiz i Altaba, A., Nguyen, V. and Palma, V.** (2003). The emergent design of the neural tube: Prepattern, SHH morphogen and GLI code. *Curr. Opin. Genet. Dev.* **13**, 513-521.
- Schmid, A., Chiba, A. and Doe, C. Q.** (1999). Clonal analysis of drosophila embryonic neuroblasts: Neural cell types, axon projections and muscle targets. *Development* **126**, 4653-4689.
- Singson, A., Leviten, M. W., Bang, A. G., Hua, X. H. and Posakony, J. W.** (1994). Direct downstream targets of proneural activators in the imaginal disc include genes involved in lateral inhibitory signaling. *Genes Dev.* **8**, 2058-2071.
- Skeath, J. B.** (1999). At the nexus between pattern formation and cell-type specification: The generation of individual neuroblast fates in the drosophila embryonic central nervous system. *Bioessays* **21**, 922-931.

- Skeath, J. B. and Carroll, S. B.** (1991). Regulation of achaete-scute gene expression and sensory organ pattern formation in the drosophila wing. *Genes Dev.* **5**, 984-995.
- Skeath, J. B. and Doe, C. Q.** (1996). The achaete-scute complex proneural genes contribute to neural precursor specification in the drosophila CNS. *Curr. Biol.* **6**, 1146-1152.
- Skeath, J. B. and Thor, S.** (2003). Genetic control of drosophila nerve cord development. *Curr. Opin. Neurobiol.* **13**, 8-15.
- Spana, E. P., Kopczynski, C., Goodman, C. S. and Doe, C. Q.** (1995). Asymmetric localization of numb autonomously determines sibling neuron identity in the drosophila CNS. *Development* **121**, 3489-3494.
- Thor, S. and Thomas, J. B.** (1997). The drosophila islet gene governs axon pathfinding and neurotransmitter identity. *Neuron* **18**, 397-409.
- Villares, R. and Cabrera, C. V.** (1987). The achaete-scute gene complex of *D. melanogaster*: Conserved domains in a subset of genes required for neurogenesis and their homology to myc. *Cell* **50**, 415-424.
- Wai, P., Truong, B. and Bhat, K. M.** (1999). Cell division genes promote asymmetric interaction between Numb and Notch in the *Drosophila* CNS. *Development* **126**, 2759-70.
- Wheeler, S. R., Kearney, J. B., Guardiola, A. R. and Crews, S. T.** (2006). Single-cell mapping of neural and glial gene expression in the developing *drosophila* CNS midline cells. *Dev. Biol.* **294**, 509-524.

CHAPTER II

MULTIPLE *NOTCH* SIGNALING EVENTS CONTROL *DROSOPHILA* CNS MIDLINE NEUROGENESIS, GLIOGENESIS, AND NEURONAL IDENTITY

Scott R. Wheeler, Stephanie B. Stagg, and Stephen T. Crews^{*}

Doctoral student contributed figures: 2.1, 2.2, and S2.1 and movie 2.1 and movie 2.2

Published in Development (Wheeler et al., 2008)

Department of Biochemistry and Biophysics; Department of Biology

Program in Molecular Biology and Biotechnology

The University of North Carolina at Chapel Hill

Chapel Hill, NC 27599-3280

^{*}Author for correspondence: steve_crews@unc.edu

Tel (919) 962-4380, Fax (919) 962-8472

Summary

The study of how transcriptional control and cell signaling influence neurons and glia to acquire their differentiated properties is fundamental to understanding CNS development and function. The *Drosophila* CNS midline cells are an excellent system for studying these issues because they consist of a small population of diverse cells with well-defined gene expression profiles. In this paper, the origins and differentiation of midline neurons and glia were analyzed. Midline precursor (MP) cells each divide once giving rise to 2 neurons; here, we use a combination of single-cell gene expression mapping and time-lapse imaging to identify individual MPs, their locations, movements, and stereotyped patterns of division. The role of *Notch* signaling was investigated by analyzing 37 midline-expressed genes in *Notch* pathway mutant and misexpression embryos. *Notch* signaling had opposing functions: it inhibited neurogenesis in MP1,3,4, and promoted neurogenesis in MP5,6. *Notch* signaling also promoted midline glial and median neuroblast cell fate. This latter result suggests that the median neuroblast resembles brain neuroblasts that require *Notch* signaling, rather than nerve cord neuroblasts, whose formation is inhibited by *Notch* signaling. Asymmetric MP daughter cell fates also depend on *Notch* signaling. One member of each pair of MP3-6 daughter cells was responsive to *Notch* signaling. In contrast, the other daughter cell asymmetrically acquired Numb, which inhibited *Notch* signaling, leading to a different fate choice. In summary, this paper describes the formation and division of MPs and describes multiple roles for *Notch* signaling in midline cell development providing a foundation for comprehensive molecular analyses.

Introduction

The central nervous system (CNS) consists of a diverse collection of neurons and glia that differ in both morphology and function. These properties arise during a sequence of developmental events that require numerous gene regulatory and signaling processes. The cells that lie along the midline of the *Drosophila* CNS provide a useful system for the comprehensive study of neurogenesis and gliogenesis. The mature, embryonic CNS midline cells consist of a functionally diverse group of ~22 cells, including midline glia (MG), local interneurons, projection neurons, peptidergic motorneurons, and neuromodulatory motorneurons (Wheeler et al., 2006). The identification and embryonic expression of almost 300 genes expressed in midline cells are known (Kearney et al., 2004), with transcriptional maps permitting detailed genetic analysis of the entire process of midline cell development (Bossing and Brand, 2006; Wheeler et al., 2006). Thus, the *Drosophila* midline cells combine cellular diversity and extensive molecular genetic characterization towards the study of CNS development.

The *Drosophila* midline cells originate from ~8 precursor cells/segment that undergo a synchronous cell division ($\delta_{14}14$) at stage 8 (Foe, 1989) to give rise to ~16 cells (Bossing and Technau, 1994). These cells are characterized by expression of the *single-minded* (*sim*) gene (Crews, 2003; Thomas et al., 1988). By late stage 11, the midline cells consist of ~10 MG, comprised of 2 populations, the anterior midline glia (AMG) and posterior midline glia (PMG), 2 midline precursor 1 (MP1) neurons, 2 MP3 neurons, 6 Ventral Unpaired Median (VUM) neurons (2 VUM4s, 2VUM5s, 2VUM6s), and the median neuroblast (MNB) (Wheeler et al., 2006). The PMG die during embryogenesis along with ~1/2 of the AMG. The remaining 3 AMG ensheath the axon

commissures. While the 2 MP1 neurons appear to be identical, the MP3 neurons differentiate into the dopaminergic H-cell and glutamatergic H-cell sib. Each VUM precursor (MP4-6) divides once giving rise to a GABAergic VUM interneuron (iVUM4-6) and a glutamatergic/octopaminergic VUM motorneuron (mVUM4-6). Thus, MPs can give rise to either 2 identical neurons (MP1) or 2 non-identical neurons (MP3-6). The MNB stem cell divides asymmetrically to generate ~8 GABAergic neurons during embryogenesis, and a much larger number post-embryonically (Truman et al., 2004). Despite the small number of embryonic midline cells, the origins of midline neurons and glia remain relatively unknown. In this study, for the first time, we identified each MP and described their patterns of cell division. This information was then utilized to reveal multiple roles of *Notch* signaling in midline neuronal and glial cell development.

Materials and methods

Drosophila strains and genetics

Drosophila strains included w^{1118} (used as wild-type), Dl^3 , Dl^7 , $numb^2$ (Uemura et al., 1989), $numb^4$ (Skeath and Doe, 1998), $spdo^{G104}$ and $spdo^{Z143}$ (Skeath and Doe, 1998), N^{55e11} , N^{ts1} , $P[12xSu(H)bs-lacZ]$ (Go et al., 1998), and $GBE-lacZ$ (Furriols and Bray, 2001). *Gal4* and *UAS* lines used were: *sim-Gal4* (Xiao et al., 1996), *UAS-numb* (Wang et al., 1997), *UAS-spdo* (O'Connor-Giles and Skeath, 2003), *UAS-Su(H).VP16* (Kidd et al., 1998), and *UAS-tau-GFP* (Brand, 1995). For *N* temperature shift experiments, N^{55e11}/N^{ts1} embryos were collected for 2 hours at 18°C, further incubated for 2 hours at 18°, then shifted to the restrictive temperature (30°C) for 6 hours, followed by fixation (~stage 14).

In situ hybridization and immunostaining

Embryo collection, in situ hybridization, and immunostaining were performed as previously described (Kearney et al., 2004). Primary antibodies used were: mouse (Promega) and rabbit (Cappel) anti- β -galactosidase, rabbit anti-Cas (Kambadur et al., 1998), mouse and rat anti-ELAV (Developmental Studies Hybridoma Bank, DSHB), mouse anti-En MAb 4D9 (Patel et al., 1989), anti-Futsch MAb 22C10 (DSHB), guinea pig anti-Hb (East Asian Distribution Center; EADC) (Kosman et al., 1998), chicken anti-GFP (Upstate), rabbit anti-GFP (Abcam), guinea pig anti-Lim1 (Broihier and Skeath, 2002), guinea pig anti-Numb (O'Connor-Giles and Skeath, 2003), rabbit anti-Odd (Ward and Skeath, 2000), rabbit anti-Period (Per) (Liu et al., 1992), rabbit anti-phosphohistone H3 (Millipore), guinea pig anti-Runt (EADC), guinea pig and rat anti-Sim (Ward et al., 1998), rabbit anti-Spdo (O'Connor-Giles and Skeath, 2003), mouse anti-tau (Sigma), and rat anti-Tup (Broihier and Skeath, 2002). Alexa Fluor-conjugated secondary antibodies were used (Molecular Probes). The Tyramide Signal Amplification System (Perkin Elmer) was employed for some immunostaining.

Microscopy and image analysis

In situ hybridization and immunostaining were carried-out as previously described (Kearney et al., 2004; Wheeler et al., 2006). Midline cells were examined in abdominal segments A1-8. Due to the 3-dimensional structure of the midline cells, it was difficult to represent all relevant cells in a single focal plane, so, for clarity, irrelevant portions of single images within a stack of confocal images were subtracted and

projections were generated. Thus, a single composite image is made from different focal planes that each contained relevant data.

Live imaging of midline cells

Time-lapse imaging of midline cell development was carried-out in *sim-Gal4 UAS-tau-GFP* and *sim-Gal4 UAS-tau-GFP; Df³/Df³* embryos by visualizing GFP. Embryos were collected for 1 hour, aged for an additional 4 hours, dechorionated, mounted on a glass coverslip, and immersed in halocarbon oil 700 on slides containing an oxygen-permeable membrane. GFP-fluorescent images were captured using a Nikon Eclipse TE300 equipped with a Perkin Elmer Ultraview confocal scanner and 40X or 60X oil objectives. Embryos were visualized for ~4 hours with an image captured every 30 seconds. Movies were assembled from images of single focal planes using Metamorph software. Ten wild-type movies viewing 29 segments and 5 *Df* mutant movies viewing 14 distinct groups of cells were analyzed.

Results

Identification of MPs and their pattern of division

As a prelude to studying the molecular mechanisms that control MP neuronal cell fate decisions, it was important to identify the MPs, and know when these cells divide. Previously, we generated molecular maps of stages 9, late 11, 13, and 17 (Wheeler et al., 2006), which allowed identification of individual midline cells. In this paper, we mapped the midline cell expression of 16 genes (Fig. 2.1 and see Fig. S2.1 in the supplementary

material) at multiple periods during stages 10-11 of embryogenesis. Each of the MPs, the MNB, and their progeny were defined and distinguished from each other by gene expression differences, position, size, and visualization of cell division. These data provided strong evidence that MP divisions occur during stage 11 and were confirmed by time-lapse imaging of midline cells in *sim-Gal4 UAS-tau-GFP* embryos (Fig. 2.2 and see Movie 2.1 in supplementary material).

At early stage 10, the midline cells constitute a monolayer along the anterior-posterior axis. However, beginning at late stage 10, MPs began to delaminate, and migrated basally (internally). As the cells migrated, they retracted a cytoplasmic process from the apical surface. The MP1,3,4 precursors acquired a flattened shape, resided internal to the MG, and were separated from other MPs by MG. The 5 MPs were arranged in a defined order, MP1→MP3→MP4→MP5→MP6 (anterior to posterior), within the segment. However, they delaminated and divided in the order MP4→MP3→MP5→MP1→MP6. The MP divisions were characterized by loss of an apical projection, retraction of the MG that separate the MPs, and the subsequent juxtaposition of neuronal progeny. The MP3-6 divisions were along the apical-basal axis, whereas the MP1 division was perpendicular to the apical-basal axis. After the MPs divided, the MNB delaminated posterior to the MP6 progeny and began dividing to generate ganglion mother cells (GMCs).

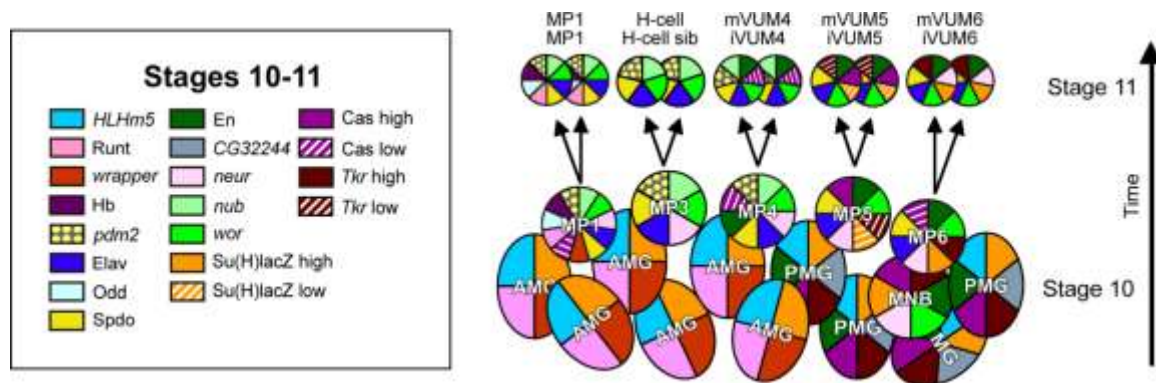


Figure 2.1. Formation of MPs and MP neurons. Molecular map of stages 10 and 11 MPs and midline neurons (circles) and glia (ovals) shown in sagittal view. One segment is shown, with anterior to the left and interior (basal) at top. Each cell is depicted by its pattern of gene expression indicated by the colors and their corresponding genes listed on the left. The 5 MPs are shown at late stage 10, and the arrows indicate MPs dividing into their neuronal progeny at stage 11. The number of MG does not change appreciably from stage 10 to 11.

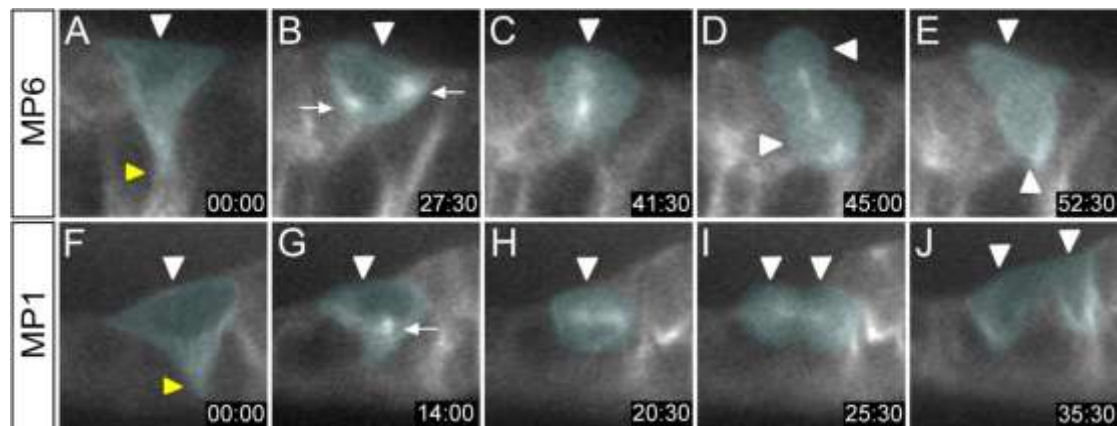


Figure 2.2. Time-lapse imaging of sequential MP division. Still images in sagittal view, internal (basal) up, from time-lapse imaging of an (A-E) MP6 division and an (F-J) MP1 division. GFP fluorescence was visualized in *sim-Gal4 UAS tau-GFP* embryos during stage 11. Time is displayed as minutes:seconds. Relevant cells in each panel are pseudocolored. (A) Prior to division, the MP6 (white arrowhead) delaminates from the apical surface and takes on a triangular shape. The tip of the retracting cell is indicated by the yellow arrowhead. (B-D) During mitosis, (B) the centrosomes (arrows) move toward opposite poles, (C) the spindle fibers have an apical-basal orientation, and (D) the MP6 divides along this axis. (E) Two MP3 neurons (arrowheads) are produced. (F) The MP1 (white arrowhead) delaminates from the apical surface, also acquiring a triangular shape (retraction point; yellow arrowhead). (G) The centrosomes (arrow) can be seen just before they separate and begin their migration. (H) The MP1 spindle maintains an orientation perpendicular to the apical-basal axis. (I-J) Cytokinesis results in the formation of 2 MP1 neurons (arrowheads).

***Notch* signaling promotes midline glia, MNB, and MP5,6 formation and inhibits MP1,3,4 formation**

Based on the important roles of *Notch* signaling in CNS development, *Delta* (*Dl*) and *Notch* (*N*) mutants were screened for midline phenotypes, including alterations in expression of midline-expressed genes. In both *Dl*³ homozygotes and *Dl*³/*Dl*⁷ transheterozygotes, an increase was observed in the number of midline neurons at the expense of MG (Fig. 2.3). At stage 14, the number of MP1 neurons increased from 2 cells/segment to 9.3 ± 1.6 (n=14 segments) cells (Fig. 2.3A,F). The number of H-cells increased from 1 cell/segment to 9.6 ± 1.1 (n=17) (Fig. 2.3B,G), and the number of mVUMs increased from 3 cells/segment to 11.5 ± 1.7 (n=51) (Fig. 2.3C,H). H-cell sib and iVUM-specific gene expression was absent in *Dl* mutants (not shown). As described below, in the absence of *Notch* signaling all MP3 neurons are H-cells and all VUMs are mVUMs due to cell fate defects. Both MP1 and MP3 neurons increased ~5X in *Dl* mutant embryos. The VUM neurons, in contrast, increased only 2X.

This disparity led us to investigate the identity of the mVUM neurons observed in *Dl* mutants. All mVUMs can be uniquely identified in the midline by *Tyramine β hydroxylase* (*Tbh*) expression, and mVUM4-6 can be distinguished from each other based on *Tyrosine kinase-related protein* (*Tkr*) and Castor (Cas) levels. The wild-type mVUM4 and mVUM5 neurons are *Tkr*⁻, whereas mVUM6 is *Tkr*⁺ (Fig. 2.4A). The expanded *Tbh*⁺ mVUMs in *Dl* mutants were *Tkr*⁻ (Fig. 4C), indicating that none were mVUM6s. The one significant difference between wild-type mVUM4 and mVUM5 is

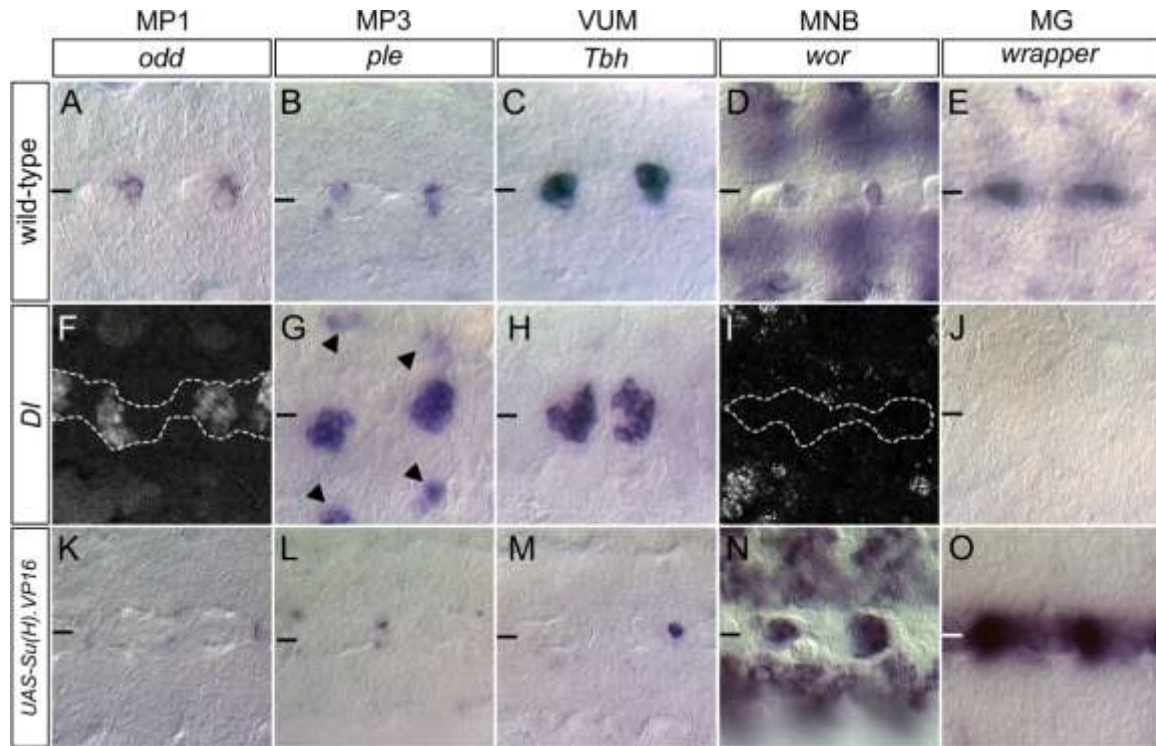


Figure 2.3. Notch signaling influences midline cell fate. Ventral views of stage 14 (A-E) wild-type, (F,G,I,J) *Dl³/Dl³*, (H) *Dl³/Dl⁷*, and (K-O) *sim-Gal4 UAS-Su(H).VP16* embryos. Cell types are listed at the top of each column, and the gene or protein assayed that identifies each cell type are listed below. Horizontal bars indicate the location of the midline. (F,I) To differentiate (F) *Odd*⁺ and (I) *wor*⁺ midline cells from lateral CNS cells, embryos were double-stained with anti-Sim (not shown, but outlined to show location of midline cells). In *Dl* mutants, there was an: (F-H) increase in MP1, MP3 (H-cell), and mVUM neurons, and an absence of the (I) MNB and (J) MG. In (G), ectopic *ple*⁺ cells (arrowheads) were present off the midline; double-staining with anti-Sim indicated that these are not midline-derived (not shown). (K-O) *sim-Gal4 UAS-Su(H).VP16* embryos showed the opposite phenotype as *Dl* mutants: (K-M) strong reduction of MP1, MP3, and mVUM neurons, and increases in (N) MNB and (O) MG.

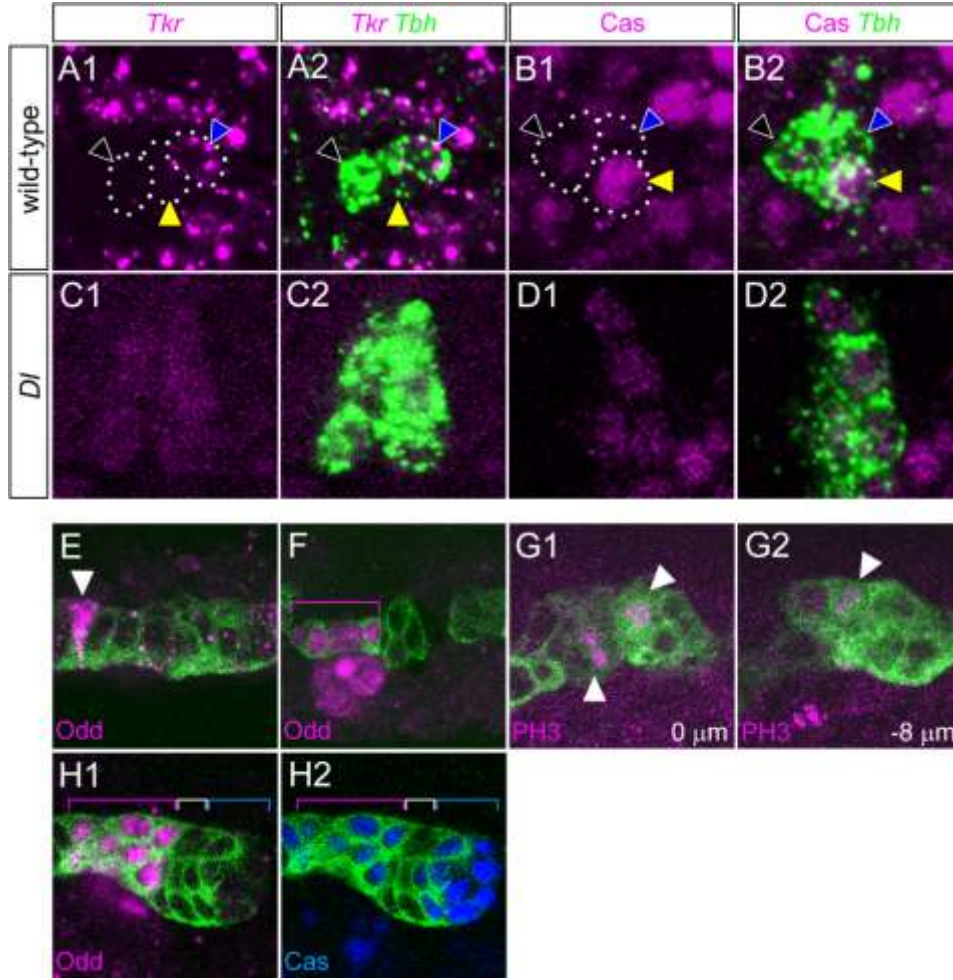


Figure 2.4. MP number increases in the absence of *Notch* signaling. (A-D) Ventral views of stage 14 (A,B) wild-type and (C,D) *Df³/Df³* mutant embryos. (A,C) Single segment stained for *Tkr* (magenta) and *Tbh* (green). The mVUM6 (blue arrowhead) was *Tkr*⁺, while mVUM4 (black arrowhead) and mVUM5 (yellow arrowhead) were *Tkr*⁻. Dotted circles show the outline of the mVUMs. (B,D) In *Df*, *Tkr* expression was absent indicating that the excess *Tbh*⁺ cells were not mVUM6s. (B) Single segment stained for *Cas* (magenta) and *Tbh* (green). There are 3 *Tbh*⁺ mVUMs in each segment: mVUM4 (black arrowhead) was *Cas*^{lo}, mVUM5 (yellow arrowhead) was *Cas*^{hi}, and mVUM6 was *Cas*⁻ (blue arrowhead). (D) Single segment of a *Df* embryo stained for *Cas* and *Tbh*. Excess *Tbh*⁺ cells were *Cas*^{lo}, indicating that they were mVUM4s. Quantitation of *Cas* staining intensity was measured using the Mean Gray Value (MGV) function of ImageJ (Abramoff et al., 2004). In wild-type (n=4 segments), mVUM4, mVUM5, and mVUM6 showed MGVs of 67, 155, and 22 respectively. In *Df* mutants (n=6 segments), all VUM neurons showed similar MGVs with an average of 67, the same as wild-type mVUM4. (E-H) Sagittal views of single segments of (E) wild-type and (F-H) *Df³/Df³* mutant embryos. Midline cells are defined as MPs based on their relatively large size and age. (E) At mid-stage 10, there is a single *Odd*⁺ (magenta) MP1 (arrowhead). (F) In *Df*, the number of *Odd*⁺ MP1s (bracket) was increased. (G) *Df* mutant embryo at two focal planes, 8 μ m apart, showing 3 dividing cells (arrowheads) in close proximity stained with anti-phosphohistone H3 (PH3; magenta). (H) In *Df*, there is an increase in *Odd*⁺ (magenta) *Cas*⁺ (blue) MP1 neurons (magenta bracket), *Odd*⁻ *Cas*⁻ MP3 neurons (white bracket), and *Odd*⁻ *Cas*⁺ MP4 neurons (blue bracket).

that mVUM4 has low levels of Cas (Cas^{lo}) and mVUM5 has high levels of Cas (Cas^{hi}) (Fig. 2.4B). The *Dl* mutant *Tbh*⁺ cells were all Cas^{lo} (Fig. 2.4D) identifying them as mVUM4s. These results, together with the observation that the 11.5 mVUMs/segment observed in *Dl* mutants were close in number to the ~9 MP1s and 10 H-cells observed, suggested an expansion of a single VUM precursor, likely the MP4.

The expanded numbers of MP1,3,4 neurons in *Dl* mutant embryos (~30) could be due to either: (1) a transformation of all of the ~15 midline cells to MP1,3,4 followed by a single division of each MP, or (2) an overproliferation of one or a few MP1,3,4 cells, accompanied by the death or unrecognizable fate change of the other midline cells. This was tested by assaying stage 10-11 *Dl* mutant embryos for gene expression and positions and timing of cell division. Late stage 10 mutant embryos revealed an increased number of Odd-skipped (Odd)⁺ MP1s (4.1 ± 1.2 ; n=17) (Fig. 2.4E,F). Live imaging of *Dl* mutant embryos during stage 11 indicated that the observable MP divisions occurred within a relatively short time interval (88 ± 16 minutes) (see Movie 2.2 in supplementary material). Divisions of closely juxtaposed cells were frequently observed occurring in close temporal sequence in both live imaging and fixed embryos stained for phosphohistone H3 (Fig. 2.4G). There was no evidence of cell death. Confocal imaging of stage 11 *Dl* embryos, after division, revealed 7.9 ± 2.1 (n=19) Odd⁺ Cas⁺ MP1 neurons, 6.9 ± 1.4 (n=12) Odd⁻ Cas⁻ MP3 neurons, and 10.0 ± 2.2 (n=7) Odd⁻ Cas⁺ MP4s (Fig. 2.4H). These data are most consistent with a model in which there is a transformation of ~16 midline cells into ~5 MP1s, ~5 MP3s, and ~6 MP4s followed by a single division of each MP.

In contrast to the expansion of MP1,3,4-derived neurons in *Dl* mutants, there was an absence of MG and the MNB. MG gene expression was reduced from 10.0 ± 1.3 (n=15) cells/segment in wild-type to 0.1 ± 0.2 (n=176) cells/segment in *Dl* mutants (Fig. 2.3E,J). The MNB has prominent wild-type expression of 3 genes: *worniu* (*wor*) (Fig. 2.3D), *miranda* (*mira*) (not shown), and *sanpodo* (*spdo*) (not shown), which are specific for the MNB after stage 11. In stage 14 *Dl* mutant embryos, *wor* (n=84) (Fig. 2.3I), *mira* (n=56), and *spdo* (n=47) expression was absent from the midline. Involvement of the Notch receptor was confirmed by analysis of a *N* mutant combination, N^{ts1}/N^{55e11} , that showed similar phenotypes, although at a reduced frequency (not shown).

***Notch* activation converts MPs to midline glia**

In experiments complementary to *Notch* and *Dl* mutant analyses, *sim-Gal4* was used to misexpress constitutively-active *Suppressor of Hairless.VP16* [*Su(H).VP16*] (Kidd et al., 1998) in all midline cells. Stage 14 *sim-Gal4 UAS-Su(H).VP16* embryos were examined, since MG undergo apoptosis beginning at stage 15. At stage 14, these embryos showed a 3X increase in the number of MG (30 ± 5.5 cells/segment, n=19) compared to wild-type (10.0 ± 1.3 , n = 15) (Fig. 2.3E,O and see Fig. S2.2A-H in the supplementary material). The expanded MG had wild-type properties: they underwent apoptosis, both AMG and PMG were present, and they wrapped commissural axons. In addition, there was a near complete absence of midline axons (see Fig. S2.3A,B in the supplementary material) and less than 1 MP-derived neuron/segment was present (Fig. 2.3K-M). Larval and adult phenotypes of these midline neuron-less animals were

assessed: 62% of embryos survived to adulthood, but were female sterile (see Fig. S2.3C in the supplementary material), and larvae had reduced motility (see Fig. S2.3D in the supplementary material). When *sim-Gal4 UAS-Su(H).VP16* embryos were stained for MNB markers *wor* (Fig. 2.3N), *mira*, and *spdo*, there was an increase in cell number from 1 cell/segment in wild-type to 4.9 ± 1.8 (n= 12). These *wor*⁺ cells also had MG gene expression. The expansion of MNB gene expression was consistent with the *Dl* mutant data indicating that *Notch* signaling was required for MNB formation. In contrast, there was no evidence that *Su(H).VP16* misexpression resulted in additional MP5,6 progeny.

To further understand the spatial and temporal dynamics of midline *Notch* signaling, the expression of 2 reporters of *Su(H)* activity were examined: *P[12xSu(H)bs-lacZ]* (Go et al., 1998) and *Gbe-lacZ* (Furriols and Bray, 2001). Reporter expression was observed in AMG and PMG during stage 10, and was maintained through the end of embryogenesis, although levels were low by stage 17 (see Fig. S2.2I-L in the supplementary material). Expression was dependent on *Notch* signaling, since it was absent in the CNS midline cells in *Dl* mutant embryos (see Fig. S2.2M,N in the supplementary material). In addition to MG, expression of *P[12xSu(H)bs-lacZ]* was present in MP5,6, and the MNB (see Fig. S2.2I-K in the supplementary material) during stage 11 prior to their division. MP5 expresses a low level of *P[12xSu(H)bs-lacZ]*, MP6 an intermediate level, and the MNB higher levels. After division, the MP5,6 and MNB progeny express *P[12xSu(H)bs-lacZ]* at the same relative levels as the precursors (see Fig. S2.2L in the supplementary material). The neuronal expression is maintained throughout embryogenesis. No expression of the reporter was observed in MP1,3,4 or their progeny. The expression pattern of *Gbe-lacZ* is similar, although levels of *lacZ*

expression were reduced, compared to *P[12xSu(H)bs-lacZ]*. These data indicate that *Notch* signaling is occurring in MG, MP5, MP6, and the MNB during stages 10-11, consistent with genetic requirements for *Notch* signaling in these cells.

***numb* and *spdo* direct sibling neuronal fates in MP asymmetric divisions**

MPs either divide symmetrically (MP1) or asymmetrically (MP3-6). One possible mechanism for generating MP asymmetric cell fates is asymmetric localization of Numb in conjunction with *Notch* signaling. Expression of 37 MP1, MP3, and VUM-expressed genes and their axonal trajectories were examined in *numb* and *spdo* mutant and overexpression embryos, as well as in *Dl* mutants.

MP3 neurons

The expression of 19 H-cell and H-cell sib-expressed genes (see Table S2.1 in the supplementary material), which includes genes encoding transcription factors, signaling molecules, neurotransmitter biosynthetic enzymes, neurotransmitter receptors, and neuropeptide receptors, as well as axonal morphology based on *sim-Gal4 UAS-tau-GFP* visualization were assayed in *numb* and *spdo* mutant embryos. H-cell specific gene expression was absent in *numb* mutant embryos (Fig. 2.5A,B,F,G) and present in both MP3 neurons in *spdo* mutants (Fig. 2.5K,L). The opposite results were observed for H-cell sib-specific gene expression (Fig. 2.5C,D,H,I,M,N). Another indicator of neuronal cell fate is axonal trajectory. Consistent with gene expression results, *numb* mutants showed an absence of H-cell axons and the presence of H-cell sib axons, while *spdo* mutants showed the opposite phenotype (see Fig. S2.4A-C in the supplementary

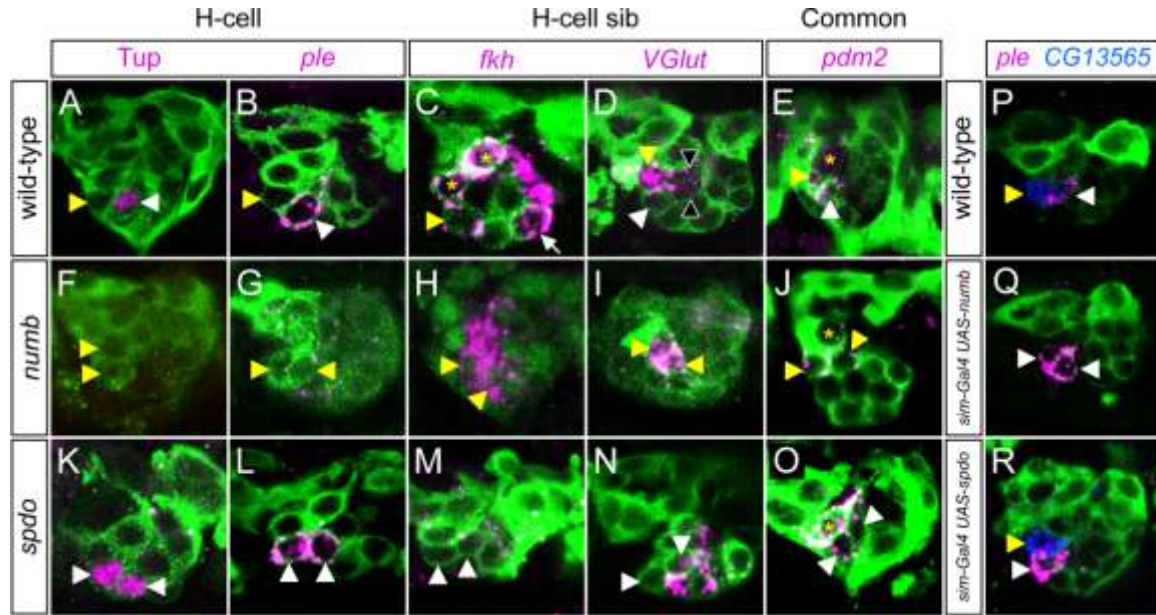


Figure 2.5. *numb* and *spdo* control MP3 neuronal cell fate. Confocal images of stages 14-15 embryos in sagittal view; (A-E, P) wild-type, (F-J) *numb*^{4/numb}, (K-O) *spdo*^{G104/spdo}^{G104}, (Q) *sim-Gal4 UAS-numb*, and (R) *sim-Gal4 UAS-spdo* embryos. All embryos had *sim-Gal4 UAS-tau-GFP* (green) in the background, except (H) that shows anti-Sim (green) staining. To identify the MP3 neurons, *numb* mutants were double-labeled with *Vesicular glutamate transporter* (*VGlut*) (not shown, except in I); *spdo* mutants were double-labeled with *ple* (not shown, except in L). In (A-O), white arrowheads denote cells expressing H-cell genes and yellow arrowheads indicate cells expressing H-cell sib genes. (A,B) In wild-type, Tailup (*Tup*) protein and *ple* were present in the H-cell, and absent in H-cell sib; (F, G) in *numb*, they were absent in both MP3 neurons; and (K,L) in *spdo*, they were present in both MP3 neurons. (C) In wild-type, *fork head* (*fkh*) was expressed in H-cell sib, the 2 MP1 neurons (*), and iVUMs (only 1 iVUM (arrow) is present in this focal plane). (H) In *numb*, *fkh* was expressed in 2 Sim⁺ MP3 neurons, and was absent (M) in *spdo* MP3 neurons. (D) In wild-type, *VGlut* was expressed in H-cell sib and at a lower level in mVUMs (black arrowheads), whereas (I) in *numb*, *VGlut* was expressed in 2 MP3 neurons and absent from VUM neurons. In contrast, (N) in *spdo*, the 2 MP3 neurons (arrowheads) lacked *VGlut* while it was present in all VUM neurons. (E) *pdm2* was expressed in the MP1 (*) neurons and both MP3 neurons in wild-type (only one MP1 neuron is present in this focal plane). The expression of *pdm2* was unaltered in (J) *numb* and (O) *spdo*. (P-R) Overexpression of *numb*, but not *spdo*, causes an MP3 cell fate change. The H-cell is marked by *ple* expression (magenta) and H-cell sib by *CG13565* expression (blue). (P) Wild-type expression of *ple* and *CG13565*. (Q) In *sim-Gal4 UAS-numb*, H-cell sib was transformed into an H-cell, as shown by the presence of 2 *ple*⁺ cells and the absence of *CG13565*-expressing cells. (R) *sim-Gal4 UAS-spdo* showed a wild-type pattern of gene expression with a single *ple*⁺ cell and a single *CG13565*⁺ cell.

material). These results were confirmed by analysis of H-cell gene expression in *numb* overexpression and *Dl* mutant embryos. When *numb* was overexpressed in all midline cells, there were 2 *pale* (*ple*)⁺ cells (H-cells), an absence of *CG13565*⁺ H-cell sib, and a duplication of H-cell axons (Fig. 2.5P,Q; see Fig. S2.4D in the supplementary material). Overexpression of *spdo* did not result in cell fate defects (Fig. 2.5R). Analysis of *Dl* mutant embryos revealed an expansion of neurons derived from the MP3. Only *ple*⁺ H-cells (Fig. 2.3G), and not *CG13565*⁺ H-cell sibs (data not shown), were present. Four genes, including *POU domain protein 2* (*pdm2*) (Fig. 2.5E,J,O), that are expressed in both cell types had no alterations in expression in either *numb* or *spdo* mutant embryos indicating that *numb* and *spdo* affect cell-type specific gene expression, but not expression present in both cells. Thus, assays of both neuronal morphology and gene expression indicated that *Notch* controls all of the divergent aspects of H-cell vs. H-cell sib cell fate.

VUM neurons

Expression of 21 VUM neuron-expressed genes (see Table S2.1 in the supplementary material) were examined in *numb* and *spdo* mutants. mVUM-specific gene expression was absent in *numb* mutant embryos and expanded in *spdo* mutants (Fig. 2.6A,B,F,G,K,L). In contrast, iVUM-specific gene expression was expanded in *numb* mutants and absent in *spdo* mutants (Fig. 2.6C,D,H,I,M,N). In *numb* mutant embryos, the mVUM axons were absent and the iVUM axons appeared thickened, suggesting a duplication; *spdo* mutants had the opposite phenotype (see Fig. S2.4E-G in the supplementary material). Embryos mutant for *Dl* showed an increase in *Tbh*⁺ mVUMs (Fig. 2.3H), but lacked *CG15236*⁺ iVUMs (data not shown). In *sim-Gal4 UAS-numb*

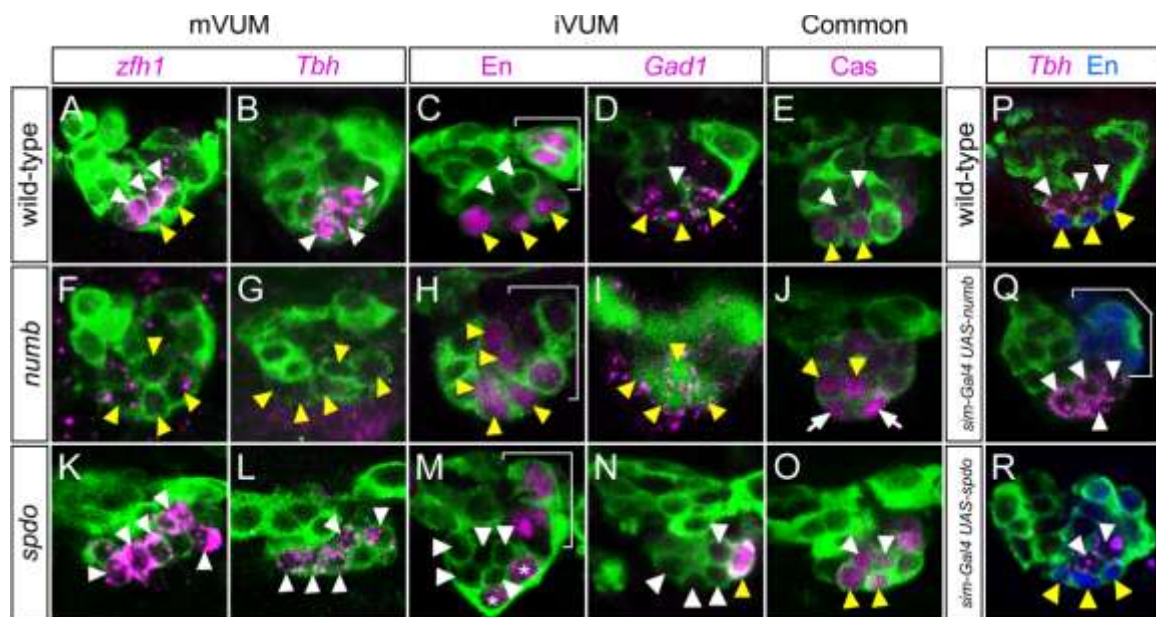


Figure 2.6. *numb* and *spdo* control VUM neuronal cell fate. Confocal images of stages 14-15 embryos in sagittal view; (A-E, P) wild-type, (F-J) *numb*⁴/*numb*⁴, (K-O) *spdo*^{G104}/*spdo*^{G104}, (Q) *sim-Gal4 UAS-numb*, and (R) *sim-Gal4 UAS-spdo* embryos. All embryos had *sim-Gal4 UAS-tau-GFP* (green) in the background except in (I) that shows anti-Sim (green) staining. To identify the VUM neurons, *numb* mutants were double-labeled with *En* (not shown, except in H); *spdo* mutants were double-labeled with *Tbh* (not shown, except in L). In (A-O), white arrowheads denote cells expressing mVUM genes and yellow arrowheads indicate cells expressing iVUM genes. (A) In wild-type, *Zn finger homeodomain 1* (*zfhl1*) was present in all 3 mVUMs and not in the iVUMs. (F) In *numb*, *zfhl1* expression was absent. (K) In *spdo*, *zfhl1* expression was expanded to 5 VUMs. (B) *Tbh* was expressed in 3 mVUMs in wild-type. (G) In *numb*, *Tbh* was not expressed. (L) In *spdo*, 5 VUMs expressed *Tbh*. (C) In wild-type, *En* was present in 3 iVUMs as well as other cell types, including the PMG (bracket). (H) In *numb*, *En* was present in 5 VUMs in addition to the PMG (bracket). (M) In *spdo*, *En* was absent in VUMs, but was present in the PMG (* and bracket). (D) *Glutamic acid decarboxylase 1* (*Gad1*) was expressed in 3 iVUMs in wild-type. (I) *Gad1* expression was expanded to 6 cells in *numb* (4 of the 6 VUMs can be seen in this focal plane). (N) In *spdo*, *Gad1* expression was present in only 1 VUM. (E) In wild-type, *Cas* was present in 2 iVUMs (iVUM4,5) and 2 mVUMs (mVUM4,5). In (J) *numb* and (O) *spdo* mutant embryos, *Cas* was also present in iVUM4,5 and mVUM4,5. (P-R) Overexpression of *numb* causes a VUM cell fate change. (P) Wild-type expression of *Tbh* (magenta) in 3 mVUMs and *En* protein (blue) in 3 iVUMs is shown. (Q) In *sim-Gal4 UAS-numb*, 6 ventral *Tbh*⁺ *En*⁻ mVUMs (2 of the 6 cells are absent in this focal plane) were present. *En* in PMG (bracket) was unaffected. (R) *sim-Gal4 UAS-spdo* had a wild-type *Tbh* and *En* pattern (2 of 3 *Tbh*⁺ mVUMs were present in this image).

was absent (Fig. 2.6P,Q). Further, mVUM but not iVUM axons were present (see Fig. S2.4H in the supplementary material). Analysis of *sim-Gal4 UAS-spdo* did not show alterations in VUM cell fate (Fig. 2.6R). Genes expressed in both iVUMs and mVUMs showed no alterations in expression in either *numb* or *spdo* mutants (Fig. 2.6E,J,O). In conclusion, *Notch* signaling, in conjunction with *numb* and *spdo*, controls iVUM/mVUM asymmetric cell fate choices.

MP1 neurons

The MP1 neurons are unique among MP progeny since they appear identical. Consequently, their development may be independent of *numb* and *spdo* regulation. This was addressed by examining mutant and overexpression embryos for 10 MP1-expressed genes (see Table S2.1 and Fig. S2.5 in the supplementary material). There were no alterations in MP1 neuronal gene expression in *numb*, *spdo*, or *sim-Gal4 UAS-numb* embryos (see Fig. S2.5 in the supplementary material), nor alterations in MP1 neuronal axonal trajectories (see Fig. S2.5A-E,G in the supplementary material). These data indicate that *numb* and *spdo* do not play a role in cell fate specification of the MP1 neurons. In *Dl* mutant embryos, we observe an expanded set of neurons that are Hunchback⁺ and Odd⁺. Since these 2 genes are uniquely expressed in the midline in only MP1s, this results suggests that *Notch* signaling is also not important for MP1 cell fate determination.

Numb and Spdo are localized asymmetrically during MP3-6 divisions

Analysis of the *numb* and *spdo* mutant phenotypes suggested that Numb and Spdo proteins would be asymmetrically localized during MP divisions. Our analysis showed that Numb localization was regulated in a cell-cycle dependent manner in MP3-6. Prior to mitosis, Numb was localized uniformly around the MP cell membrane (Fig. 2.7A), then enriched along the basolateral surface (Fig. 2.7B), and finally segregated into only the basal H-cell daughter (Fig. 2.7C,D). During mitosis (Fig. 2.7G-I), Spdo was localized around the MP membrane and in puncta throughout the cytoplasm. Immediately after division, Spdo was localized uniformly around the membrane of the Numb⁻ daughter cell at a low level (Fig. 2.7J), whereas Spdo membrane localization was reduced and was, instead, found in intracellular puncta (Fig. 2.7J) in the Numb⁺ cell. These puncta are likely intracellular vesicles (Hutterer and Knoblich, 2005; O'Connor-Giles and Skeath, 2003). In summary, MPs asymmetrically generate a Numb⁺ intracellular Spdo⁺ neuron (H-cell, mVUM) and a Numb⁻ cortical Spdo⁺ neuron (H-cell sib, iVUM).

What happens in the MP1, which generates 2 identical neurons? In this case, Numb was uniformly localized to the membrane prior to, during, and after MP1 cell division (Fig. 2.7E,F). Spdo was found at the membrane and in cytoplasmic puncta prior to and during division, and in both progeny after division (Fig. 2.7K,L). Although Numb is present in both MP1 neurons, other mechanisms must cause these cells to be refractory to *Notch* signaling, since *numb* mutants do not cause changes in MP1 gene expression.

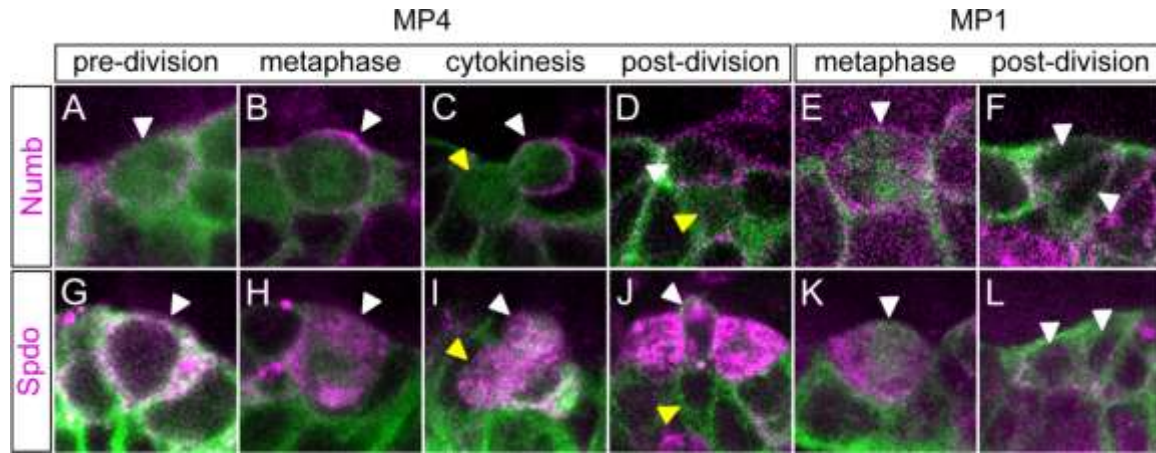


Figure 2.7. Numb and Spdo localization during MP divisions. Confocal images of MP1 and MP4 divisions in *sim-Gal4 UAS-tau-GFP* (green) stage 11 embryos stained with (A-F) anti-Numb (magenta) and (G-L) anti-Spdo (magenta). Sagittal views with anterior left and internal (basal) up. White arrowhead indicates: (A,B,G,H) MP4, (C,D) Numb⁺ VUM4 neuron, (I,J) basal VUM4 neuron with cytoplasmic punctate Spdo, (E,K) MP1, (F,L) MP1 neurons. Yellow arrowhead indicates: (C,D) Numb⁻ VUM4 neuron, (I) apical VUM4 neuron with cytoplasmic punctate Spdo, and (J) membranous Spdo VUM4 neuron.

Discussion

Patterns of stages 10-11 midline cell divisions and gene expression

The *Drosophila* MPs form at specific positions and divide in a reproducible sequence. Descriptive work in grasshopper indicated that MPs each undergo a single division (Bate and Grunewald, 1981; Goodman et al., 1981; Jia and Siegler, 2002). We propose that the *Drosophila* cells described here are homologous, and that MP4 gives rise to the anterior pair of VUMs (VUM4s), MP5 to the medial VUM pair (VUM5s), and MP6 to the posterior VUM pair (VUM6s). This picture of *Drosophila* stage 11 MP divisions runs counter to the prevailing *Drosophila* models, which proposed that the MP divisions occurred at stage 8 during the $\delta_{14}14$ synchronous cell division (Bossing and Technau, 1994; Jacobs, 2000; Klambt et al., 1991). Instead, we propose that the precursors dividing at stage 8 give rise to glial-glial, neuronal-neuronal, and mixed glial-neuronal lineages (Fig. 2.8). In general, this new model fits published *Dil* labeling data that noticed mixed clones (Bossing and Technau, 1994; Schmid et al., 1999), but had no compelling arguments for how they arose.

Notch signaling directs the formation of midline glia and inhibits neurogenesis

Dl mutants and *Su(H)* misexpression experiments indicated that: (1) *Notch* signaling was required for the formation of both AMG and PMG, (2) *Dl* was a ligand for N, and (3) transcriptional output involved *Su(H)* beginning at stage 10. Consistent with

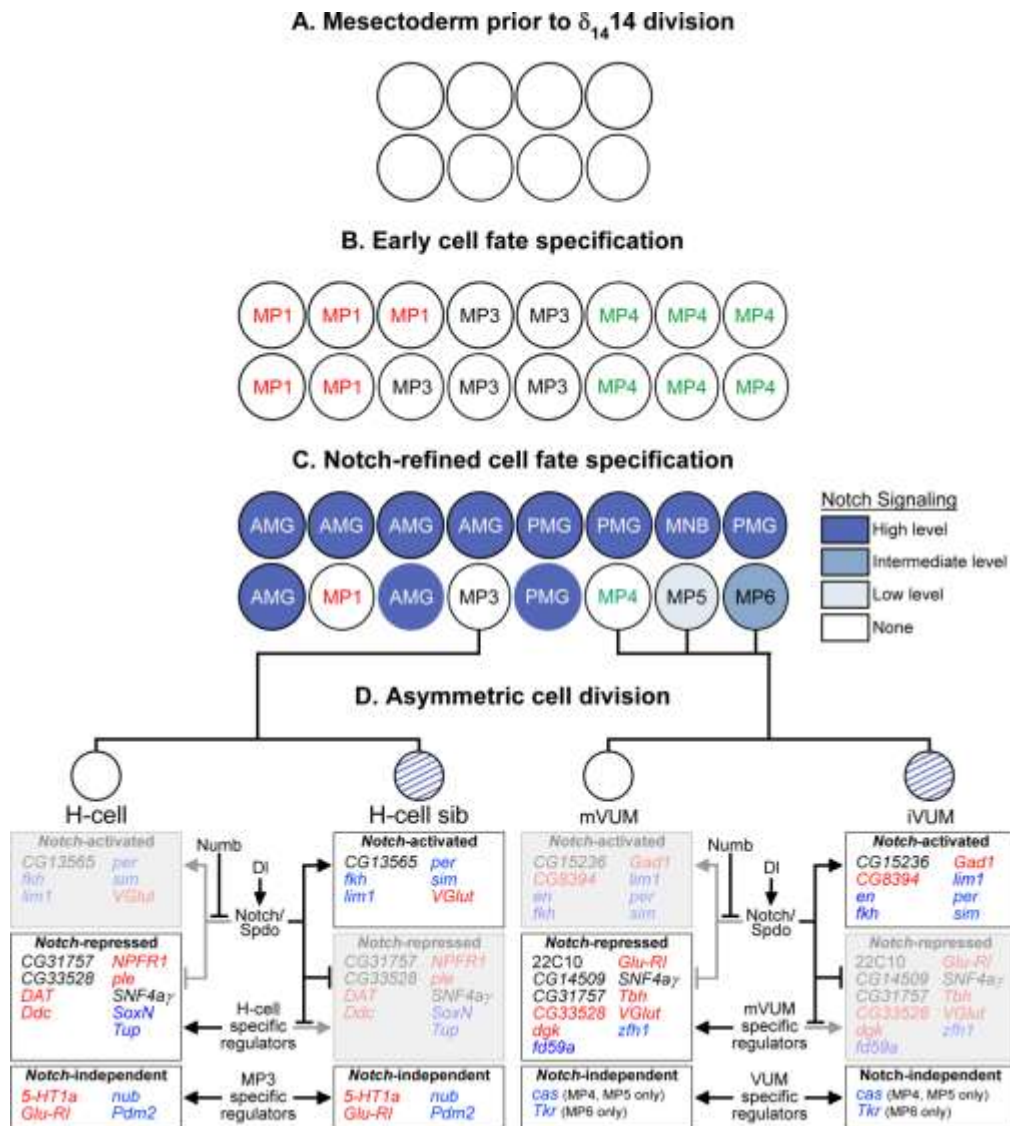


Figure 2.8. Model of *Notch* regulation of midline cell fate. (A) Mesectodermal cells meet at the ventral midline before the stage 8 δ_{14} division. Little is known regarding influences on midline cell development at this stage. (B) After the stage 8 division, but before *Notch* signaling, the 16 midline cells can be considered as 3 equivalent groups of cells: MP1s, MP3s, and MP4s. (C) After *Notch* signaling, the 16 cells acquire specific fates, and differ in their levels of *Notch* signaling as indicated by the expression of *Su(H)-lacZ* reporter. For simplicity midline cells are shown as paired cells along the anterior-posterior axis. The precise anterior-posterior and left-right positions of individual cells are unknown, except that AMG, MP1, MP3 tend to reside in the anterior half, and PMG, MP5, MP6, and MNB in the posterior half. Different shades of blue indicate relative levels of *Notch* signaling. (D) Asymmetric cell division. *Notch* signaling is required for MP3-6 asymmetric cell fates. *Notch* signaling is active (blue diagonals) in H-cell sib and iVUMs, and inhibited in H-cell and mVUMs. Assayed genes expressed in the MP3 and VUM lineages are shown below each neuron: dark indicates expression, and shaded indicates repression. Genes are categorized as either: *Notch*-activated, *Notch*-repressed, or *Notch*-independent. Functional classes of genes are color-coded: transcription factors (blue), neural function genes (red), and others (black).

these results, analysis of a N^{ts} mutant showed changes in expression of MG and neuronal enhancer trap lines, but lacked specific markers to fully characterize the phenotype (Menne and Klambt, 1994). Genes of the *Enhancer of split-Complex* [*E(spl)-C*] are commonly activated upon *Notch* signaling, where they act to repress transcription. We note that the *HLHm5 E(spl)-C* gene is expressed specifically in MG at stages 10-11 (Fig. 2.1), and other *E(spl)* members are also expressed in midline cells (Kearney et al., 2004; Wech et al., 1999). While *E(spl)-C* genes could be direct targets of Su(H) and repress midline neuronal gene expression, the *sim* gene could also be a direct target that activates MG gene expression, a role previously shown for *sim* (Ma et al., 2000; Wharton et al., 1994).

Dl mutants not only showed a complete lack of MG gene expression, but an expansion of anterior midline neurons (MP1,3,VUM4) and absence of posterior neurons (VUM5,6,MNB). Expanded MP1s were also noted in work describing the role of *Notch* signaling on MP2 development (Spana and Doe, 1996). Do the expanded *Dl* mutant MP1,3,4 neurons result from transformation of MG precursors to MPs, or from excessive division of a small number of MPs? Analysis of *Dl* mutants at stages 10-11 suggest that the midline cells at those stages consist of ~5 MP1s, ~5 MP3s, and ~6 MP4s. If each divided once, this would equal the observed 10 MP1 neurons, 10 H-cells, and 12 mVUM4s observed in *Dl* mutant embryos at later stages. In this model (Fig. 2.8), *Notch* signaling promotes MG development, while a single MP1,3,4 is selected from their respective MP fields. This midline role for *Notch* parallels functions of *Notch* in both *Drosophila* and vertebrates, in which it promote gliogenesis and inhibit neurogenesis (Gaiano et al., 2000; Morrison et al., 2000; Udolph et al., 2001).

***Notch* signaling promotes MNB and MP5,6 formation**

The progeny of MP5,6 and the MNB were absent in *Dl* mutants, indicating that *Notch* signaling is required for the formation of the MNB, as well as VUM5,6. This was a surprising result for the MNB, since in the ventral nerve cord, *Notch* signaling inhibits NB formation (Campos-Ortega, 1993), and does not affect NB number (Almeida and Bray, 2005). However, *Notch* signaling controls central brain NB number (Lee et al., 2006; Wang et al., 2007), indicating a parallel between the MNB and brain NBs. Thus, the MNB has a number of properties distinct from other nerve cord NBs, since it is not part of an neural/epidermal equivalence group, and does not utilize the Hunchback>Krüppel>Pdm>Cas cascade (Isshiki et al., 2001). Similarly, it is unusual that VUM5,6 required *Notch* function, since *Notch* signaling inhibited MP1,3, and MP4 neurogenesis. Consistent with the genetic data, *P[12xSu(H)bs-lacZ]* expression is restricted to the MP5,6 and MNB. This suggests that the different responses to *Notch* signaling may reflect anterior-posterior location. However, there may also be differences with respect to cell type, since *sim-Gal4 UAS-Su(H).VP16* embryos have expanded MNB-like cells, but the MP5,6 cells were not expanded. One potential model involves successive waves of signaling, either by *Notch* or other signaling molecules to generate the MNB, MP5, MP6, and MG, similar to development of the *Drosophila* retina (e.g. Doroquez and Rebay, 2006). Bossing and Brand have proposed an equivalence group in which *Notch* signaling would inhibit cells from becoming a MNB, and instead promote the VUM cell fate (Bossing and Brand, 2006). However, our *Dl* mutant and *Su(H).VP16* misexpression data indicate that *Notch* signaling promotes, not inhibits, MNB formation. Another view is that the presence of PMG is required for MP5,6 and MNB formation,

and the absence of PMG in *Dl* mutants also results in the loss of the neural precursors. In summary, alterations in *Notch* signaling have revealed a requirement in the formation of MP5,6 and the MNB, but additional work will be required for mechanistic insight.

***Notch* signaling and *numb* generate asymmetric midline neuronal cell fates**

Asymmetric neuronal cell fates of MP3-6 progeny are determined by Numb and Spdo asymmetric localization in one of the two daughter cells (Fig. 2.8), similar to asymmetric cell fate determination of the non-midline MP2 cell and GMCs (O'Connor-Giles and Skeath, 2003; Spana and Doe, 1996; Spana et al., 1995). In H-cell sib and the iVUMs, Numb is absent, and *Notch* signaling, in combination with cortical Spdo, activates H-cell sib and iVUM-specific gene expression and represses H-cell and mVUM gene expression. Genes that are expressed in both siblings are not dependent on *Notch* signaling. The MP1 progeny are identical by gene expression and morphological criteria. Numb is present in both MP1 neurons, but the significance of this is unclear, since MP1 gene expression and morphology were unaffected in *numb* mutants, nor were defects observed in *Dl* mutants. This suggests that *Notch* signaling does not influence MP1 development.

Another difference between MP1 and the other MPs is that MP1 divides perpendicular to the apical-basal axis, while, MP3-6 rotate their spindles during cell division along the apical-basal axis. The basal cell is always the Numb⁺ cell, which is the *Notch*-independent H-cell or mVUM. The orientations of the divisions may aid in positioning the cells towards their final locations in the CNS. In the mature CNS, the iVUMs are apical to the mVUMs, and during MP divisions, the iVUM is the more apical

sibling. In the case of the MP1s, it may be important that both cells are in the same position along the basal/apical axis.

Previously, the development of grasshopper MP3 was examined experimentally by Kuwada and Goodman (Kuwada and Goodman, 1985). Their data suggested a model in which the two MP3 neurons are born equivalent with an H-cell sib dominant fate, and within 5 hours, signaling between the two cells generates different fates. These data appear inconsistent with the *Drosophila* results, since the *Drosophila* MP3 neurons asymmetrically localize Numb and are inherently different at birth. However, it is important to recognize that the grasshopper and *Drosophila* results are based on different types of experiments (genetic vs. experimental ablation), and the grasshopper data may be revealing additional levels of regulation or different mechanisms for generating cell fates.

Towards a molecular basis for neuronal and glial cell fate determination

Nearly 300 genes are known to be expressed in the developing *Drosophila* CNS midline cells, and many have been mapped at the single-cell level by confocal microscopy. The work described here examined the role of *Notch* signaling on the expression of 37 MG and neuronal-expressed genes (Fig. 2.8). Molecular analysis can now be carried-out on these genes to identify direct targets of *Notch* action. Additional studies are also beginning to identify transcription factors that regulate the *Notch*-independent neuronal pathways (unpublished). The large number of identified genes, in combination with the utility of *Drosophila* molecular and genetic tools, will facilitate a

detailed understanding of the regulatory pathways controlling midline neurogenesis and gliogenesis.

Acknowledgements

The authors would like to thank Amaris Guardiola, Catarina Homem, Joe Kearney, Tony Perdue, Nasser Rusan, and Ferrin Wheeler for valuable advice and assistance, Stephanie Freer for her investigation of larval phenotypes, and Joe Pearson for helpful comments on the manuscript. We are grateful to Spyros Artavanis-Tsakonas, Nipam Patel, and Francois Schweisguth for contributing antibodies and fly stocks, and particularly appreciative of the endless advice and supplies from Jim Skeath and Beth Wilson. We also would like to thank the Developmental Studies Hybridoma Bank for monoclonal antibodies and the Bloomington *Drosophila* stock center for fly stocks. This work was supported by NIH grant R37 RD25251 to STC, an NRSA postdoctoral fellowship to SRW, and UNC Developmental Biology NIH training grant support to SBS.

Supplemental Figures

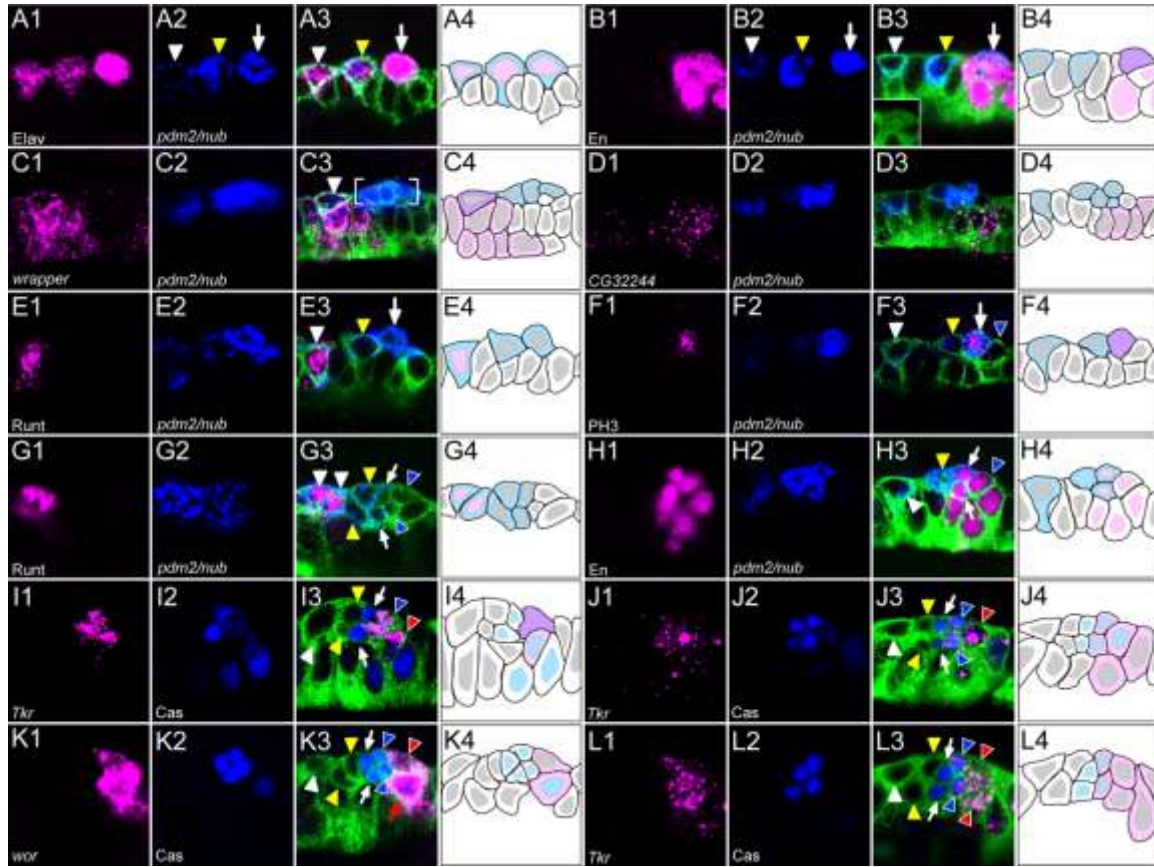


Figure S2.1. Midline precursor divisions occur during stage 11. (A-L) Representative images that document construction of the stages 10-11 molecular maps. Sagittal views of single segments of *sim-Gal4 UAS-tau-GFP* embryos; all images were from stage 11, except (A,B,E,F), which were at stage 10. Column 1 (magenta): midline cell-type specific probe; (A-H) Column 2 (blue): combined *pdm2* and *nubbin* (*nub*) expression; (I-L) Column 2: anti-Cas immunostaining; Column 3: merge image showing all CNS midline cells (green) revealed by anti-GFP staining; Column 4: schematic of expression. Pink corresponds to magenta gene expression, blue corresponds to blue gene expression, and purple indicates co-localization. Colored outlines represent cytoplasm staining, colored nuclei indicate nuclear staining, and absence of a nucleus indicates that the cell is undergoing division. (A) The undivided MP1,3,4 can be identified at late stage 10. The MP1 (white arrowhead), MP3 (yellow arrowhead) and MP4 (white arrow) are Embryonic lethal, abnormal vision (*Elav*)⁺ *pdm2/nub*⁺. (B) The MP4 (white arrow) can be distinguished from the MP3 (yellow arrowhead), and MP1 (white arrowhead) based on the presence of *En*. In this late stage 10 segment, MP4 can be seen dividing, based on dispersed localization of tau-GFP, while MP3 and MP1 are yet to divide. (C-D) 2 populations of MG can be distinguished based on gene expression. (C) During stage 11, *wrapper* was present in the AMG and the MP1 (white arrowhead), but not other MPs and their progeny (bracket). MP1 *wrapper* expression diminished by late stage 11 while *wrapper* expanded to both AMG and PMG. (D) *CG32244* was expressed in the PMG at stage 11. (E) The MP1 (white arrowhead) could be distinguished from the MP3 (yellow arrowhead) and the MP4 (white arrow) at late stage 10 based on *Runt* localization in MP1. (F) Anti-PH3 staining of a late stage 10 embryo showed a dividing MP4 (white arrow). The

MP1 (white arrowhead), MP3 (yellow arrowhead) and MP5 (blue arrowhead) had not yet divided. **(G)** The MP1 neurons (white arrowheads) could be distinguished by expression of Runt. The VUM5 neurons were *pdm2/nub*⁻ (blue arrowheads), which distinguished them from the MP1, MP3 (yellow arrowheads), and VUM4 (arrows) neurons, which were *pdm2/nub*⁺. MP6 had not yet divided. **(H)** Segment showing the temporal sequence of MP cell division. The MP4 divided to give rise to 2 VUM4 neurons (white arrows) that were *En*⁺ *pdm2/nub*⁺. The MP3 (yellow arrowhead; *En*⁻ *pdm2/nub*⁺) was beginning to divide, whereas the MP1 (white arrowhead) and MP5 (blue arrowhead; *En*⁺ *pdm2/nub*⁻) had not yet divided. **(I)** Segment in which the MP3 (yellow arrowheads) and MP4 (arrows) cells have divided, and MP5 (blue arrowhead) has initiated division. MP5 (*Tkr*⁺ *Cas*^{hi}) could be distinguished from the VUM4 neurons (*Tkr*⁻ *Cas*^{lo}) based on *Tkr* expression. *Cas* was transiently present at low levels in the MP6 (red arrowhead; *Tkr*⁺ *Cas*^{lo}) before the MP5 divided, and was absent after MP5 division. **(J)** MP5 (blue arrowheads; *Tkr*⁺ *Cas*^{hi}) division preceded MP1 (white arrowhead) and MP6 (red arrowhead; *Tkr*⁺ *Cas*^{lo}) divisions. The VUM4 neurons (white arrows) were *Tkr*⁻ *Cas*^{lo} and the MP3 neurons (yellow arrowhead) were *Tkr*⁻ *Cas*⁻. **(K)** The MNB (red arrow; *wor*⁺ *Cas*^{lo}) was identified prior to its delamination and MP6 (red arrowhead; *wor*⁺ *Cas*⁻) division. The MP3 (yellow arrowheads), VUM4 (white arrows), and VUM5 (blue arrowheads) neurons are shown, post-division. Only one of the 2 MP1 neurons (white arrowhead) is apparent in this focal plane. **(L)** All MPs have divided. Only one MP1 neuron (white arrowhead) is visible in this projection, and the MNB is also absent from this image. The MP3 (yellow arrowheads; *Tkr*⁻ *Cas*⁻), VUM4 (white arrows; *Tkr*⁻ *Cas*^{lo}), VUM5 (blue arrowheads; *Tkr*⁺ *Cas*^{hi}), and VUM6 (red arrowheads; *Tkr*⁺ *Cas*⁻) neurons are shown. Note that *Cas* was absent from the MP6 neurons.

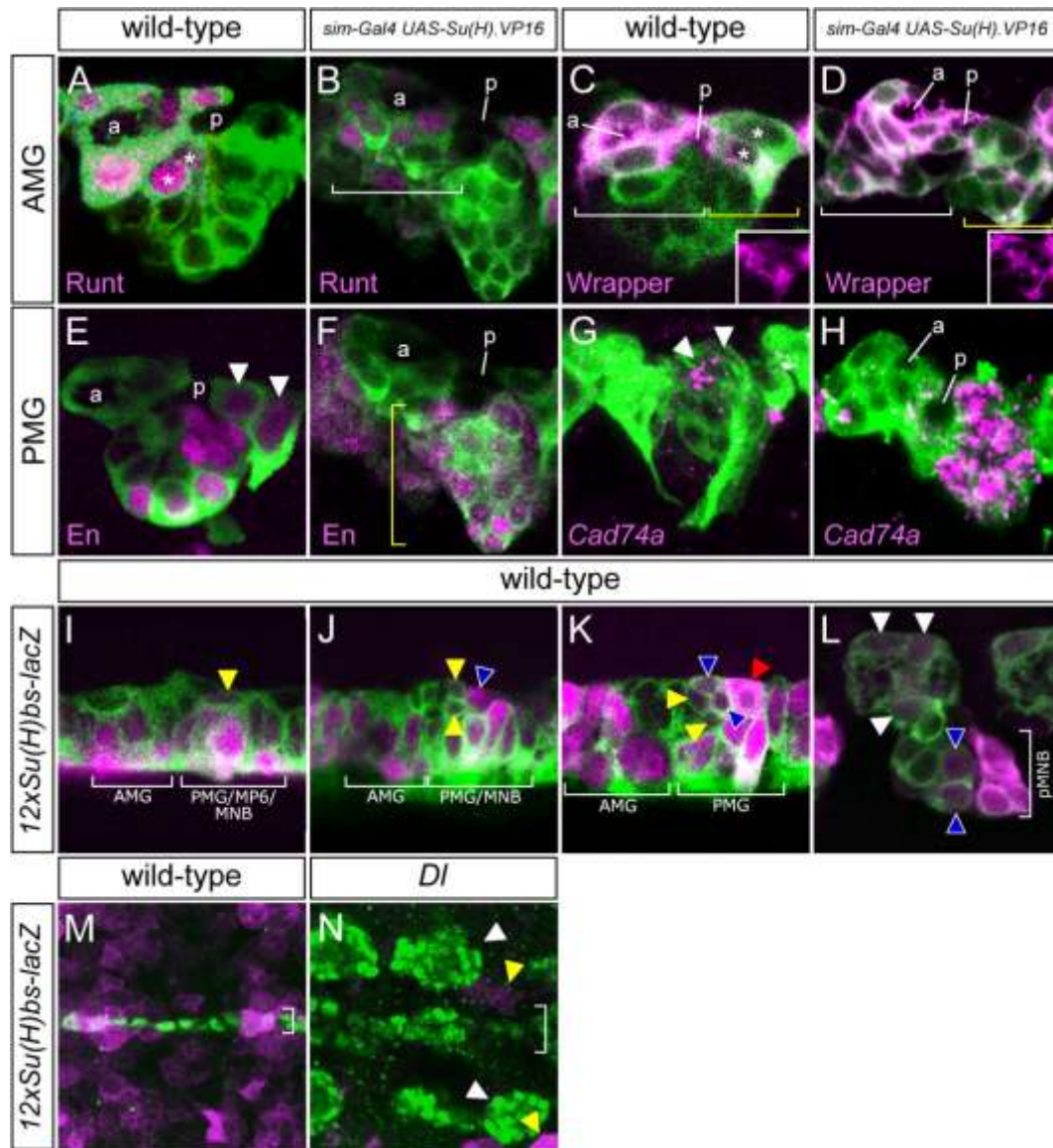


Figure S2.2. Notch signaling is active in midline glia, MPs, and neurons. (A,L) Sagittal views of single segments of stage 14 *sim-Gal4 UAS-tau-GFP* embryos are shown as confocal images. Midline cells are visualized by anti-GFP staining (green). (A,C,E,G) wild-type; (B,D,F,H) *sim-Gal4 UAS-Su(H).VP16* misexpression embryos. (A) Immunostaining showed Runt (magenta) in wild-type AMG and MP1s (*). The AMG completely surround the anterior commissure (a) and partially surround the posterior commissure (p). (B) Misexpression of *Su(H).VP16* resulted in excess anterior Runt⁺ cells (bracket). (C) Wild-type embryos showed high levels of Wrapper (magenta) in AMG (anterior cells) and lower levels in PMG (*). Brackets denote relative positions of AMG (white) and PMG (yellow). Inset corresponds to the yellow bracketed area and shows Wrapper staining at low levels in PMG. (D) In *sim-Gal4 UAS-Su(H).VP16*, all midline cells were Wrapper⁺ with anterior cells Wrapper^{hi}, indicative of AMG (white bracket), and posterior cells Wrapper^{lo} (PMG, yellow bracket) indicative of PMG. Inset corresponds to yellow bracketed area and shows Wrapper staining at low levels in all cells in this region. (E) In wild-type, En (magenta) was present in PMG (arrowheads), as well as MNB, MNB progeny, and iVUMs. (F) In *sim-Gal4 UAS-Su(H).VP16*, the number of En⁺ PMG was increased in the

posterior region (yellow bracket). **(G)** In situ hybridization showed *Cad74a* expression (magenta) exclusively in wild-type PMG (arrowheads), and **(H)** the number of *Cad74a*⁺ cells was expanded in *sim-Gal4 UAS-Su(H).VP16*. **(I)** During stage 11, *P[12xSu(H)bs-lacZ]* was expressed at high levels in AMG, and a posterior cell cluster containing MP6, the MNB, and PMG. MP5 (yellow arrowhead) expressed *P[12xSu(H)bs-lacZ]* at low levels. **(J)** After the MP5 division, low-level *P[12xSu(H)bs-lacZ]* expression was present in the VUM5 neurons (yellow arrowheads) and at a high level in MP6 (blue arrowhead). **(K)** After the MP6 division, *P[12xSu(H)bs-lacZ]* expression was present at low levels in the VUM5s (yellow arrowheads), medium levels in VUM6s (blue arrowheads), and high levels in the MNB (red arrowhead). **(L)** At stage 17, *P[12xSu(H)bs-lacZ]* was expressed in the MG (white arrowheads), the MNB and its progeny (pMNB, bracket), VUM5s (absent in this focal plane), and VUM6s (blue arrowheads). **(M,N)** Ventral views of stage 14 *P[12xSu(H)bs-lacZ]* **(M)** wild-type and **(N)** *Dl* embryos stained with anti-Sim (green) and anti-LacZ (magenta). The *Dl* mutant showed that midline and CNS expression of *P[12xSu(H)bs-lacZ]* was absent, indicating that *P[12xSu(H)bs-lacZ]* is dependent on *N* signaling. Expanded Sim⁺ muscle precursor cells (white arrowheads) and a few *P[12xSu(H)bs-lacZ]*⁺ cells (yellow arrowheads) with residual Dl protein (not shown) were present.

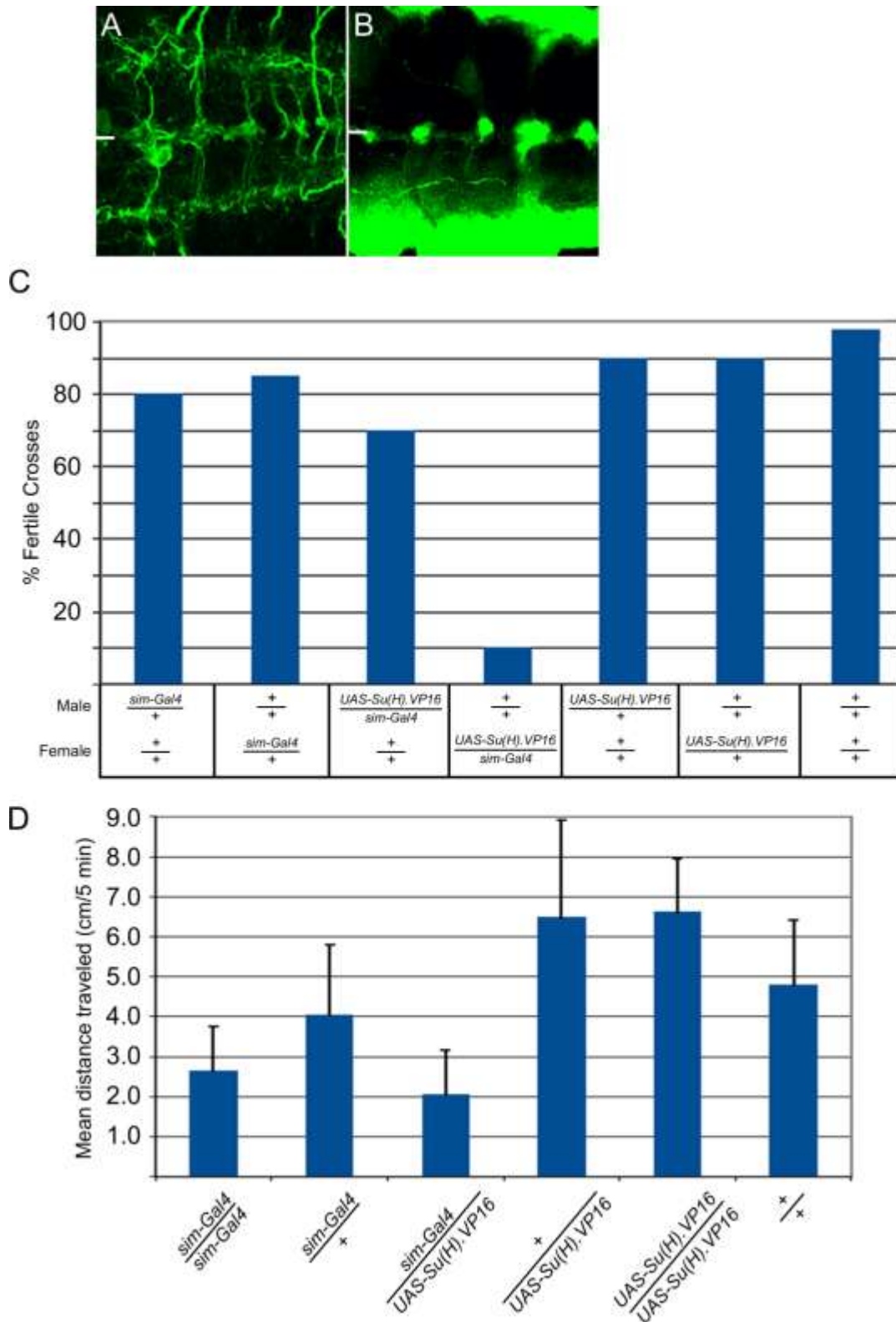


Figure S2.3. *sim-Gal4/UAS-Su(H).VP16* females have reduced fertility

Figure S2.3. *sim-Gal4/UAS-Su(H).VP16* females have reduced fertility. (A) Ventral view of a *sim-Gal4 UAS-tau-GFP* 3rd instar larval nerve cord showing midline neuronal axons visualized by anti-GFP staining. Horizontal bar indicates the midline. (B) In *sim-Gal4 UAS-tau-GFP UAS-Su(H).VP16* larvae, there is a severe reduction in the number of midline neuronal axons, consistent with the absence of midline neurons observed in the embryo (Fig. 3K-M). The effect is highly penetrant, and >90% of midline cells were absent. This allowed a worst-case test of the physiological and behavioral consequences of depleting all midline neurons. (C) Fertility was measured by scoring 20 crosses of each genotype for: % vials with progeny. Individual flies were crossed to 3 *w* flies. The majority of the *sim-Gal4 UAS-Su(H).VP16* embryos formed normal-appearing adults. Females showed low fertility, while males were relatively fertile. Previously, it was shown that octopaminergic/glutamatergic neurons residing along the CNS midline innervate the female genitalia and control oviduct contraction (Hardie et al., 2007; Monastirioti, 2003; Rodriguez-Valentin et al., 2006). These are likely mVUMs, and their loss would explain the female sterility. (D) The mean distance traveled (cm) in 5 minutes by larvae was measured for 6 genotypes. Wandering 3rd instar larvae were removed from the walls of food containers and placed on a grape juice agar plate for 1 minute. Larvae were then transferred to a clean grape juice agar plate and allowed to move freely for 5 minutes. The indentations in the grape juice agar plate caused by moving larvae were scanned on a flatbed scanner, and analyzed for distance traveled using ImageJ software. The larval path was traced using the freehand lines tool and the distance travelled expressed in cm. For each genotype, distances traveled for 16-25 individual larvae were averaged and the standard deviation (error bars) calculated. The number and identity of midline neurons and glia were wild-type in each of the genotypes examined with the exception of *sim-Gal4/UAS-Su(H).VP16*. The mean distance traveled by *sim-Gal4/UAS-Su(H).VP16* larvae was reduced compared to the controls: *sim-Gal4/+* (2X reduction) and *UAS-Su(H).VP16/+* (3X reduction). The larval locomotory defects resemble abnormalities associated with octopaminergic mVUM control of larval body wall muscles and movement (Nishikawa and Kidokoro, 1999; Saraswati et al., 2004). Thus, the results with *sim-Gal4 UAS-Su(H).VP16* animals were validated by other studies, and suggest that the remaining neurons, while likely important, do not have dramatic effects on behavior or physiology. Use of a *sim* temperature sensitive strain previously showed that reduction in *sim* function in the late embryo resulted in adult female sterility and defects in locomotion (Pielage et al., 2002). However, in these flies, it is unknown whether midline neurons, including mVUMs, are present and functional, and thus, contribute to these phenotypes. In contrast, defects in *sim^{ts}* male and female genitalia, gonadogenesis, and male courtship behavior could lead to sterility, and the locomotory defects could be due to defects in the central brain.

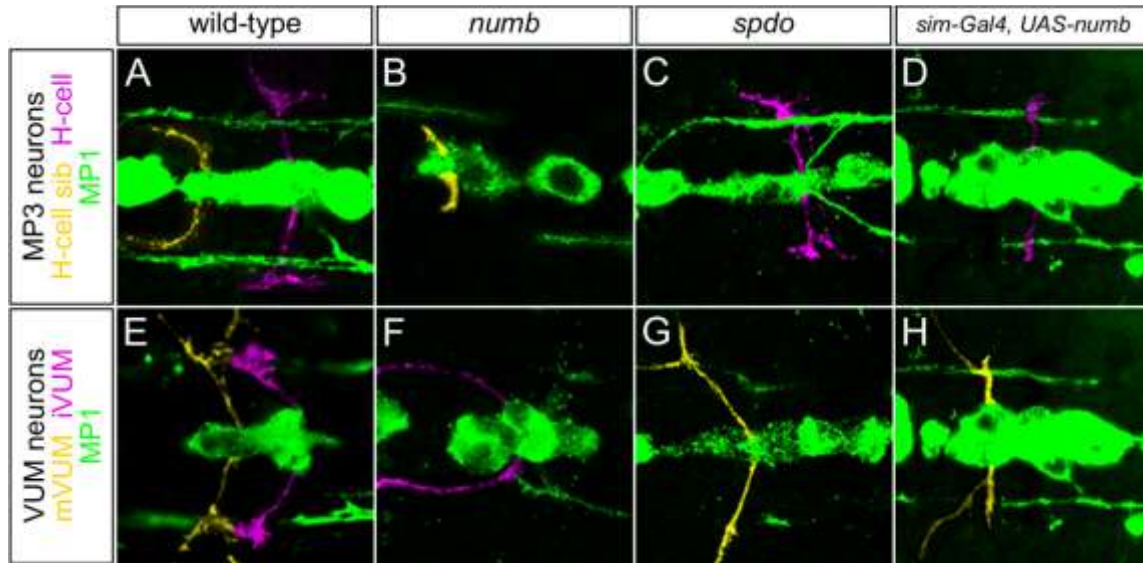


Figure S2.4. *numb* and *spdo* regulate axonal trajectory. Composite confocal images of single segments from stage 15 (**A,E**) wild-type, (**B,F**) *numb*⁴/*numb*⁴, (**C,G**) *spdo*^{G104}/*spdo*^{G104}, and (**D,H**) *sim-Gal4 UAS-numb* embryos in ventral view with anterior to the left. All embryos had *sim-Gal4 UAS-tau-GFP* (green) in the background to visualize all midline cells and their axons. The midline axons can be discerned based on their characteristic positions along the anterior-posterior and dorsal-ventral axes. For clarity, non-relevant axons have been subtracted and relevant axons have been pseudocolored. MP1 axons were not significantly affected in any of the mutant embryos. (**A-D**) MP3 neurons. H-cell sib (yellow), H-cell (magenta), MP1 neurons (green). (**A**) In wild-type, the H-cell sib axon bifurcated in the anterior commissure and sent projections on both sides of the midline in an anterior direction. The H-cell axon bifurcated in the posterior commissure and sent projections into the longitudinal tract lateral to the MP1 axons. The MP1 axons emanated from the lateral face of the cell body and extended posteriorly to the longitudinal tract where they bifurcated and sent axons in both anterior and posterior directions. (**B**) In *numb*, the H-cell sib axons were present and appeared thickened while the H-cell axons were absent. (**C**) In *spdo*, the H-cell sib axon was absent while the H-cell axons were duplicated and characteristically extended past the MP1 axons. (**D**) Overexpression of *numb* in all midline cells resulted in the absence of H-cell sib axons, but possessed thickened H-cell axons similar to the *spdo* mutant phenotype. (**E-H**) VUM neurons. mVUMs (yellow), iVUMs (magenta), MP1 neurons (green). (**E**) In wild-type, the mVUM axons bifurcated in the anterior commissure and projected along the segmental and intersegmental nerves into the muscle fields. The iVUM axons bifurcated in the posterior commissure and extended projections anteriorly within the longitudinal tracts. (**F**) In *numb*, the iVUM axons were present while the mVUM axons were absent. (**G**) In *spdo*, the iVUM axons were absent while the mVUM axons were present and appeared thicker. (**H**) *numb* overexpression resulted in the presence of thickened mVUM axons and the absence of iVUM axons.

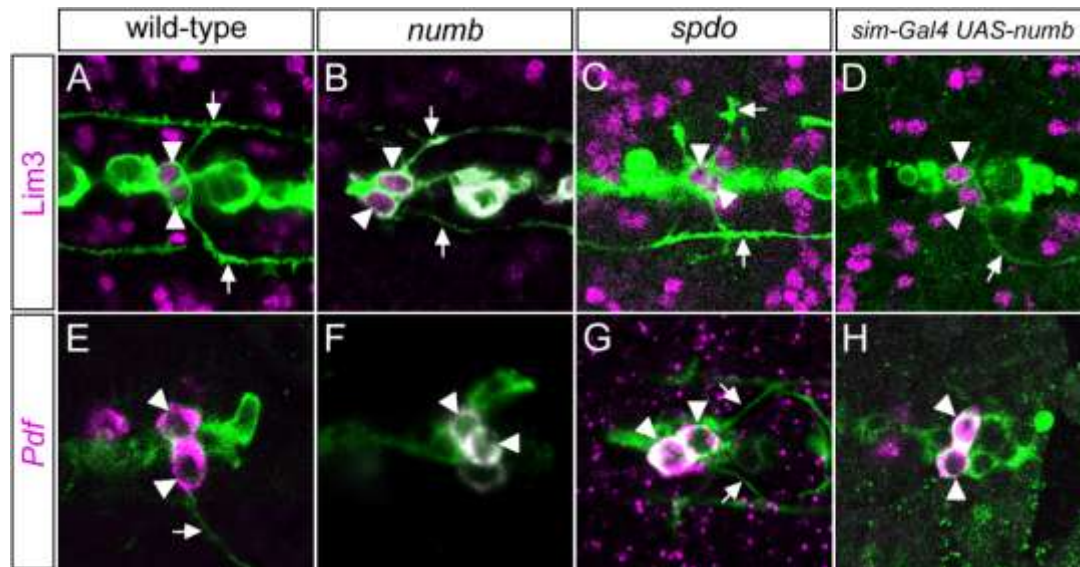


Figure S2.5. *numb* and *spdo* are not required for MP1 neuronal fate. Confocal images of single midline segments in stage 14 *sim-Gal4 UAS-tau-GFP* embryos. Anterior is left and all views are ventral. (**A,E**) Wild-type, (**B,F**) *numb*⁴/*numb*⁴, (**C,G**) *spdo*^{G104}/*spdo*^{G104}, (**D,H**) *sim-Gal4 UAS-numb*. (**A-D**) Anti-Lim3 immunostaining (magenta) shows prominent localization to the MP1 neurons (arrowheads) in (**A**) wild-type, (**B**) *numb*, (**C**) *spdo*, and (**D**) *sim-Gal4 UAS-numb* embryos. (**E-H**) *Pigment-dispersing factor* (*Pdf*) (magenta) is expressed in both MP1 neurons (arrowheads) in (**E**) wild-type, (**F**) *numb*, (**G**) *spdo*, and (**H**) *sim-Gal4 UAS-numb* embryos. MP1 axonal trajectories (arrows) were not altered in mutant or overexpression backgrounds.

Table S2.1. Midline genes

Name	Function	Name	Function
MP1		All MP3	
<i>5-HT1A</i>	Serotonin receptor	<i>5-HT1A</i>	Serotonin receptor
<i>CG31757</i>	Phosphodiesterase	<i>Glu-RI</i>	Glutamate-gated ion channel
<i>exex</i>	Lim homeobox transcription factor	<i>nub</i>	POU homeobox transcription factor
<i>fkf</i>	Fork head transcription factor	<i>pdm2</i>	POU homeobox transcription factor
<i>Glu-RI</i>	Glutamate-gated ion channel	mVUM	
<i>hb</i>	Zinc finger transcription factor	<i>futsch</i>	Microtubule binding
<i>Lim3</i>	Lim homeobox transcription factor	<i>CG14509</i>	Unknown
<i>nub</i>	POU homeobox transcription factor	<i>CG31757</i>	Phosphodiesterase
<i>Pdf</i>	Neuropeptide	<i>CG33528</i>	Monoamine transporter
<i>pdm2</i>	POU homeobox transcription factor	<i>dgk</i>	Diacylglycerol kinase
H-cell		<i>fd59a</i>	Fork head transcription factor
<i>CG31757</i>	Phosphodiesterase	<i>Glu-RI</i>	Glutamate-gated ion channel
<i>CG33528</i>	Monoamine transporter	<i>SNF4aγ</i>	Receptor serine/threonine kinase
<i>DAT</i>	Dopamine transporter	<i>Tbh</i>	Octopamine biosynthesis
<i>Ddc</i>	Dopamine biosynthesis	<i>VGlut</i>	Vesicular glutamate transporter
<i>NPFR1</i>	Neuropeptide receptor	<i>zfh1</i>	Zinc finger transcription factor
<i>ple</i>	Tyrosine 3-monooxygenase	iVUM	
<i>SNF4aγ</i>	Receptor serine/threonine kinase	<i>CG15236</i>	Unknown
<i>SoxN</i>	HMG transcription factor	<i>CG8394</i>	GABA vesicular transporter
<i>tup</i>	Lim homeobox transcription factor	<i>en</i>	Homeobox transcription factor
H-cell sib		<i>fkf</i>	Fork head transcription factor
<i>CG13565</i>	Unknown	<i>Gad1</i>	Glutamate decarboxylase
<i>fkf</i>	Fork head transcription factor	<i>Lim1</i>	Lim homeobox transcription factor
<i>Lim1</i>	Lim homeobox transcription factor	<i>per</i>	PAS transcription factor
<i>per</i>	PAS transcription factor	<i>sim</i>	bHLH-PAS transcription factor
<i>sim</i>	bHLH-PAS transcription factor	All VUM4,5	
<i>VGlut</i>	Vesicular glutamate transporter	<i>cas</i>	Zinc finger transcription factor
		All VUM6	
		<i>Tkr</i>	BTB/POZ domain

Supplemental Movie Legends

Movie 2.1. Time-lapse imaging of MP and MNB divisions. Live *sim-Gal4 UAS-tau-GFP* embryo imaged for GFP fluorescence for 144 minutes during stages 10-11. Sagittal view of one segment is shown (brackets), with anterior (Ant) to the left and interior (Int) at top. The movie pauses periodically to indicate the appearance of MPs (arrowheads) and their neuronal progeny (arrows), followed by the stem cell division of the MNB (arrowhead) into an MNB and GMC (arrow). Movie 2.1 can be found at: <http://dev.biologists.org/content/suppl/2008/08/18/135.18.3071.DC1/022343-movie1.mov>

Movie 2.2. Time-lapse imaging of *Dl* mutant embryos. Sagittal view of a 80 minutes excerpt from a stage 11 *sim-Gal4 UAS-tau-GFP; Dl³/Dl³* embryo that was imaged for GFP fluorescence for 127 minutes total. Anterior (Ant) is to the left and interior (Int) at top. The midline cells are pushed inward by the hypertrophied lateral CNS. Note near-simultaneous divisions occurring in neighboring cells. Movie 2.2 can be found at: <http://dev.biologists.org/content/suppl/2008/08/18/135.18.3071.DC1/022343-movie2.mov>

References

- Abramoff, M. D., Magelhaes, P. J. and Ram, S. J.** (2004). Image Processing with ImageJ. *Biophotonics International* **11**, 36-42.
- Almeida, M. S. and Bray, S. J.** (2005). Regulation of post-embryonic neuroblasts by *Drosophila* Grainyhead. *Mech. Dev.* **122**, 1282-93.
- Bate, C. M. and Grunewald, E. B.** (1981). Embryogenesis of an insect nervous system II: a second class of neuron precursor cells and the origin of the intersegmental connectives. *J. Embryol. Exp. Morphol.* **61**, 317-30.
- Bossing, T. and Brand, A. H.** (2006). Determination of cell fate along the anteroposterior axis of the *Drosophila* ventral midline. *Development* **133**, 1001-12.
- Bossing, T. and Technau, G. M.** (1994). The fate of the CNS midline progenitors in *Drosophila* as revealed by a new method for single cell labelling. *Development* **120**, 1895-906.
- Brand, A.** (1995). GFP in *Drosophila*. *Trends Genet.* **11**, 324-5.
- Broihier, H. T. and Skeath, J. B.** (2002). *Drosophila* homeodomain protein dHb9 directs neuronal fate via crossrepressive and cell-nonautonomous mechanisms. *Neuron* **35**, 39-50.
- Campos-Ortega, J. A.** (1993). Early neurogenesis in *Drosophila melanogaster*. In *The Development of Drosophila melanogaster*, vol. II (ed. M. Bate and A. M. Arias), pp. 1091-1129. Cold Spring Harbor, NY: Cold Spring Harbor Laboratory Press.
- Crews, S. T.** (2003). *Drosophila* bHLH-PAS developmental regulatory proteins. In *PAS proteins: regulators and sensors of development and physiology*, (ed. S. T. Crews): Kluwer.
- Doroquez, D. B. and Rebay, I.** (2006). Signal integration during development: mechanisms of EGFR and Notch pathway function and cross-talk. *Crit. Rev. Biochem. Mol. Biol.* **41**, 339-85.
- Foe, V. E.** (1989). Mitotic domains reveal early commitment of cells in *Drosophila* embryos. *Development* **107**, 1-22.
- Furriols, M. and Bray, S.** (2001). A model Notch response element detects Suppressor of Hairless-dependent molecular switch. *Curr. Biol.* **11**, 60-4.
- Gaiano, N., Nye, J. S. and Fishell, G.** (2000). Radial glial identity is promoted by Notch1 signaling in the murine forebrain. *Neuron* **26**, 395-404.

- Go, M. J., Eastman, D. S. and Artavanis-Tsakonas, S.** (1998). Cell proliferation control by Notch signaling in *Drosophila* development. *Development* **125**, 2031-40.
- Goodman, C. S., Bate, M. and Spitzer, N. C.** (1981). Embryonic development of identified neurons: origin and transformation of the H cell. *J. Neurosci.* **1**, 94-102.
- Hardie, S. L., Zhang, J. X. and Hirsh, J.** (2007). Trace amines differentially regulate adult locomotor activity, cocaine sensitivity, and female fertility in *Drosophila melanogaster*. *Dev. Neurobiol.* **67**, 1396-405.
- Hutterer, A. and Knoblich, J. A.** (2005). Numb and alpha-Adaptin regulate Sanpodo endocytosis to specify cell fate in *Drosophila* external sensory organs. *EMBO Rep.* **6**, 836-42.
- Isshiki, T., Pearson, B., Holbrook, S. and Doe, C. Q.** (2001). *Drosophila* neuroblasts sequentially express transcription factors which specify the temporal identity of their neuronal progeny. *Cell* **106**, 511-21.
- Jacobs, J. R.** (2000). The midline glia of *Drosophila*: a molecular genetic model for the developmental functions of glia. *Prog. Neurobiol.* **62**, 475-508.
- Jia, X. X. and Siegler, M. V.** (2002). Midline lineages in grasshopper produce neuronal siblings with asymmetric expression of Engrailed. *Development* **129**, 5181-93.
- Kambadur, R., Koizumi, K., Stivers, C., Nagle, J., Poole, S. J. and Odenwald, W. F.** (1998). Regulation of POU genes by castor and hunchback establishes layered compartments in the *Drosophila* CNS. *Genes Dev.* **12**, 246-60.
- Kearney, J. B., Wheeler, S. R., Estes, P., Parente, B. and Crews, S. T.** (2004). Gene expression profiling of the developing *Drosophila* CNS midline cells. *Dev. Biol.* **275**, 473-92.
- Kidd, S., Lieber, T. and Young, M. W.** (1998). Ligand-induced cleavage and regulation of nuclear entry of Notch in *Drosophila melanogaster* embryos. *Genes Dev.* **12**, 3728-40.
- Klamt, C., Jacobs, J. R. and Goodman, C. S.** (1991). The midline of the *Drosophila* central nervous system: a model for the genetic analysis of cell fate, cell migration, and growth cone guidance. *Cell* **64**, 801-15.
- Kosman, D., Small, S. and Reinitz, J.** (1998). Rapid preparation of a panel of polyclonal antibodies to *Drosophila* segmentation proteins. *Dev. Genes Evol.* **208**, 290-4.
- Kuwada, J. Y. and Goodman, C. S.** (1985). Neuronal determination during embryonic development of the grasshopper nervous system. *Dev. Biol.* **110**, 114-26.
- Lee, C. Y., Andersen, R. O., Cabernard, C., Manning, L., Tran, K. D., Lanskey, M. J., Bashirullah, A. and Doe, C. Q.** (2006). *Drosophila* Aurora-A kinase inhibits

neuroblast self-renewal by regulating aPKC/Numb cortical polarity and spindle orientation. *Genes Dev.* **20**, 3464-74.

Liu, X., Zwiebel, L. J., Hinton, D., Benzer, S., Hall, J. C. and Rosbash, M. (1992). The period gene encodes a predominantly nuclear protein in adult *Drosophila*. *J. Neurosci.* **12**, 2735-44.

Ma, Y., Certel, K., Gao, Y., Niemitz, E., Mosher, J., Mukherjee, A., Mutsuddi, M., Huseinovic, N., Crews, S. T., Johnson, W. A. et al. (2000). Functional interactions between *Drosophila* bHLH/PAS, Sox, and POU transcription factors regulate CNS midline expression of the slit gene. *J. Neurosci.* **20**, 4596-605.

Menne, T. V. and Klammt, C. (1994). The formation of commissures in the *Drosophila* CNS depends on the midline cells and on the Notch gene. *Development* **120**, 123-33.

Monastirioti, M. (2003). Distinct octopamine cell population residing in the CNS abdominal ganglion controls ovulation in *Drosophila melanogaster*. *Dev. Biol.* **264**, 38-49.

Morrison, S. J., Perez, S. E., Qiao, Z., Verdi, J. M., Hicks, C., Weinmaster, G. and Anderson, D. J. (2000). Transient Notch activation initiates an irreversible switch from neurogenesis to gliogenesis by neural crest stem cells. *Cell* **101**, 499-510.

Nishikawa, K. and Kidokoro, Y. (1999). Octopamine inhibits synaptic transmission at the larval neuromuscular junction in *Drosophila melanogaster*. *Brain Res.* **837**, 67-74.

O'Connor-Giles, K. M. and Skeath, J. B. (2003). Numb inhibits membrane localization of Sanpodo, a four-pass transmembrane protein, to promote asymmetric divisions in *Drosophila*. *Dev. Cell* **5**, 231-43.

Patel, N. H., Martin-Blanco, E., Coleman, K. G., Poole, S. J., Ellis, M. C., Kornberg, T. B. and Goodman, C. S. (1989). Expression of engrailed proteins in arthropods, annelids, and chordates. *Cell* **58**, 955-68.

Pielage, J., Steffes, G., Lau, D. C., Parente, B. A., Crews, S. T., Strauss, R. and Klammt, C. (2002). Novel behavioral and developmental defects associated with *Drosophila* single-minded. *Dev. Biol.* **249**, 283-99.

Rodriguez-Valentin, R., Lopez-Gonzalez, I., Jorquera, R., Labarca, P., Zurita, M. and Reynaud, E. (2006). Oviduct contraction in *Drosophila* is modulated by a neural network that is both, octopaminergic and glutamatergic. *J. Cell. Physiol.* **209**, 183-98.

Saraswati, S., Fox, L. E., Soll, D. R. and Wu, C. F. (2004). Tyramine and octopamine have opposite effects on the locomotion of *Drosophila* larvae. *J. Neurobiol.* **58**, 425-41.

Schmid, A., Chiba, A. and Doe, C. Q. (1999). Clonal analysis of *Drosophila* embryonic neuroblasts: neural cell types, axon projections and muscle targets. *Development* **126**, 4653-89.

- Skeath, J. B. and Doe, C. Q.** (1998). Sanpodo and Notch act in opposition to Numb to distinguish sibling neuron fates in the *Drosophila* CNS. *Development* **125**, 1857-65.
- Spana, E. P. and Doe, C. Q.** (1996). Numb antagonizes Notch signaling to specify sibling neuron cell fates. *Neuron* **17**, 21-6.
- Spana, E. P., Kopczynski, C., Goodman, C. S. and Doe, C. Q.** (1995). Asymmetric localization of numb autonomously determines sibling neuron identity in the *Drosophila* CNS. *Development* **121**, 3489-94.
- Thomas, J. B., Crews, S. T. and Goodman, C. S.** (1988). Molecular genetics of the *single-minded* locus: a gene involved in the development of the *Drosophila* nervous system. *Cell* **52**, 133-141.
- Truman, J. W., Schuppe, H., Shepherd, D. and Williams, D. W.** (2004). Developmental architecture of adult-specific lineages in the ventral CNS of *Drosophila*. *Development* **131**, 5167-84.
- Udolph, G., Rath, P. and Chia, W.** (2001). A requirement for Notch in the genesis of a subset of glial cells in the *Drosophila* embryonic central nervous system which arise through asymmetric divisions. *Development* **128**, 1457-66.
- Uemura, T., Shepherd, S., Ackerman, L., Jan, L. Y. and Jan, Y. N.** (1989). numb, a gene required in determination of cell fate during sensory organ formation in *Drosophila* embryos. *Cell* **58**, 349-60.
- Wang, H., Ouyang, Y., Somers, W. G., Chia, W. and Lu, B.** (2007). Polo inhibits progenitor self-renewal and regulates Numb asymmetry by phosphorylating Pon. *Nature* **449**, 96-100.
- Wang, S., Younger-Shepherd, S., Jan, L. Y. and Jan, Y. N.** (1997). Only a subset of the binary cell fate decisions mediated by Numb/Notch signaling in *Drosophila* sensory organ lineage requires Suppressor of Hairless. *Development* **124**, 4435-46.
- Ward, E. J. and Skeath, J. B.** (2000). Characterization of a novel subset of cardiac cells and their progenitors in the *Drosophila* embryo. *Development* **127**, 4959-69.
- Ward, M. P., Mosher, J. T. and Crews, S. T.** (1998). Regulation of bHLH-PAS protein subcellular localization during *Drosophila* embryogenesis. *Development* **125**, 1599-608.
- Wech, I., Bray, S., Delidakis, C. and Preiss, A.** (1999). Distinct expression patterns of different enhancer of split bHLH genes during embryogenesis of *Drosophila melanogaster*. *Dev. Genes Evol.* **209**, 370-5.
- Wharton, K. A., Jr., Franks, R. G., Kasai, Y. and Crews, S. T.** (1994). Control of CNS midline transcription by asymmetric E-box-like elements: similarity to xenobiotic responsive regulation. *Development* **120**, 3563-9.

- Wheeler, S. R., Kearney, J. B., Guardiola, A. R. and Crews, S. T.** (2006). Single-cell mapping of neural and glial gene expression in the developing *Drosophila* CNS midline cells. *Dev. Biol.* **294**, 509-24.
- Xiao, H., Hrdlicka, L. A. and Nambu, J. R.** (1996). Alternate functions of the single-minded and rhomboid genes in development of the *Drosophila* ventral neuroectoderm. *Mech. Dev.* **58**, 65-74.

CHAPTER III

**THE *DROSOPHILA* H-CELL DOPAMINERGIC NEURON:
GENETIC REGULATION OF CELL-TYPE SPECIFIC GENE
EXPRESSION**

Stephanie Stagg,^{1,3} Amaris R. Guardiola,^{3,5} and Stephen T. Crews^{1,2,3,4*}

Manuscript in preparation for submission.

¹Curriculum in Neurobiology

²Department of Biochemistry and Biophysics

³Program in Molecular Biology and Biotechnology

⁴Department of Biology

The University of North Carolina at Chapel Hill, Chapel Hill, NC 27599-3280

⁵Department of Biology

Angelo State University

San Angelo, TX 76909

*Author for correspondence: steve_crews@unc.edu

Tel (919) 962-4380, Fax (919) 962-8472

Summary

Dopaminergic neurons play important neurobiological roles in vertebrates and invertebrates in reward and aggressive behaviors and locomotion. The *Drosophila* H-cell is dopaminergic neuron that resides at the midline of the ventral nerve cord. The midline precursor MP3 gives rise to H-cell and H-cell sib. While H-cell sib fate requires *Notch* signaling, H-cell asymmetrically inherits Numb during division, and blocks *Notch* signaling. Screening transcription factor genes for expression in H-cell discovered 5 that are prominently expressed in H-cell. In particular Lethal of scute and Tailup are initially localized to both H-cell and H-cell sib, but then become preferentially localized to H-cell. Instead of *Notch* signaling, the Lethal of scute bHLH transcription factor is required for H-cell differentiation. Misexpression of *lethal of scute* results in ectopic expression of all H-cell-specific gene expression and *lethal of scute* mutant analysis revealed an absence of H-cell differentiation gene expression. The *lethal of scute* gene is expressed in all midline neuronal precursors, including MPs and the median neuroblast stem cell. The related *achaete* and *scute* genes are also expressed in subsets of midline neuronal precursors. Genetic experiments revealed that *lethal of scute* also plays a proneural role in the midline, and is required for formation of MP4, MP5, MP6, and the median neuroblast. However, it is not required for formation of MP3, only in H-cell-specific gene expression. The Tailup and SoxNeuro transcription factors are each required for different aspects of H-cell differentiation: Tailup for genes involved in dopamine metabolism, and SoxNeuro for a peptide neurotransmitter receptor. Thus, H-cell fate is a combination of *lethal of scute* control of H-cell specific gene expression with contributions of *tailup* and *SoxNeuro* controlling specific aspects of H-cell differentiation.

Introduction

Complex behaviors require the coordinated action of diverse ensembles of neurons. Each neuron contains a distinct combination of neural function genes, which include genes encoding neurotransmitter biosynthetic enzymes, neuropeptides, vesicular transporters, membrane transporters, neurotransmitter receptors, and axon guidance proteins. One of the key issues in developmental neuroscience is to molecularly describe the unique patterns of gene expression that define each neuron and its precursors during development, and understand how neural gene expression is regulated. Not only will this explain how neuronal diversity is generated, but, in the case of humans, provide the experimental basis for generating specific types of neurons for cell-based therapies of nervous system disease.

These goals have been systematically applied towards studying the development of dopaminergic neurons because of their prominent neurobiological roles in reward, emotion, and locomotory pathways, and their importance in neurodegenerative diseases. Parkinson's disease is characterized by the loss of midbrain dopaminergic neurons, and one of the major goals of contemporary neural stem cell research is to generate sufficient quantities of dopaminergic neurons for cell replacement therapies to counteract Parkinson's disease. Studies in vertebrates have identified multiple regulatory proteins that are required for controlling gene expression and development of dopaminergic neurons. Recent work further showed that an Ets-family transcription factor is evolutionarily conserved between *C. elegans* (AST-1) and mammals (ETV1), and controls dopaminergic cell gene expression (Flames and Hobert, 2009). In insects, dopaminergic neurons are found in both the nerve cord and brain. One of the best-

described insect dopaminergic neurons is the H-cell (named for its “H”-like axonal trajectories), which is present in the CNS midline cells of the nerve cord. H-cell was first described in grasshopper as one of the two progeny of the Midline Precursor 3 (MP3) cell (Goodman et al., 1981), and shown in the moth *Manduca sexta* to be dopaminergic. H-cell is also present in *Drosophila* (Bossing and Technau, 1994; Budnik and White, 1988; Schmid et al., 1999; Wheeler et al., 2006) and in this paper we address how H-cell acquires its dopaminergic cell fate.

The *Drosophila* CNS midline cells are an attractive system for studying CNS development. The mature embryonic midline cells consist of a small number (~22) of neurons and glia, yet they are comprised of diverse motoneurons, interneurons, neurosecretory cells, and glia (Bossing and Technau, 1994; Wheeler et al., 2006). The development of the wild-type midline cells has been carefully analyzed, and a large number of midline-expressed genes identified and their expression analyzed at the single-cell level throughout embryonic development (Kearney et al., 2004; Wheeler et al., 2006). The H-cell midline interneuron is dopaminergic, and similar to other dopaminergic neurons, expresses a set of genes encoding dopamine biosynthetic enzymes including *pale* (*ple*; encodes tyrosine hydroxylase) and *dopa decarboxylase* (*Ddc*), as well as a vesicular monoamine transporter (*Vmat*), and the dopamine membrane transporter (*DAT*) (Wheeler et al., 2006). H-cell also expresses neurotransmitter receptors that receive input for serotonin (*5-HT1A*), glutamate (*Glu-RI*), and neuropeptide F (*NPFRI*). These characteristic traits, as well as its “H” pattern of axonal connections, to a large degree, constitute the unique character of the H-cell.

Around the time of gastrulation, the *single-minded* master regulatory gene activates the midline developmental program (Crews, 1998), and soon after 3 MP equivalence groups (MP1, MP3, MP4) of 5-6 cells/each form (Wheeler et al., 2008). *Notch* signaling ensues, and from the MP1 group, one cell is selected to become an MP1 and the others become midline glia (MG). The same occurs for the MP3 group with one cell becoming an MP3 and the others MG. Development of the MP4 group is more complex, with sequential development of MP4 followed by MP5, MP6, and the median neuroblast (MNB). MP3 undergoes a single asymmetric cell division giving rise to the dopaminergic H-cell and the glutamatergic H-cell sib interneuron. The differences in MP3 neuron cell fate are due to the asymmetric localization of the Numb protein, which is high in H-cell, but low in H-cell sib (Wheeler et al., 2008). Another round of *Notch* signaling directs H-cell sib to its fate, but is blocked in H-cell due to the presence of Numb. Thus, H-cell sib cell fate and gene expression is dependent on *Notch* signaling and its transcriptional effector, Suppressor of Hairless [Su(H)], and H-cell is governed by a different regulatory program.

In this paper, we ask the complementary question: what regulatory proteins govern H-cell fate and gene expression? We demonstrate that two transcription factors, the Lethal of scute [L(1)sc] bHLH protein (Alonso and Cabrera, 1988) and Tailup (Tup; Islet) Lim-homeodomain protein (Thor and Thomas, 1997), while initially present in MP3, H-cell and H-cell sib become preferentially localized to H-cell. L(1)sc plays the more prominent genetic role, and is required for all H-cell specific gene expression, but does not repress H-cell sib expression. Tup plays a more specific role and is required for expression of *ple* and *DAT*, two genes that encode proteins involved in DA metabolism.

Another genetic pathway is required for expression of genes present in both H-cell and H-cell, including the *5-HT1A* and *Glu-R1* neurotransmitter receptor genes. Another transcription factor, the Sox2 family protein, SoxNeuro (SoxN) (Buescher et al., 2002; Cremazy et al., 2000; Overton et al., 2002), is required for expression of another neurotransmitter receptor, NPFR1. Thus, while L(1)sc directs all H-cell specific gene expression, both Tup and SoxN regulate specific subsets of H-cell gene expression. L(1)sc does not play a proneural role regarding MP1 and MP3, since they form in *l(1)sc* mutants. However, the presence of MP4-6 and the MNB does require *l(1)sc*, indicating that it plays a proneural role in those cells. L(1)sc also likely directs mVUM-specific gene expression, just as *Notch* signaling directs iVUM-specific gene expression. Thus, the role of *l(1)sc* is dependent on the precursor cell type (e.g. MP3 vs. MP4-6 and MNB), and can play both proneural and neural identity roles. However, the Tup and SoxN proteins contribute to specifying different characteristics of the H-cell phenotype.

Materials and Methods

Drosophila Strains

Drosophila strains used included: *ase*¹, *BarH1*^{PL21}, *Df(1)sc*¹⁰⁻¹, *Df(1)sc*^{B57}, *SoxN*⁴, and *tup*¹. *Gal4* and *UAS* lines employed were: *sim-Gal4*, *UAS-BarH1*, *UAS-l(1)sc*, *UAS-sc*, *UAS-SoxN*, and *UAS-tau-GFP*. All *sim-Gal4* *UAS* embryos were analyzed by in situ hybridization with the relevant probes and shown to be strongly expressed in all midline cells.

L(1)sc and Sc Antisera

Polyclonal antibodies against L(1)sc and Sc were generated by injecting both guinea pigs and rats (Pocono Rabbit Farm) with N-terminal 6xHis-L(1)sc and 6xHis-Sc fusion proteins (S. Wheeler, J. Skeath; pers. comm.). The L(1)sc and Sc sequences were the full-length proteins. After transformation into *E. coli* BL21 (DE3), 6xHis-L(1)sc and 6xHis-Sc protein synthesis was induced by IPTG. Inclusion bodies were isolated, solubilized in 10% SDS, followed by sequential dialysis in: (1) 0.05% SDS, 1xPBS, (2) 0.01% SDS, 1xPBS, and (3) 1xPBS. The specificity of both antibodies was confirmed by the following observations: (1) the lateral CNS staining was identical to published accounts for L(1)sc and Sc, and (2) immunoreactivity was absent in the corresponding deficiency strains: *Df(1)sc^{B57}* for L(1)sc and Sc, and *Df(1)sc¹⁰⁻¹* for Sc.

In Situ Hybridization and Immunostaining

Embryo collection, in situ hybridization, and immunostaining were performed as previously described (Kearney et al., 2004). Only embryonic abdominal segments (A1-8) were examined. Primary antibodies used were: mouse (Promega) and rabbit (Cappel) anti- β -galactosidase, rabbit anti-Cas (Kambadur et al., 1998), mouse and rat anti-ELAV (Developmental Studies Hybridoma Bank), rabbit anti-GFP (Abcam), guinea pig anti-Lim3 (Broihier and Skeath, 2002), rabbit anti-SoxN (also cross-reacts with Dichaete; John Nambu, personal communication), mouse anti-Tau (Sigma), and rat anti-Tup (Broihier and Skeath, 2002). Alexa Fluor-conjugated secondary antibodies were used

(Molecular Probes), and the Tyramide Signal Amplification System (Perkin Elmer) was employed for some experiments.

Microscopy and Image Analysis

Fluorescently-stained embryos were imaged on Zeiss LSM-510 and LSM-PASCAL confocal microscopes using a 40x objective. Images were processed as previously described (Wheeler et al., 2008). It is uncommon for all midline cells to be present in a single focal plane, so, for clarity, multiple focal planes for a given Z-series were combined as composite images.

Results

Expression of H-Cell Neural Function and Regulatory Genes

MP3 divides at early stage 11 (~5 hr post-fertilization (pf)) to give rise to H-cell and H-cell sib. Expression of H-cell neural function genes that are involved in dopamine biosynthesis, dopamine transport, and neurotransmitter receptors begins at late stage 13 (~10 hr pf). Fig. 3.1A-D shows the expression of the *ple*, *DAT*, *NPFR1*, *Vmat*, and 5-*HT1A* neural function genes in H-cell. Note that analysis of H-cell transcription utilizes multi-label immunostaining and in situ hybridization in *sim-Gal4 UAS-tau-GFP* embryos. In this background, the outline of each midline cell is revealed assisting in analysis of gene expression. Imaging is usually carried-out on sagittal views of the CNS, which allows all midline cells to be viewed in relationship to each other. Analysis of 36 transcription factors expressed in the midline cells (Wheeler et al., 2008;

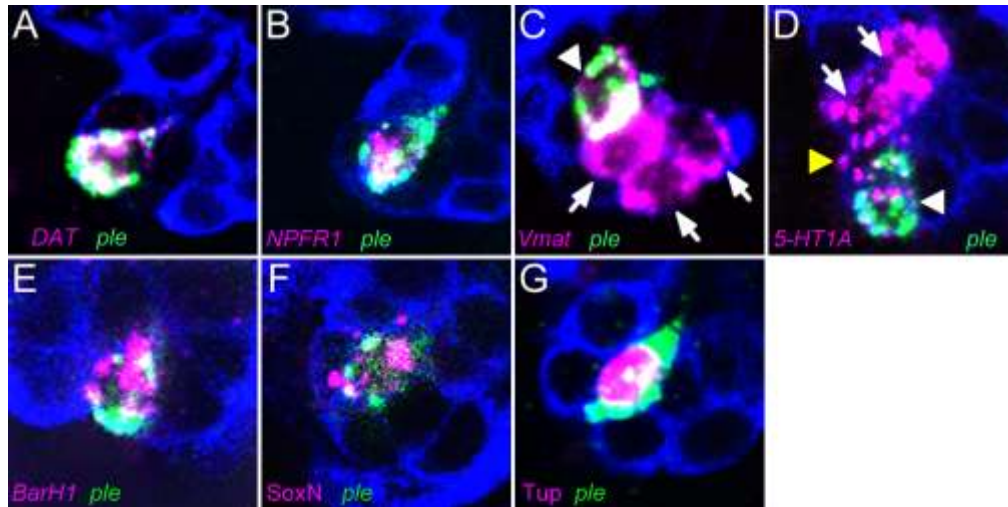


Figure 3.1. H-Cell gene expression. Sagittal views of single segments of *sim-Gal4 UAS-tau-GFP* embryos at stage 14. Embryos were stained for GFP or Tau (blue; midline cell cytoplasm is GFP⁺ and cell nuclei are GFP⁻) and additional antibody and in situ hybridization probes. Italicized gene names represent RNA and unitalicized gene names represent protein. (**A-G**) In all panels, *ple* expression (green), which is H-cell specific, is shown. (**A-D**) The neural function genes: (**A**) *DAT*, (**B**) *NPFR1*, (**C**) *Vmat*, and (**D**) *5-HT1A* (all magenta) colocalize with *ple* in H-cell. (**C**) The *Vmat* gene is expressed in H-cell (arrowhead) and 3 mVUMs (arrows). (**D**) The *5-HT1A* gene is expressed in H-cell (white arrowhead), H-cell sib (yellow arrowhead), and 2 MP1 neurons (arrows). (**E-G**) The transcription factor genes: (**E**) *BarH1*, (**F**) *SoxN*, and (**G**) *tup* (all magenta) colocalize with *ple* in H-cell.

Wheeler et al., 2009) revealed 5 that were prominently expressed in H-cell: *BarH1* (Reig et al., 2007), *lethal of scute* [*l(1)sc*], *scute* (*sc*), *SoxNeuro* (*SoxN*), and *tailup* (*tup*) (Fig 3.1E-G; Fig. 2A-N). The *BarH1*, *SoxN*, and *tup* genes are each expressed at stage 11 and remain on until the end of embryonic development. *BarH1* is not expressed in MP3, but is present in H-cell beginning at late stage 11, and is absent in H-cell sib. *Tup* is absent in MP3, initially present in both H-cell and H-cell sib, but by stage late stage 11 is preferentially localized to only H-cell (Fig. 3.2A-C). *SoxN* is expressed in MP3, present in both H-cell and H-cell sib until the end of stage 13, and then becomes localized to only the H-cell. Each of these genes is expressed before the appearance of H-cell neural function gene expression, and could regulate their expression either directly or indirectly.

AS-C Genes are Expressed in Midline Precursors and their Neuronal Progeny

The *l(1)sc* and *sc* bHLH *achaete-scute* complex (AS-C) genes are both expressed in H-cell (Fig. 3.2). The AS-C consists of 3 proneural basic-helix-loop-helix (bHLH) genes, *achaete* (*ac*), *l(1)sc*, and *sc* (Campuzano and Modolell, 1992), and the *asense* (*ase*) bHLH neural precursor gene (Brand et al., 1993; Dominguez and Campuzano, 1993; Gonzalez et al., 1989). The proneural bHLH genes play important roles in CNS and sensory cell development although relatively little is known regarding the function of *l(1)sc* and its downstream target genes. The *l(1)sc* gene was previously shown to control *engrailed* (*en*) expression in the CNS midline cells (Bossing and Brand, 2006). However, these results were based on the assumption that *ac* and *sc* were not expressed in the midline cells, which, as shown below, is incorrect. Since detailed expression analysis of the AS-C genes has not been carried-out, we examined expression using antibodies we

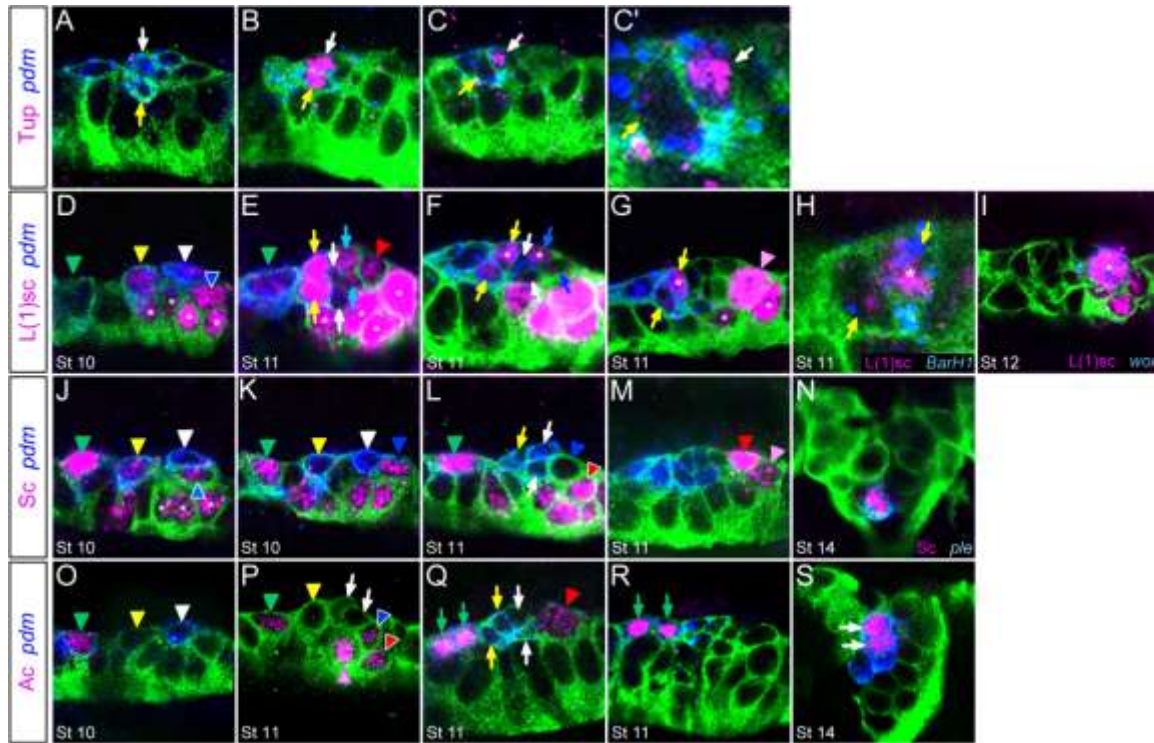


Figure 3.2. Tup and AS-C Genes are expressed in precursors and neurons. Sagittal views of single segments of *sim-Gal4 UAS-tau-GFP* embryos stained with (A-C) anti-Tup, (D-I) anti-L(1)sc (magenta), (J-N) anti-Sc (magenta), (O-S) anti-Ac (magenta), and (A-S) anti- τ FP (green). (A-G, J-M, O-S) Combined *pdm2* and *nubbin* expression (*pdm*; blue) mark MP1, MP3, MP4, and their neuronal progeny, but is absent in MP5 and MP6 and their progeny, MNB, and MG. Arrowheads indicate MPs and arrows indicate neurons. Embryonic stages (St) are indicated in each panel, and embryos at the same stage are progressively older moving from left-to-right. (A-C) Tup is preferentially localized to H-cell. (A) At early stage 11 immediately after MP3 division, Tup (magenta) was absent from H-cell (white arrow) and H-cell sib (yellow arrow). (B) Later during stage 11, Tup was present in both H-cell and H-cell sib. (C) By the end of stage 11, Tup was present in H-cell, and absent from H-cell sib. (C') Higher magnification view. (D-I) L(1)sc is present in all MPs, their newly divided neurons, MNB, and PMG. (D) At stage 10, L(1)sc was present in *pdm*⁺ MP3 (yellow arrowhead), *pdm*⁺ MP4 (white arrowhead), *pdm*⁻ MP5 (blue arrowhead), and MP6, MNB, and PMG (*; these cell types cannot be distinguished at this time). L(1)sc was absent in MP1 (green arrowhead) at this time. (E) At early stage 11, L(1)sc was present at low levels in MP1 (green arrowhead), at high levels in the newly-divided MP3 neurons (H-cell and H-cell sib; yellow arrows), low in the MP4 neurons (white arrows), and present in both MP5 neurons (mVUM5 and iVUM5; blue arrows) and in MP6 (red arrowhead). Levels were high in the PMG and MNB (*). (F) L(1)sc levels were higher in H-cell (*; yellow arrow) than H-cell sib (yellow arrow), absent in VUM4s (white arrows), and present in mVUM5 (*; blue arrow), but not iVUM5 (blue arrow). (G) L(1)sc was present in H-cell (*), but greatly reduced in H-cell sib, absent in VUMs, and present in MNB (purple arrowhead), and PMG (*). (H) High magnification view of a late stage 11 embryo stained with L(1)sc (magenta) and BarH1 (blue). BarH1 expression is restricted to H-cell, and this image demonstrated the higher levels of L(1)sc in the *BarH1*⁺ H-cell (*) compared to H-cell sib. (I) L(1)sc (magenta) overlapped in expression with *wor* (green), which is expressed in the MNB (*; purple arrowhead). (J-N) Sc (magenta) is present in MPs, MNB, and H-cell. (J) At stage 10, Sc was high in MP1 (green arrowhead), present in MP3 (yellow arrowhead), MP5 (blue arrowhead), and additional midline cells (MP6,

MNB, PMG; *). Sc was low in MP4 (white arrowhead). **(K)** Prior to the MP3 and MP4 divisions (late stage 10), Sc was present in MP1 and MP5, but low in MP3 and MP4. **(L)** Prior to the MP5 division (early stage 11), Sc was present in MP1 and MP6 (red arrowhead), but was absent in MP3 neurons (yellow arrow; second neuron is out of the focal plane), MP4 neurons (white arrows), and MP5 (blue arrowhead). **(M)** After the MP1 division, but before the MP6 division, Sc was absent from all MP neurons, but was present in MP6 (red arrowhead) and MNB (purple arrowhead). **(N)** Sc was present in H-cell beginning at stage 14, as shown by colocalization with *ple* (blue). **(O-S)** Ac is present in MP1 and MP1 neurons and transiently in MP5, MP6, and MNB. **(O)** At stage 10, Ac was present in MP1 (green arrowhead) and absent from all other MPs. **(P)** At stage 11 when MP5 was delaminating, Ac was present in MP5 (blue arrowhead), MP6 (red arrowhead), and MNB (purple arrowhead), while still present in MP1 (green arrowhead). **(Q)** Later during stage 11, Ac was highly expressed in the newly divided MP1 neurons (green arrows), present at low levels in MP6 (red arrowhead) and absent in MP5 (out of the focal plane of this image) and MNB. **(R)** At late stage 11, Ac was present only in the MP1 neurons. **(S)** At stage 14, Ac was present in the MP1 neurons, and remained present until the end of embryogenesis.

generated against the L(1)sc and Sc proteins, as well as an existing Ac monoclonal antibody.

L(1)sc. L(1)sc was present in all midline neuronal precursors, including MP1, MP3, MP4, MP5, and MP6 at stages 10-11 and MNB at stages 10-12 (Fig. 3.2D-G,I). L(1)sc remained present in the newly divided neurons of MP3 (H-cell, H-cell sib), MP5 (mVUM5, iVUM5), and MP6 (mVUM6 and iVUM6) (Fig. 3.2E,F). Although both H-cell and H-cell sib initially possessed high levels of L(1)sc protein (Fig. 3.2F), the amount was greatly reduced in H-cell sib as stage 11 progressed, whereas levels remained high in the H-cell (Fig. 3.2G,H). Similar L(1)sc dynamics were observed for the VUMs: L(1)sc was initially present in both mVUM5,6 and iVUM5,6 (Fig. 3.2E), but levels became higher in the mVUMs with respect to iVUMs (Fig. 3.2F). In contrast, L(1)sc was present in MP1 and MP4 (Fig. 3.2D), but not in their progeny (Fig. 3.2E-G). By the end of stage 11, L(1)sc was no longer detectable in midline neurons (Fig. 3.2I), including H-cell and mVUMs. L(1)sc was present in PMG from stages 10-12, but was absent in AMG (Fig. 3.2D-G,I).

Sc. Sc was present in the MP1, MP3, MP5, MP6, and MNB precursors, but was absent in MP4 (Fig. 3.2J-M). Unlike L(1)sc, the Sc protein was absent in the newly-divided MP and MNB neurons. Sc appeared in H-cell beginning at stage 14 (Fig. 3.2N) and remained on throughout embryonic development. Sc was not expressed in any other midline neurons. Sc was present in PMG from stages 10-11, but was absent in AMG.

Ac. Ac was present in MP1 and transiently in MP5, MP6, and MNB at stages 10-11 (Fig. 3.2O-Q). Ac prominently remained on in the MP1 neurons after division

throughout embryogenesis (Fig. 3.2R,S). In contrast, *Ac* was absent in all other midline neurons and MG.

In summary, the 3 *AS-C* proneural genes are all expressed in the midline cells in a dynamic manner. While they partially overlap in expression, each gene has a unique pattern of midline expression. In the case of *ac* and *sc*, this contrasts with their expression in other cell types, including embryonic lateral neuroblasts and sensory precursors, where their expression closely overlaps. Regarding H-cell development, *L(1)sc* and *Sc*, but not *Ac*, are present in MP3 and could be involved in MP3 formation. Most significantly, *L(1)sc* remains on early in H-cell development, but is reduced in H-cell sib, consistent with playing a role in H-cell-specific gene expression and development. *Sc* is also present specifically in H-cell but relatively late in development, and unlikely to control H-cell fate. Similarly, expression of *l(1)sc*, *ac*, and *sc* in MP1, MP4 (weakly but present), MP5, MP6, and MNB could influence MP formation and division, and *l(1)sc* could control mVUM cell type-specific expression, since it is preferentially expressed in mVUMs compared to iVUMs.

***L(1)Sc* Misexpression Activates H-Cell Gene Expression**

Based on the expression of *l(1)sc* and *sc* (but not *ac*) in H-cell and their potential roles in H-cell development, we individually misexpressed *l(1)sc* and *sc* in all midline cells in *sim-Gal4 UAS-l(1)sc* and *sim-Gal4 UAS-sc* embryos. Stage 14-16 embryos were then screened for alterations in H-cell specific gene expression. When *l(1)sc* was misexpressed, *ple* expression was observed in an extra cell in addition to H-cell in 22% of segments analyzed (Fig. 3.3A,B; Table 3.1). The additional *ple*⁺ cell was H-cell sib based

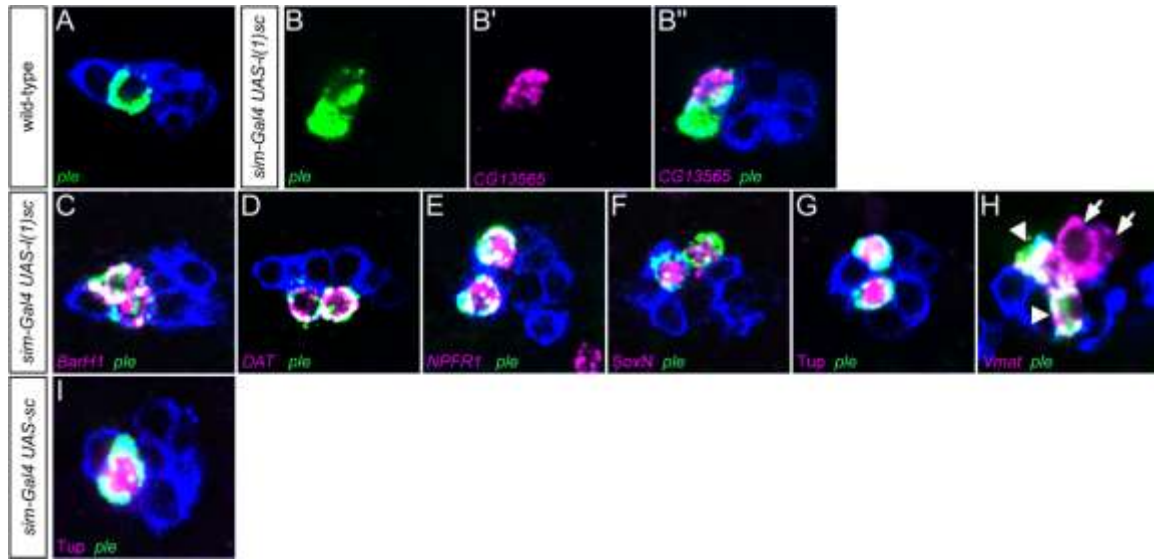


Figure 3.3. *l(1)Sc* activates H-Cell gene expression. Horizontal views of single segments of stages 14-16: (A) wild-type (B-H) *sim-Gal4 UAS-l(1)sc*, and (I) *sim-Gal4 UAS-sc* embryos stained for *ple* expression (green) and various H-cell expressed genes (magenta). All embryos had *sim-Gal4 UAS-tau-GFP* (blue). (A) Shown is the single wild-type *ple*⁺ H-cell. (B) Misexpression of *l(1)sc* resulted in 2 *ple*⁺ cells in 22% segments scored. The additional cell was *CG13565*⁺ (magenta), which indicated that it was H-cell sib. (C-G) Misexpression of *l(1)sc* resulted in expression of: (C) *BarH1*, (D) *DAT*, (E) *NPFR1*, (F) *SoxN*, and (G) *Tup* in an additional *ple*⁺ cell in 14-24% of segments scored. (H) Misexpression of *l(1)sc* resulted in the expansion of *Vmat* expression from 4 cells in wild-type to 5-8 cells. In this segment, there were 5 *Vmat*⁺ cells, 2 of which were *ple*⁺ (arrowheads; H-cell and H-cell sib) and the other 3 mVUMs (only 2 *Vmat*⁺ mVUMs are shown in this image). (I) Misexpression of *sc* had no affect on *ple* or *Tup* expression; only expression in H-cell was observed.

on coexpression of *ple* with *CG13565*, an H-cell sib-specific marker (Fig. 3.3B). Since *CG13565* was still expressed in the *ple*⁺ cell, this indicated that H-cell sib was not completely transformed into an H-cell, but rather that *l(1)sc* was able to activate H-cell-specific gene expression in H-cell sib. Ectopic *ple* expression was not observed in any other midline cell type besides H-cell sib, suggesting that only H-cell sib has the requisite transcriptional coactivators, chromatin structure, or other factors required for *L(1)sc* to activate H-cell-specific transcription. *l(1)sc* misexpression also induced the expression of additional H-cell specific genes, including *BarH1*, *DAT*, *NPFR1*, *SoxN*, *tup*, and *Vmat* in an extra cell in 14-22% segments analyzed (Fig. 3.3C-H; Table 3.1). In all cases, both cells were *ple*⁺, indicating that the two cells were H-cell and H-cell sib. The *Vmat* gene, which is expressed in both H-cell and mVUMs in wild-type embryos, showed an increase in *l(1)sc* misexpression embryos from 4 cells in wild type to 5-8 cells (Fig. 3.3H). One of the additional cells was H-cell sib, based on coexpression with *ple*, and the others were presumably iVUMs that ectopically expressed *Vmat*. This demonstrated that *l(1)sc* can ectopically activate both H-cell and mVUM gene expression. In contrast, misexpression of *sc* did not result in expanded *ple* or *Tup* (Fig. 3.3I). These results indicated that *l(1)sc* has the ability to activate most, if not all, H-cell-specific gene expression, whereas *sc*, despite its close sequence homology to *l(1)sc*, is not able to induce ectopic H-cell specific gene expression.

***L(1)Sc* is Required for H-Cell Gene Expression**

Since *l(1)sc* was able to ectopically activate H-cell transcription, we utilized mutants of the *AS-C* to further assess the role of the *AS-C* genes in H-cell development.

The mutants analyzed included: (1) *Df(1)sc^{B57}* (deficient for *ac*, *l(1)sc*, *sc*, and *ase*), (2) *sc¹⁰⁻¹* (deficient for *ac* and *sc*), (3) *ase¹* (mutant for *ase*) (Garcia-Bellido, 1979; Jimenez and Campos-Ortega, 1990). In *Df(1)sc^{B57}* mutant embryos, there was often an absence of expression of the H-cell neural function genes: *DAT*, *NPFRI*, *ple*, and *Vmat* (Fig. 3.4A-D, H-K; Table 3.1). *DAT* was absent in 100% of segments, and *NPFRI* absent in 45% of segments. *ple* expression was absent in 76% of segments, and when present, at reduced levels. In wild-type embryos (Fig. 3.4D), *Vmat* was expressed in the *pdm⁺* H-cell and the 3 *pdm⁻* mVUMs. In *Df(1)sc^{B57}* embryos (Fig. 3.4K), *Vmat* was absent in H-cell in 43% of segments, absent from all mVUMs in 39% of segments, present in only one mVUM in 43% of segments, and present in 2 mVUMs in 18% of segments. Analysis of *BarHI*, *SoxN*, and *tup* transcription factor gene expression in *Df(1)sc^{B57}* mutant embryos was assayed in stage 14-16 embryos, when expression of these genes is restricted to only H-cell in wild-type (Fig. 3.4E-G, L-O; Table 3.1). *BarHI* expression was absent in 100% of segments, and *SoxN* absent in 47% of segments. In contrast, Tup protein was present in *Df(1)sc^{B57}* embryos in either one cell (72% of segments) or two cells (28% of segments). Costaining with *ple* (H-cell marker) and *CG13565* (H-cell sib marker) indicated that in *Df(1)sc^{B57}* embryos, Tup is always present in H-cell and the additional cell is H-cell sib (Fig. 3.4 N,O). The *CG13565* gene was expressed in H-cell sib in *Df(1)sc^{B57}* mutant embryos at the same frequency and levels as wild-type indicating that AS-C genes do not clearly influence H-cell sib gene expression. Thus, in segments in which H-cell gene expression is absent in *Df(1)sc^{B57}*, H-cell is not transformed into H-cell sib.

The *5-HT1A* gene is expressed in both H-cell and H-cell sib (Wheeler, S.R. 2006), and its expression was unaffected in *Df(1)sc^{B57}* mutants (Fig. 3.4P,R). Similarly, *nub* and

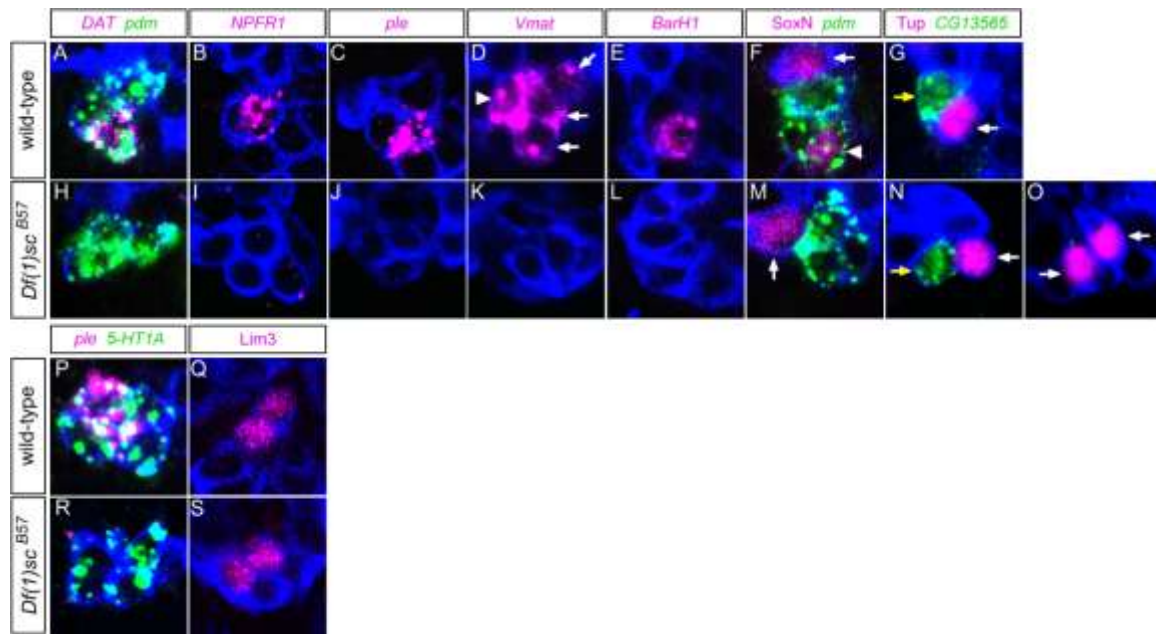


Figure 3.4. Mutants of *l(1)sc* affect H-Cell gene expression. Confocal images of stages 14-16 (A-G, O-Q) wild-type and (H-N, R-T) *Df(1)sc^{B57}* embryos. All embryos contained *sim-Gal4* *UAS-tau-GFP* and were stained for GFP (blue), and all segments, except P,Q,S,T, were stained for *pdm2/nub* (*pdm*; green) to identify H-cell, H-cell sib, and MP1 neurons. For simplicity, *pdm2/nub* staining is omitted from most panels, except for A,F,H,M. (A-F) In wild-type control embryos, (A) *DAT*, (B) *NPFR1*, (C) *ple*, (D) *Vmat*, (E) *BarH1*, and (F) *SoxN* (all magenta) were present in H-cell. In (A) *pdm* staining was present to illustrate that MP1 neurons, H-cell, and H-cell sib could be identified, and note that *DAT* overlaps with *pdm* in the H-cell. In wild-type, (D) *Vmat* expression was present in the H-cell (arrowhead; identified by *pdm* staining, which is not shown) and in the mVUMs (arrows). (F) *SoxN* was present in the *pdm⁺* H-cell (arrowhead) and *pdm⁻* MG (arrows). (H-M) In *Df(1)sc^{B57}* embryos, (H) *DAT*, (I) *NPFR1*, (J) *ple*, (K) *Vmat*, (L) *BarH1*, and (M) *SoxN* were absent from H-cell in the segments shown. (M) In *Df(1)sc^{B57}*, *SoxN* was absent from *pdm⁺* cells, including H-cell, but remained present in *pdm⁻* MG (arrow). (K) In *Df(1)sc^{B57}*, *Vmat* was absent from H-cell and all 3 mVUMs. (G,N,O) In (G) wild type, *Tup* (magenta) was present in H-cell (white arrow) and *CG13565* (green) was present in H-cell sib (yellow arrow)., In (N) *Df(1)sc^{B57}*, *Tup* (magenta) was present in H-cell (white arrow) and H-cell was not transformed to H-cell sib (yellow arrow), since H-cell sib-specific gene expression (*CG13565*; green) was not present in H-cell. In (O) *Df(1)sc^{B57}*, *Tup* (magenta) was present in an additional cell in 28% of segments scored. (P,R) Expression of the *5-HT1A* gene (green), which is present in H-cell, H-cell sib, and MP1 neurons in wild-type embryos, was unaffected in *Df(1)sc^{B57}*. Note the absence of *ple* expression (magenta) in *Df(1)sc^{B57}*. (Q,S) *Lim3* expression in the two MP1 neurons (magenta) was unaffected in *Df(1)sc^{B57}* mutant embryos.

Table 3.1. Quantitative summary of H-cell genetic data

	Wild-type			<i>Df(1)sc^{B57}</i>			<i>sim-Gal4 UAS-l(1)sc</i>		
Gene	0 cell	1 cell	2 cells	0 cell	1 cell	2 cells	0 cell	1 cell	2 cells
<i>BarH1</i>	0	10	0	8	0	0	0	12	2
<i>DAT</i>	0	10	0	8	0	0	0	25	7
<i>NPFR1</i>	0	10	0	10	12	0	0	19	6
<i>ple</i>	0	10	0	13	4	0	0	125	29
<i>SoxN</i>	0	10	0	7	8	0	0	25	4
<i>Vmat</i>	0	10	0	10	12	1	0	19	3
<i>Tup</i>	0	10	0	0	23	9	0	25	7

Numbers = number of segments in which 0, 1, or 2 cells expressed the RNA or protein of the gene

pdm2 are both expressed in MP1 neurons, H-cell, and H-cell sib, and their expression was unaffected in *Df(1)sc^{B57}* (not shown). This suggests that *Df(1)sc^{B57}* only affects H-cell-specific gene expression, and not genes expressed in both H-cell and H-cell sib. In the midline cells, *Lim3* is expressed only in the MP1 neurons, and its expression was unaffected in *Df(1)sc^{B57}* mutant embryos (Fig. 3.4Q,S). In summary, these results indicated that the AS-C does not control MP1 or H-cell sib gene expression, precursor formation, or neuronal cell fate, nor do they regulate the expression of genes present in both H-cell and H-cell sib. The AS-C does control H-cell-specific gene expression, but loss of AS-C function in H-cell does not result in transformation to its sibling cell, H-cell sib.

The *Df(1)sc^{B57}* mutant strain provided strong evidence for defects in H-cell gene expression, but it is deficient for 4 genes (*ac*, *ase*, *l(1)sc*, *sc*). The analysis of additional mutations in the AS-C locus indicated that only the *l(1)sc* gene was required for H-cell gene expression, since H-cell gene expression was unaltered in mutants for *ac*, *sc*, and *ase*. The *Df(1)sc¹⁰⁻¹* mutant is deficient for *ac* and *sc*, and *ple* and *NPFRI* expression were present in 100% of segments examined in mutant embryos (Fig. S3.1A,B in the supplementary material; Table 1). In *ase¹* mutants, which are deficient for only *ase*, *ple* and *DAT* were present in 100% of segments (Fig. S3.1C,D in the supplementary material; Table 1). While *l(1)sc* single-gene mutants were unavailable, the fact that null mutants in *ac*, *ase*, and *sc* do not show defects in H-cell gene expression indicated that the loss of *l(1)sc* is responsible for the effects on H-cell gene expression observed in *Df(1)sc^{B57}* mutant embryos. This is consistent with misexpression data showing the ability of *l(1)sc*

to ectopically activate H-cell gene expression in H-cell sib, as well as the prominent H-cell-specific localization of L(1)sc protein.

***l(1)Sc* is Required for Formation of a Subset of Midline Neuronal Precursors**

Examination of *Df(1)sc^{B57}* mutant embryos revealed that they had a deficiency of midline neurons compared to wild-type (Fig. 3.5). Midline cells were identified by *tau-GFP* expression in *sim-Gal4 UAS-tau-GFP Df(1)sc^{B57}* mutant embryos that were also stained for either neurons (anti-Elav) or MG (anti-Wrapper). In stage 12 wild-type embryos, there are 10 neurons present (Fig. 3.5A). They are the recently created progeny of the 5 MPs (the MNB is just beginning to generate neurons). The number of Elav⁺ neurons increased to 14 at stage 14 (Fig. 3.5B) and 16 at stage 16 (Fig. 3.5C). In stage 12 *Df(1)sc^{B57}* mutants, there were 6 Elav⁺ cells (Fig. 3.5F), and this number was maintained at stages 14 and 16 (Fig. 3.5G,H). Since the 6 Elav⁺ cells were present soon after the MP divisions and they did not decrease in cell number over time, this suggested that the reduction in neurons was due to a lack of neuron formation rather than cell death. Four of the 6 neurons in *Df(1)sc^{B57}* mutant embryos were the 2 MP1 neurons, H-cell, and H-cell sib, since their presence was revealed by positive staining for *Lim3* (MP1 neurons), *tup* (H-cell), *CG13565* (H-cell sib), *5-HT1A* and *nub/pdm2* (MP1 neurons, H-cell, H-cell sib, VUM4s) (Fig. 3.4). This implied that the missing neurons were VUMs.

To further address which VUMs were affected, we examined the expression of 3 VUM-expressed genes: (1) *Tyramine β hydroxylase* (*Tbh*), which is expressed in mVUM4-6 and encodes an octopamine biosynthetic enzyme, (2) *castor* (*cas*), which is present in iVUM4,5 and mVUM4,5, and (3) *CG16778* (also *Tyrosine kinase-related*; *Tkr*

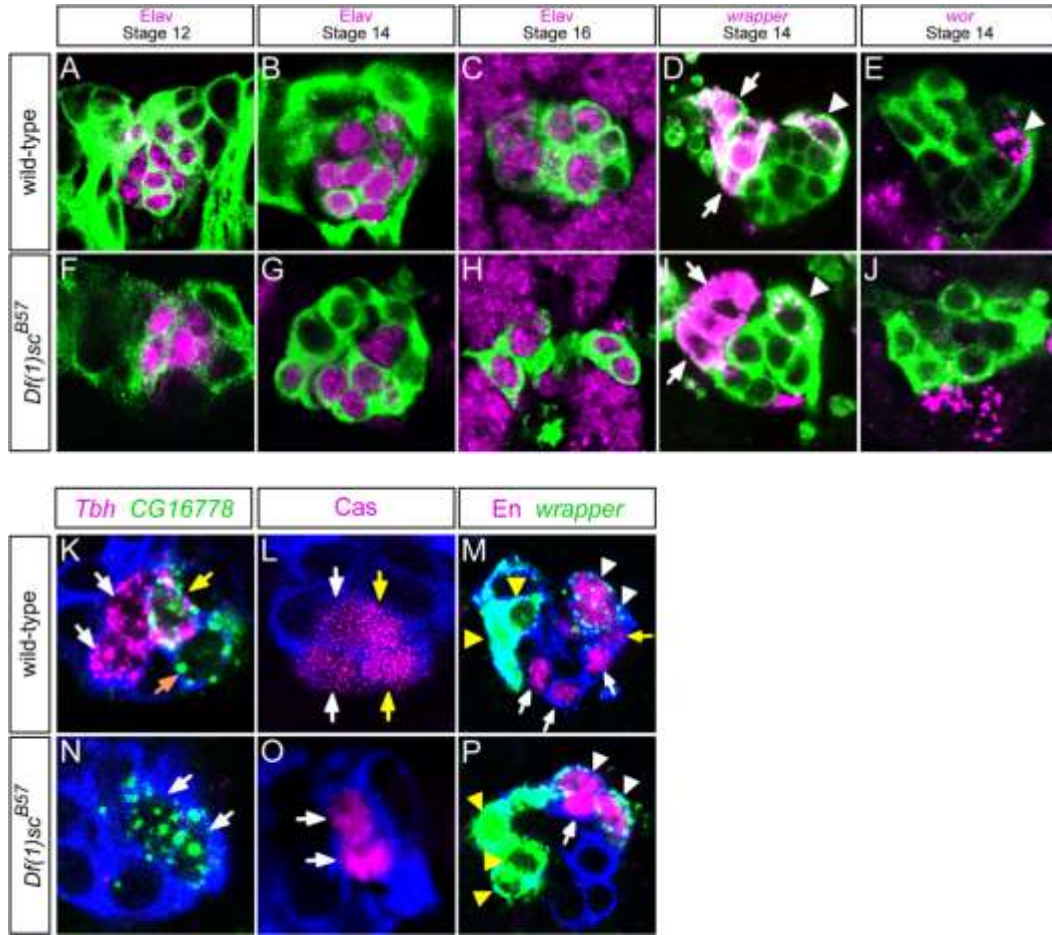


Figure 3.5. *l(1)sc* controls VUM neuron and MNB formation. Confocal images of (A-E,L,M) wild-type and (F-J,N,O) *Df(1)sc^{B57} sim-Gal4 UAS-tau-GFP* embryos are shown with the embryonic stages indicated at top. All views are sagittal, except (C,H), which are horizontal views. Embryos were stained with anti-GFP (A-J, green; L-O, blue). (A-C) In wild-type embryos, there were 10 *Elav*⁺ (magenta) neurons at stage 12, 14 *Elav*⁺ neurons at stage 14, and 16 *Elav*⁺ neurons at stage 16 (not all *Elav*⁺ neurons can be observed in the focal planes shown). (F-H) In *Df(1)sc^{B57}* embryos, there were 6 *Elav*⁺ neurons at stages 12, 14, and 16. (D,I) Expression of *wrapper* was high in AMG (arrows) and low in PMG (arrowheads) in both wild-type and *Df(1)sc^{B57}* embryos, and the same number of MG were present in wild-type and mutant. These results indicated that MG number, sub-type (AMG, PMG) and gene expression were not perturbed in *Df(1)sc^{B57}*. (E,J) Expression of *wor* was present in the MNB (arrowhead) in wild-type embryos, but was absent in *Df(1)sc^{B57}* embryos. (K) In wild-type, *CG16778* (green) was present in iVUM6 (yellow arrow) and mVUM6 (orange arrow). *Tbh* expression (magenta) marks the three mVUMs (white and yellow arrows). (N) In *Df(1)sc^{B57}*, 2 *CG16778*⁺ (green) cells (arrows) were present in 60% of segments. *Tbh* expression was absent. (L) In wild-type, *Cas* was present in mVUM4 and iVUM4 (white arrows), present at higher levels in mVUM5 and iVUM5 (yellow arrows), and absent in mVUM6 and iVUM6. (O) In *Df(1)sc^{B57}*, only 2 *Cas*⁺ cells (arrows; either VUM4s or VUM5s) were present in 50% of segments. (M) In wild-type, *En* (magenta) was present in *wrapper_{low}*⁺ (green) PMG (white arrow heads) and in the *wrapper*⁻ MNB (yellow arrow) and 3 mVUMs (white arrows). (P) In *Df(1)sc^{B57}* embryos, *En* was present in *wrapper_{low}*⁺ (green) PMG (white arrow heads) and in 1 *wrapper*⁻ cell (white arrow) which is likely to be an iVUM.

and Jim Lovell; *Lov*), which is expressed in iVUM6 and mVUM6. In *Df(1)sc^{B57}* mutant embryos, *Tbh* expression was absent in 82% of segments, and *CG16778* was absent in 40% of segments and present in 2 cells in 60% of segments (Fig. 3.5K,N). Cas protein was absent in 50% of segments, and reduced to only 2 cells in another 50% of segments (instead of 4 in wild-type) (Fig. 3.5L,O). While additional markers need to be discovered that can distinguish between different VUM neurons, the present results indicated that *l(1)sc* is required for formation of MP4-6 (*cas*, *CG16778*, *Elav*, and *nub/pdm2* results), and may also control mVUM cell-type specific gene expression (*Tbh* results). Regarding the latter point, expression of both *dgk* and *zfh1*, which are present in mVUMs, but not iVUMs, was absent in *Df(1)sc^{B57}* (Fig. S3.2A,B,D,E in the supplementary material), as was *Vmat* (Fig. 3.4K). However, iVUM-expressed genes, including *CG15236* and *en*, were not affected (Fig. S3.2C,F; Fig. 3.5M,P). The MG were present in normal numbers and both sub-types (AMG, PMG) were present in *Df(1)sc^{B57}* mutants, as determined by the presence of *wrapper*⁺ MG (Fig. 3.5D,I). The reduction of midline neurons observed in *Df(1)sc^{B57}* was not observed in *Df(1)sc¹⁰⁻¹* or *ase¹* (Fig. S3.1E,F in the supplementary material) and accordingly, is due to *l(1)sc*. In summary, *l(1)sc* is required for the formation of functional MP4-6s that can generate VUM neurons, but has no effect on the formation and division of MP1, MP3, and MG.

The *l(1)sc* gene plays an important proneural role in the formation of neuroblasts in the *Drosophila* embryonic CNS (Jimenez and Campos-Ortega, 1990). Since it is also prominently expressed in the MNB, we assayed *Df(1)sc^{B57}* embryos for defects in MNB formation by assaying for *wor* expression, a NB marker. Analysis of *Df(1)sc^{B57}* mutant embryos indicated that *wor* expression was absent from the MNB in 93% of segments

(Fig. 3.5E,J; Table 3.1). Expression of *wor* was unaffected in *ase^l* mutant embryos and in *Df(1)^{sc10-1}* mutant embryos no defects in cell number were seen, indicating that MNB formation was dependent on *l(1)sc* function. These results are consistent with the reduced number and identity of *Elav⁺* cells observed in *Df(1)sc^{B57}*; all were either MP1 neurons H-cell, H-cell sib and VUMs. The absence of *wor* expression and any apparent MNB progeny in *Df(1)sc^{B57}* indicated that *l(1)sc* is required for MNB formation, similar to its proneural role in the lateral CNS. Previous work indicated that a deficiency strain removing AS-C genes, including *l(1)sc* resulted in a reduction in *en⁺* midline cells, although the identity of both the affected and unaffected *en⁺* cells was not determined (Bossing and Brand, 2006). The *en⁺* cells in stage 12 or older embryos include iVUMs, MNB, MNB progeny, and PMG (Fig. 3.5 M,Q). In *Df(1)sc^{B57}* embryos, *en* remained on in 4 cells/segment, and these are *wrapper_{low}⁺*, indicating they are PMG (Fig. 3.5N,R). In addition, a single *wrapper⁻* cell was often observed, which is likely to be an iVUM. Thus, *l(1)sc* does not control *en* expression in PMG, even though it is expressed in PMG. Generally, only a single non-PMG *en⁺* cells was observed, which was not surprising, since we showed that most *en⁺* MPs, iVUMs, MNB, and MNB progeny were absent in *Df(1)sc^{B57}*. Thus, *l(1)sc* is required for formation of neural precursors, including MP4-6 and MNB, in the posterior region of the midline cells, but not in the anterior region, which includes MP1 and MP3.

***Tup* And *SoxN* Regulate Different Components of H-Cell Gene Expression**

L(1)sc protein is present in MP3, its newly-divided progeny (H-cell and H-cell sib), and then becomes restricted in expression to only H-cell. Genetically, *l(1)sc* influences expression of all H-cell-specific gene expression tested, but *L(1)sc* protein is

absent by the end of stage 11, which is before the neural function genes we tested are expressed. Thus, other H-cell-expressed transcription factors are required to control their expression. Potential candidates that could regulate H-cell gene expression are the transcription factors *BarH1*, *SoxN*, and *tup* (*sc* is removed from consideration since *Df(1)sc¹⁰⁻¹*, which removes *sc* function, does not affect expression of the H-cell genes tested). *Tup* is an attractive candidate because, like *L(1)sc*, it is expressed in H-cell and H-cell sib, before becoming localized to only H-cell (Fig. 3.2A-C) (Thor and Thomas, 1997). Unlike *L(1)sc*, *Tup* remains on in H-cell throughout embryonic development. Genetic analysis of *tup* mutant embryos indicated that *tup* function was required for *ple* and *DAT* expression (Fig. 3.6A,B,E,F) but *Vmat* and *NPFRI* were unaffected (Fig. 3.6A-C,E-G). Misexpression of *tup* in *sim-Gal4 UAS-tup* embryos failed to activate *ple* or *DAT* expression, revealing a difference in regulatory function compared to *l(1)sc* (data not shown). Since *tup* is expressed in transiently in H-cell sib, *tup* mutant embryos were analyzed for expression of *CG13565*, *sim*, and *Vglut*, which are expressed in H-cell sib in wild-type embryos. Expression of these 3 genes was unaffected (data not shown). In addition, expression of *pdm2/nub* and *5-HT1A*, which are expressed in both H-cell and H-cell sib, was unchanged between wild-type and *tup* (data not shown). These results indicated that *tup* regulates expression of two genes involved in dopamine biosynthesis and transport, but not other aspects of H-cell development, and consequently, has a more limited role than *l(1)sc*.

SoxN, one of the two *Drosophila* Sox2 family of transcription factors (Cremazy et al., 2000), was assayed for effects on H-cell transcription by analyzing *SoxN⁴* null

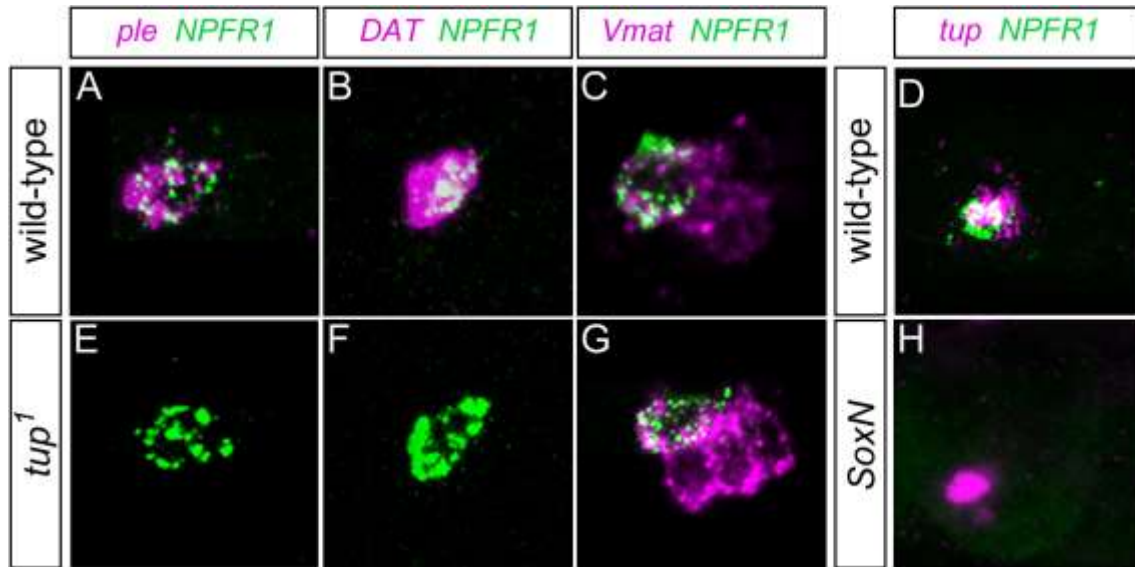


Figure 3.6. SoxN and Tup control aspects of H-Cell gene expression. Confocal images of stages 14-16 (A-D) wild-type, (E-G) *tup*¹ embryos, and (H) *SoxN* embryos. Compared to (A-D) wild-type embryos, *tup*¹ mutant embryos showed an absence of (E) *ple* and (F) *DAT* expression (magenta), but (E-G) *NPFR1* (green) and (G) *Vmat* (magenta) expression were not affected. In *tup*¹ mutants, *NPFR1* acts as a marker for H-cell. (C,G) *Vmat* (magenta) was present in both H-cell (*NPFR1*⁺; green) and mVUMs (*NPFR1*⁻; arrows) in *tup*¹. (D-H) Compared to wild-type, *SoxN* mutant embryos had an absence of *NPFR1* expression. Expression of *tup*, which is unaffected in *SoxN*, acts as an H-cell marker.

mutant embryos (Fig. 3.6D,H). Expression of the *NPFRI* neuropeptide receptor was absent in *SoxN^Δ* mutant embryos. The expression of *5-HT1A* or *Glu-RI*, another neurotransmitter receptor expressed in H-cell, was not affected in *SoxN* mutants. Expression of other H-cell expressed genes was unaffected in *SoxN* mutants, nor was additional expression observed in *sim-Gal4 UAS-SoxN* embryos (data not shown). While *l(1)sc* is required for much (if not all) H-cell gene expression, the SoxN and Tup transcription factors act downstream (and possibly parallel in the case of Tup) to regulate subsets of H-cell gene expression: a dopamine biosynthetic enzyme gene and membrane transporter in the case of Tup, and a neurotransmitter receptor in the case of SoxN.

Discussion

The MP3 cell divides asymmetrically to give rise to the H-cell and H-cell sib neurons. Whereas *Notch* signaling and *Su(H)* control the fate of H-cell sib, in this paper we propose that *l(1)sc* plays a major role in directing the fate of H-cell. In addition, the Tup and SoxN transcription factors play major roles in regulating aspects of H-cell neuronal differentiation.

L(1)sc and Tup are Preferentially Localized to H-cell and Control Neural Differentiation

The L(1)sc protein is present in MP3 and both H-cell and H-cell sib after MP3 division. However, L(1)sc levels quickly decline in H-cell sib, but persist in H-cell for the duration of stage 11. L(1)sc levels are undetectable after stage 11. Tup appears after

MP3 division in both H-cell and H-cell sib, and like *L(1)sc* soon becomes restricted to only H-cell. However, *Tup* persists in H-cell throughout the rest of embryonic development. Genetically, both transcription factors play important roles in controlling H-cell gene expression. However, our current data supports the view that *L(1)sc* acts as a master regulator of H-cell development, since it is genetically required for all H-cell specific gene expression, and can induce expression of H-cell-specific gene expression when misexpressed. In contrast, *Tup* is required only for expression of *DAT* and *ple*, but no other H-cell-specific gene expression, and is unable to activate H-cell gene expression in misexpression assays. Thus, *tup* has a more limited role in H-cell differentiation in comparison to *l(1)sc*. H-cell neural function gene expression begins at stage 14, well after *l(1)sc* expression is absent, indicating that *l(1)sc* is unlikely to directly regulate neural function gene expression. However, *Tup* is present and could directly regulate *DAT* and *ple*. This can be tested using biochemical approaches combined with transgenic enhancer analysis of *DAT* and *ple*.

The relationship between *l(1)sc* and *tup* is complex. Misexpression of *l(1)sc* resulted in the ectopic expression of *tup* in H-cell sib, similar to other H-cell specific genes. However, *l(1)sc* mutants did not result in absence of H-cell expression, but instead *tup* expression was either unaffected in H-cell or present in another cell in addition to H-cell. While the *l(1)sc* misexpression studies suggested that *l(1)sc* has the potential to positively regulate *tup* expression, the *l(1)sc* mutants suggested that *l(1)sc* represses *tup*, possibly in H-cell sib. The identity of the additional *tup*⁺ cell is likely to be H-cell sib, based on proximity to H-cell. However, the expression of *CG13565*, a good H-cell sib marker that is present in only 50% of wild-type segments, was absent in the additional

tup⁺ cells, suggesting that either *tup* negatively regulates H-cell sib gene expression or not enough segments were assayed to observe coexpression of *tup* and *CG13565*. Thus, paradoxically, while *l(1)sc* has the ability to activate transcription of *tup*, it appears to have little, if any role, in controlling its expression in H-cell, and may repress it in H-cell sib. While *l(1)sc* is required for all H-cell specific transcription, it does not repress H-cell sib transcription in H-cell (i.e. *l(1)sc* mutants do not results in a transformation of H-cell to H-cell sib, unlike mutants affecting *Notch* signaling that cause H-cell sib to H-cell transformations. Consequently, at least 3 distinct genetic programs control H-cell gene expression: (1) *l(sc)*, which control H-cell specific gene expression, (2) an unknown factor that represses H-cell sib gene expression, and (3) an unknown factor that controls gene expression present in both H-cell and H-cell sib.

Negative Regulation of L(1)Sc and Tup in H-cell sib and H-cell

One of the key aspects of H-cell gene expression is the restriction of both *l(1)sc* and *tup* to H-cell. Since both genes initially appear in both H-cell and H-cell sib, what triggers the reduction of their levels in H-cell sib? *Notch* signaling and repression by E(spl) are likely. Previous work demonstrated that *tup* expression in H-cell was duplicated in *spdo* mutants, which results in a loss of *Notch* signaling and a transformation of H-cell sib to H-cell sib (Wheeler et al., 2008). Similarly, *numb* mutants, which result in an H-cell to H-cell sib transformation, resulted in an absence of *tup* expression. It is likely that *Notch* signaling represses *l(1)sc* expression in H-cell sib, since proneural genes are targets of *Notch* signaling in other cell types, and proneural genes are directs targets of E(spl) and Notch signaling.

Active protein degradation may also reduce L(1)sc and Tup protein levels in H-cell sib, and L(1)sc in H-cell. For example, the Phyllopod/Seven-in-absentia components of the E3 ubiquitin ligase complex were shown to downregulate Ac and Sc proneural proteins levels during sensory cell development (Chang et al., 2008), and *phyl* is present in midline cells (as likely is *sina*, which is ubiquitously expressed). The degradation in H-cell sib is presumably under the control of *Notch* signaling, and degradation of the human hASH1 AS-C homolog is dependent on *Notch* signaling in cancer cells (Sriuranpong et al., 2002). It should also be noted that when misexpressed in all midline cells using *sim-Gal4*, *l(1)sc* is significantly more stable in midline glia (present at stage 14 and later) compared to midline neurons (absent by stage 12). This may reflect the presence of an active L(1)sc degradation activity in midline neurons that is absent in midline glia.

L(1)sc Selectively Controls Midline Precursor Formation

The formation of midline neural precursors is a dynamic, yet stereotypical process. Two distinct types of precursors are present: (1) MPs that only divide once into two neurons (and resemble ganglion mother cells (GMCs), and (2) the MNB, which divides asymmetrically into a self-renewing NB and a GMC, with each GMC dividing into 2 neurons. The MPs undergo cellular changes in which their nuclei delaminate from an apical position within the ectoderm and move to the basal (internal) surface. There they divide after orienting their spindles. The MPs arise in a distinct order: MP4→MP3→MP5→MP1→MP6→MNB (Wheeler et al., 2008). Key issues concern the identity of regulatory proteins controlling the timing and morphological changes that accompany delamination and division. *Drosophila* proneural proteins control the

formation of neuroblasts and sensory organ precursors (Bertrand et al., 2002). While *l(1)sc* is the major proneural gene controlling formation of embryonic neuroblasts (Jimenez and Campos-Ortega, 1990), relatively little is known regarding how it functions and the identity of relevant target genes. In one study, it was shown that morphological changes that accompany neuroblast formation were dependent on *l(1)sc* function (Stollewerk, 2000). All of the MPs express *l(1)sc*. However, analysis of *Df(1)sc^{B57}*, which lacks *l(1)sc* indicated that the formation of MP1 and MP3 were unaffected, whereas mutant embryos generally only had a single MP4, MP5, or MP6 cell. MP6 was absent in 40% of mutant embryos, and either MP4 or MP5 was absent in 50% embryos (these cells cannot be distinguished in *Df(1)sc^{B57}* embryos). While there is a correlation between levels of *L(1)sc* and MP formation (levels relatively low in MP1, MP3, and MP4; higher in MP5, MP6, and MNB), another possibility is that the origins of each cell type from different MP equivalence groups may dictate how neural precursor formation occurs. Despite the cell-type specific differences, our results provide strong evidence that *L(1)sc* acts to control both MP and MNB formation (proneural role) and in neuron-specific gene regulation (differentiation role)

Although *sc* it is expressed in all MPs except MP4 and *ac* is prominently expressed in MP1, neither has an effect on MP or MP neuron formation, since *Df(1)^{sc10-1}*, which deletes both genes, showed no defects in MP or midline neuron formation. The roles of *ac* and *sc* in midline development remain unknown, and despite the presence of *sc* in H-cell after stage 14, it does not influence H-cell neural function gene expression. Interestingly, the non-midline MP2 cell requires both *ac* and *sc* for MP formation and neuronal differentiation, whereas *l(1)sc* does not play a role in MP2 development, nor can

it compensate for *ac* and *sc* in transgenic rescue experiments. Thus, whereas MP2 and MP4-6 require proneural bHLH activity to form, they utilize different combinations of AS-C family members.

It was proposed that MP2 is transformed into a neuroblast in an *ac sc* double mutant (Skeath, J.B. 1996). This is unlikely to be the case for the MP4-6 cells in *Df(1)sc^{B57}*, since no *wor*⁺ NBs, including the MNB, were detected in mutant embryos. Most noteworthy, is that despite the expression of *l(1)sc* in MP1 and MP3, it is not required for formation of either cell type or its progeny, in contrast to MP4-6. It will be important to understand what factors substitute for *l(1)sc* to control MP1 and MP3 formation, and whether the regulation and expression of *l(1)sc* in MP4-6 controls the timing of their formation.

Defining H-Cell Gene Expression

While *l(1)sc* is required for all H-cell specific gene expression, *tup* function is required for only *ple* and *DAT* expression, and *SoxN* only for *NPFR1* expression. Since both overlap in expression with the genes they regulate, it is possible that they directly regulate their genetic target genes. Neither is required for *Vmat* expression. In addition, genes expressed in both H-cell and H-cell sib (*Glu-RI*, *5-HT1A*; *pdm2*, *nub*) are not dependent on *l(1)sc*, *sc*, *SoxN*, or *tup*, and thus are under the control of a different regulatory system. Thus, H-cell gene-specific gene expression is dependent on *l(1)sc* and additional H-cell gene expression is dependent on additional unknown regulatory inputs. Since *ple*, *DAT*, *Ddc*, and VMAT are all involved in DA metabolism, it might be

expected that their corresponding genes would be directly regulated by the same transcription factors. In fact, this is what was observed in *C. elegans*, in which all were directly regulated by *ast-1* (Flames et al., 2009). In the case of H-cell, *tup* genetically regulates *ple* and *DAT*, but, surprisingly, not *Vmat*. Since different DA neurons may contain a different complement of neurotransmitter receptors, it is perhaps expected that different transcription factors will control their expression. In the case of H-cell, *SoxN* controls *NPFRI* expression, but not expression of the other H-cell-expressed genes assayed, including the *Glu-RI* and *5-HT1A* receptor genes. Future work will involve genetically identifying additional regulatory proteins activating H-cell gene expression, as well as the repression of H-cell-sib gene expression in H-cell, and then understanding biochemically how these proteins function together to directly regulate gene expression.

Evolutionary Aspects of *Drosophila* Dopaminergic Neuron Regulation

Because of the key neurobiological and medical importance of dopaminergic neurons, there has been intensive analysis of the regulatory factors that control their development in vertebrates and *C. elegans*. Two issues regarding evolutionary similarities exist: anatomical homology and conservation of gene regulatory mechanisms. While it is difficult to assess evolutionary homology, in both insects and vertebrates there are dopaminergic neurons residing at the midline of the CNS. In vertebrates, there are DA neurons that comprise the ventral tegmental area (emotional and reward behaviors), substantia nigra (motor control), and retrorubral region. When neurons of the substantia nigra that project to the striatum degenerate, Parkinson's disease ensues.

The two key regulatory proteins that control H-cell differentiation are *l(1)sc* and *tup*. In vertebrates the bHLH genes *Mouse achaete-scute homolog* (*Mash1*; homolog of *l(1)sc*) and *Neurogenin 2* (*Ngn2*) play roles in midbrain DA neuron development, although the role of *Mash1* is secondary to *Ngn2*, which has a key function in DA differentiation (Kele et al., 2006). In contrast, *Mash1* (as well as *Ngn2*) can initiate neurogenic programs of other neuronal cell types. This was emphatically demonstrated in recent work in which forced expression of *Mash1* and two other transcription factor genes converted murine fibroblast cells to neurons (Vierbuchen et al., 2010). Thus, while both vertebrate and insect bHLH proteins regulate DA neuron development, their precise roles and target genes likely differ.

Recently, the *C. elegans ast-1* ETS family transcription factor gene was shown to directly regulate 5 worm DA pathway genes (Flames and Hobert, 2009). In vertebrates, the related *Etv1* (and possibly *Etv5*) ETS gene also functions in controlling DA gene expression (Flames and Hobert, 2009), demonstrating an impressive evolutionary link. In *Drosophila*, there are 8 ETS proteins (Hsu and Schulz, 2000), and it unknown whether any are expressed in DA neurons or function in regulating DA cell differentiation. This needs to be tested, since it would be surprising if *C. elegans* and mammals both utilized ETS transcription factors to regulate DA neuron gene expression, and *Drosophila* did not. Whether ETS proteins or other *Drosophila* regulatory proteins, such as *Tup*, it will be important to identify the regulatory proteins directly regulating *Drosophila* H-cell gene expression.

Acknowledgements

The authors are grateful to Jim Skeath and Stefan Thor for reagents and advice. We thank the Developmental Studies Hybridoma Bank for monoclonal antibodies and The Bloomington Drosophila Stock Center for *Drosophila* strains. This work was supported by NIH grant R37 RD25251 to S.T.C., an NIH/UNC SPIRE fellowship to A.R.G, and a UNC Developmental Biology NIH training grant fellowship to S.B.S.

Supplemental Figures

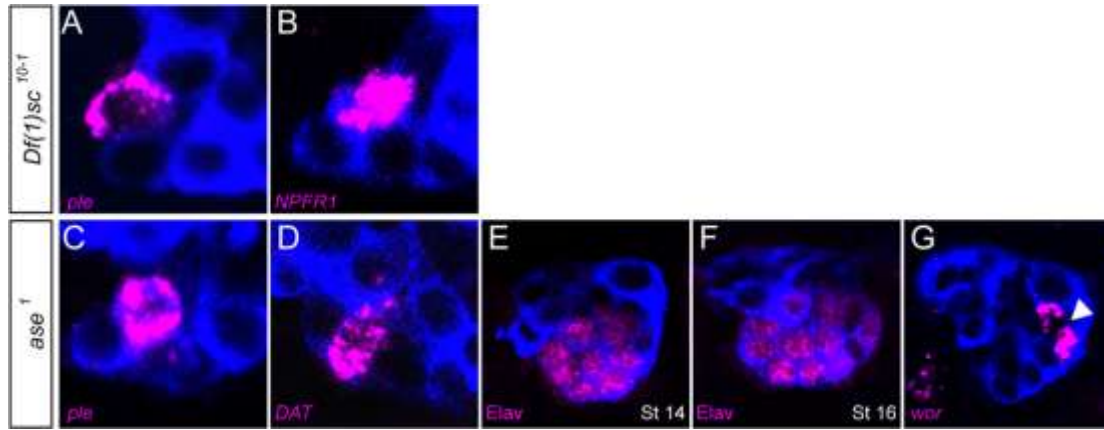


Figure S3.1. *ac*, *sc*, and *ase* do not affect H-cell gene expression. Sagittal views of (A,B) *Df(1)sc¹⁰⁻¹* and (C-G) *ase¹ sim-Gal4 UAS-tau-GFP* embryos at stages 14-16. In *Df(1)sc¹⁰⁻¹* mutant embryos, (A) *ple* and (B) *NPFR1* expression (magenta) were present in H-cell at wild-type levels. In *ase¹* mutant embryos, (C) *ple* and (D) *DAT* (magenta) were present in H-cell. (E-F) In *ase¹* embryos, there were 14 *Elav⁺* (magenta) neurons at stage 14 and 16 *Elav⁺* neurons at stage 16 (not all *Elav⁺* neurons can be observed in the focal planes shown) which is comparable to wild-type. (G) Expression of *wor* (magenta) was present in the MNB (arrowhead) at wild-type levels.

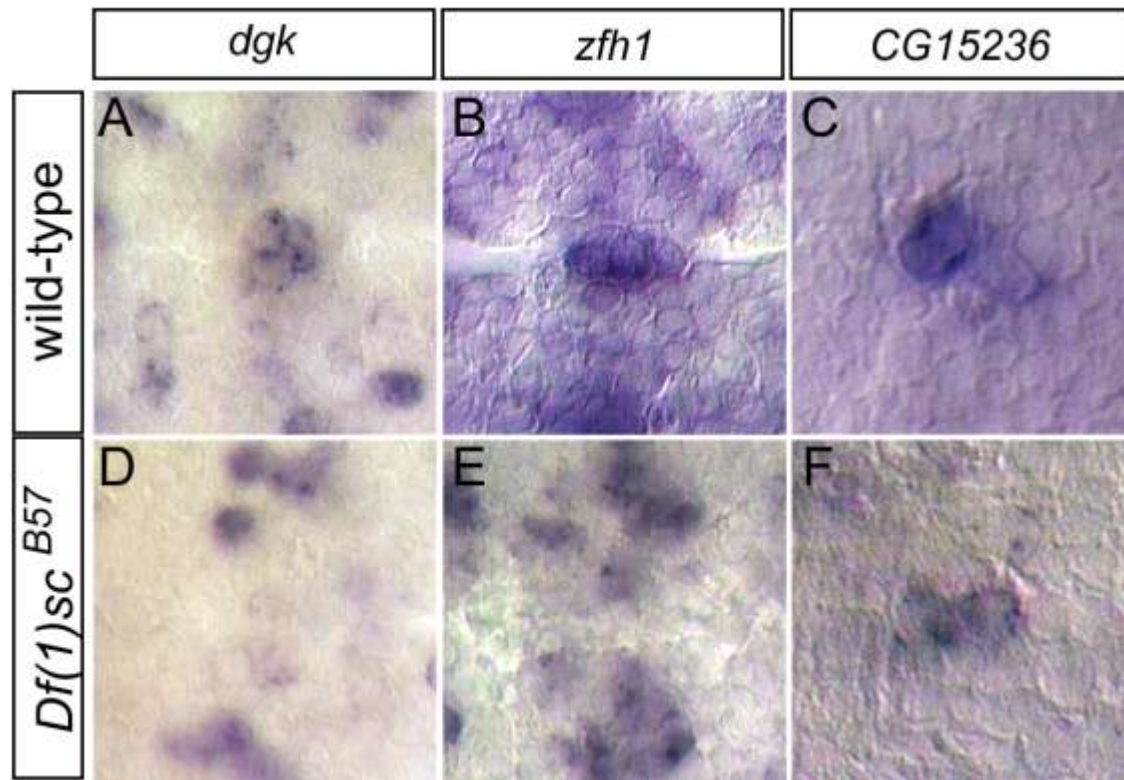


Figure S3.2. *l(1)sc* affects mVUM, but not iVUM, gene expression. Horizontal views of stage 14 (A-C) wild-type and (D-F) *Df(1)sc^{B57}* mutant embryos hybridized in situ to the mVUM-expressed genes: (A,D) *dgk*, (B,E) *zfh1*, and iVUM-expressed gene, (C,F) *CG15236*. In the mutant, *dgk* and *zfh1* midline expression was absent, but *CG15236* expression was present.

References

- Alonso, M. C. and Cabrera, C. V.** (1988). The achaete-scute gene complex of *Drosophila melanogaster* comprises four homologous genes. *EMBO J.* **7**, 2585-2591.
- Bertrand, N., Castro, D. S. and Guillemot, F.** (2002). Proneural genes and the specification of neural cell types. *Nat. Rev. Neurosci.* **3**, 517-530.
- Bossing, T. and Brand, A. H.** (2006). Determination of cell fate along the anteroposterior axis of the *Drosophila* ventral midline. *Development* **133**, 1001-1012.
- Bossing, T. and Technau, G. M.** (1994). The fate of the CNS midline progenitors in *Drosophila* as revealed by a new method for single cell labelling. *Development* **120**, 1895-1906.
- Brand, M., Jarman, A. P., Jan, L. Y. and Jan, Y. N.** (1993). asense is a *Drosophila* neural precursor gene and is capable of initiating sense organ formation. *Development* **119**, 1-17.
- Broihier, H. T. and Skeath, J. B.** (2002). *Drosophila* homeodomain protein dHb9 directs neuronal fate via crossrepressive and cell-nonautonomous mechanisms. *Neuron* **35**, 39-50.
- Budnik, V. and White, K.** (1988). Catecholamine-containing neurons in *Drosophila melanogaster*: distribution and development. *J. Comp. Neurol.* **268**, 400-413.
- Buescher, M., Hing, F. S. and Chia, W.** (2002). Formation of neuroblasts in the embryonic central nervous system of *Drosophila melanogaster* is controlled by SoxNeuro. *Development* **129**, 4193-4203.
- Campuzano, S. and Modolell, J.** (1992). Patterning of the *Drosophila* nervous system: the achaete-scute gene complex. *Trends Genet.* **8**, 202-208.

- Chang, P. J., Hsiao, Y. L., Tien, A. C., Li, Y. C. and Pi, H.** (2008). Negative-feedback regulation of proneural proteins controls the timing of neural precursor division. *Development* **135**, 3021-3030.
- Cremazy, F., Berta, P. and Girard, F.** (2000). Sox neuro, a new Drosophila Sox gene expressed in the developing central nervous system. *Mech. Dev.* **93**, 215-219.
- Crews, S. T.** (1998). Control of cell lineage-specific development and transcription by bHLH-PAS proteins. *Genes Dev.* **12**, 607-620.
- Dominguez, M. and Campuzano, S.** (1993). asense, a member of the Drosophila achaete-scute complex, is a proneural and neural differentiation gene. *EMBO J.* **12**, 2049-2060.
- Flames, N. and Hobert, O.** (2009). Gene regulatory logic of dopamine neuron differentiation. *Nature* **458**, 885-889.
- Garcia-Bellido, A.** (1979). Genetic Analysis of the Achaete-Scute System of DROSOPHILA MELANOGASTER. *Genetics* **91**, 491-520.
- Gonzalez, F., Romani, S., Cubas, P., Modolell, J. and Campuzano, S.** (1989). Molecular analysis of the asense gene, a member of the achaete-scute complex of Drosophila melanogaster, and its novel role in optic lobe development. *EMBO J.* **8**, 3553-3562.
- Goodman, C. S., Bate, M. and Spitzer, N. C.** (1981). Embryonic development of identified neurons: origin and transformation of the H cell. *J. Neurosci.* **1**, 94-102.
- Hsu, T. and Schulz, R. A.** (2000). Sequence and functional properties of Ets genes in the model organism Drosophila. *Oncogene* **19**, 6409-6416.
- Jimenez, F. and Campos-Ortega, J. A.** (1990). Defective neuroblast commitment in mutants of the achaete-scute complex and adjacent genes of D. melanogaster. *Neuron* **5**, 81-89.

- Kambadur, R., Koizumi, K., Stivers, C., Nagle, J., Poole, S. J. and Odenwald, W. F.** (1998). Regulation of POU genes by castor and hunchback establishes layered compartments in the Drosophila CNS. *Genes Dev.* **12**, 246-260.
- Kearney, J. B., Wheeler, S. R., Estes, P., Parente, B. and Crews, S. T.** (2004). Gene expression profiling of the developing Drosophila CNS midline cells. *Dev Biol* **275**, 473-92.
- Kele, J., Simplicio, N., Ferri, A. L., Mira, H., Guillemot, F., Arenas, E. and Ang, S. L.** (2006). Neurogenin 2 is required for the development of ventral midbrain dopaminergic neurons. *Development* **133**, 495-505.
- Overton, P. M., Meadows, L. A., Urban, J. and Russell, S.** (2002). Evidence for differential and redundant function of the Sox genes Dichaete and SoxN during CNS development in Drosophila. *Development* **129**, 4219-4228.
- Reig, G., Cabrejos, M. E. and Concha, M. L.** (2007). Functions of BarH transcription factors during embryonic development. *Dev. Biol.* **302**, 367-375.
- Schmid, A., Chiba, A. and Doe, C. Q.** (1999). Clonal analysis of Drosophila embryonic neuroblasts: neural cell types, axon projections and muscle targets. *Development* **126**, 4653-4689.
- Sriuranpong, V., Borges, M. W., Strock, C. L., Nakakura, E. K., Watkins, D. N., Blaumueller, C. M., Nelkin, B. D. and Ball, D. W.** (2002). Notch signaling induces rapid degradation of achaete-scute homolog 1. *Mol. Cell. Biol.* **22**, 3129-3139.
- Stollewerk, A.** (2000). Changes in cell shape in the ventral neuroectoderm of Drosophila melanogaster depend on the activity of the achaete-scute complex genes. *Dev. Genes Evol.* **210**, 190-199.
- Thor, S. and Thomas, J. B.** (1997). The Drosophila islet gene governs axon pathfinding and neurotransmitter identity. *Neuron* **18**, 397-409.

Vierbuchen, T., Ostermeier, A., Pang, Z. P., Kokubu, Y., Sudhof, T. C. and Wernig, M. (2010). Direct conversion of fibroblasts to functional neurons by defined factors. *Nature* **463**, 1035-1041.

Wheeler, S. R., Kearney, J. B., Guardiola, A. R. and Crews, S. T. (2006). Single-cell mapping of neural and glial gene expression in the developing *Drosophila* CNS midline cells. *Dev Biol* **294**, 509-524.

Wheeler, S. R., Stagg, S. B. and Crews, S. T. (2008). Multiple Notch signaling events control *Drosophila* CNS midline neurogenesis, gliogenesis and neuronal identity. *Development* **135**, 3071-3079.

Wheeler, S. R., Stagg, S. B. and Crews, S. T. (2009). MidExDB: a database of *Drosophila* CNS midline cell gene expression. *BMC Dev. Biol.* **9**, 56.

CHAPTER IV

MidExDB: A DATABASE OF *DROSOPHILA* CNS MIDLINE CELL GENE EXPRESSION

Scott R Wheeler, Stephanie B Stagg and Stephen T Crews[§]

Doctoral student participated in the design of the web pages and their content.

Published in BMC Developmental Biology

Program in Molecular Biology and Biophysics

Department of Biochemistry and Biophysics

The University of North Carolina at Chapel Hill

Chapel Hill, NC 27599-3280

[§]Corresponding author

Email addresses:

Scott R Wheeler – wheelers@email.unc.edu

Stephanie B Stagg – sstagg@med.unc.edu

Stephen T Crews – steve_crews@unc.edu

Abstract

Background

The *Drosophila* CNS midline cells are an excellent model system to study neuronal and glial development because of their diversity of cell types and the relative ease in identifying and studying the function of midline-expressed genes. In situ hybridization experiments generated a large dataset of midline gene expression patterns. To help synthesize these data and make them available to the scientific community, we developed a web-accessible database.

Description

MidExDB (*Drosophila* CNS Midline Gene Expression Database) is comprised of images and data from our in situ hybridization experiments that examined midline gene expression. Multiple search tools are available to allow each type of data to be viewed and compared. Descriptions of each midline cell type and their development are included as background information.

Conclusion

MidExDB integrates large-scale gene expression data with the ability to identify individual cell types providing the foundation for detailed genetic, molecular, and biochemical studies of CNS midline cell neuronal and glial development and function. This information has general relevance for the study of nervous system development in other organisms, and also provides insight into transcriptional regulation.

Background

The neurons and glia that comprise the *Drosophila* CNS midline cells are an excellent model system to study neurogenesis and gliogenesis (Jacobs, 2000; Kearney et al., 2004). This is due to their highly recognizable location at the midline of the embryo, small number of cells, diversity of cell types, large number of identified genes and associated expression patterns, and the ability to identify individual cell types across embryonic development. In each ganglion, there are ~18 midline neurons including glutamatergic/octopaminergic motoneurons, peptidergic motoneurons, dopaminergic interneurons, and glutamatergic interneurons (Wheeler et al., 2006). There are two molecularly distinct populations of midline glia (MG): the anterior MG (AMG) ensheath the commissural axons that cross the midline and the posterior MG (PMG) have unknown function. Study of the midline cells has been instrumental in studying programmed cell death, the role of the Single-minded (Sim) master regulatory transcription factor protein, neuronal and glial cell fate, neuron-glia interactions, and how diffusible factors control axon guidance. The insect midline cells strongly resemble the floorplate cells that reside at the midline of the vertebrate spinal cord (Jacobs, 2000). Both the *Drosophila* midline cells and vertebrate floorplate cells are important embryonic signaling centers – in *Drosophila*, the midline cells are a source of signals responsible for axon commissure formation, muscle cell migration, and the formation of the ventral epidermis and mesodermal dorsal median cells.

While *Drosophila* midline cell gene expression has been studied for over 20 years, a major advance was a large-scale in situ hybridization screen, in which the

midline expression patterns of 224 genes were identified and documented throughout embryonic development (Figures 4.1A) (Kearney et al., 2004). The genes analyzed were identified based on a variety of approaches, including enhancer trap screens, microarray experiments, the existing scientific literature, and in situ hybridization screens, including midline-expressed genes identified from the Berkeley Drosophila Genome Project (BDGP) embryonic in situ hybridization gene expression database (Tomancak et al., 2002). These data are referred to as “AP data”, since the in situ-hybridized embryos were stained using alkaline phosphatase (AP) histochemistry and imaged by differential interference contrast (DIC) microscopy. Subsequently, the expression of 77 genes was mapped at 5 stages of embryonic development using multi-label fluorescence confocal microscopy (Figure 4.1B) (Wheeler et al., 2006; Wheeler et al., 2008). These fluorescent data are referred to as “confocal data”. The confocal data provided the ability to: (1) identify individual midline cell types at all stages of embryonic development, (2) analyze how gene expression changes in individual cells during development, and (3) carry-out sophisticated genetic experiments for studying midline cell gene function and transcriptional circuitry. In addition, this work provided key insights allowing a refinement of how midline cells develop (Wheeler et al., 2008). Consequently, to facilitate the ability of the scientific community to access and use both types of midline gene expression data, we created a web-based searchable database, MidExDB (*Drosophila* CNS Midline Gene Expression Database; <http://www.unc.edu/~crews/MidExDB> or accessible from the Crews Lab home page at <http://www.unc.edu/~crews>). MidExDB contains CNS midline cell gene expression data at both low-resolution (AP data) and high-resolution (confocal data).

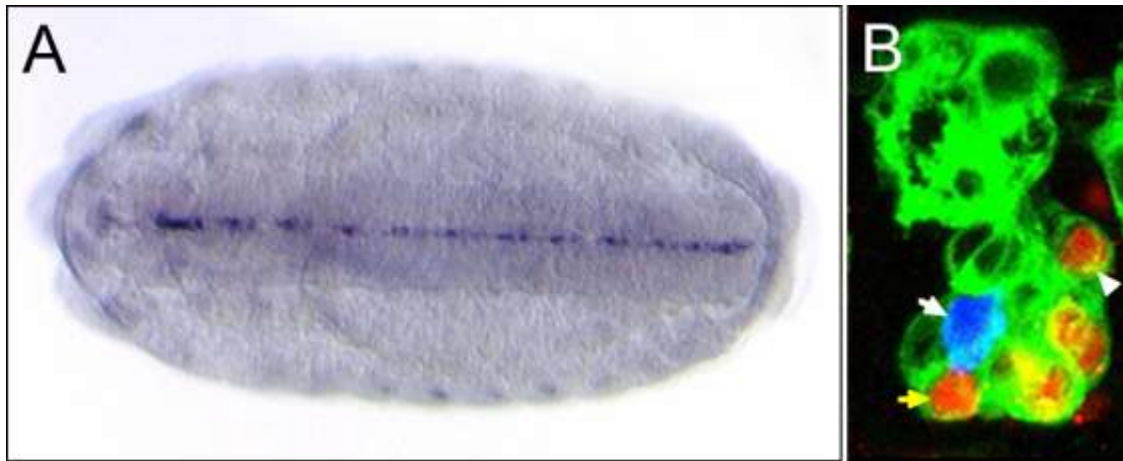


Figure 4.1. CNS midline gene expression. (A) In situ hybridization (AP histochemistry) of the *Poly-glutamine tract binding protein 1 (PQBP-1)* gene at stage 15 of embryonic development showing prominent midline cell expression. Ventral view; anterior left. (B) Sagittal view of a *sim-Gal4 UAS-tau-GFP* embryo at stage 17, in which *tau-GFP* is expressed in all midline cells and facilitates midline cell identification by confocal microscopy. The embryo was immunostained with: (1) anti-GFP (green) to visualize the cytoplasm of all midline cells and (2) anti-Engrailed (red), which stains the nuclei of ventral unpaired median interneurons (iVUMs; yellow arrow points to 1 iVUM), median neuroblast (MNB), and MNB neuronal progeny (arrowhead points to 1 MNB progeny). The embryo was also hybridized to a probe for *pale* (blue) which stains the H-cell (white arrow). Dorsal top; anterior left.

Construction and content

MidExDB is a relational database created using Microsoft SQL server 2000 and Visual Studio. At the top of each page, there is a navigation bar with links and pull-down menus entitled: Home, Confocal Query Tool, Cell Types, Development, and Information (Figure 4.2). The Home page provides access to AP and Confocal data searches. The Confocal Query Tool allows the user to search for cell-type and stage-specific gene expression data. The Cell Type and Development menus provide links describing the individual midline cell types and summaries of developmental events. The Information menu includes links to Help, Protocols, References, the Crews Lab homepage, and email address.

AP or confocal data is retrieved from MidExDB using one of the search modes on the Home page (described in detail in Utility and discussion section). For example, when using Gene Search to find a gene (Figure 4.2A), the resulting Images link returns DIC images of whole-mount AP in situ hybridization gene expression data arranged by stage. The Confocal link returns a tabular summary of confocal expression data and a link to the raw data displayed as movies.

AP data. MidExDB currently contains 6987 images acquired from in situ hybridization experiments documenting the embryonic expression patterns of 286 identified midline-expressed genes. All images in MidExDB were derived from wild-type embryos. The 286 genes include the previously-published 249 (Kearney et al., 2004; Wheeler et al., 2006; Wheeler et al., 2008) and an additional 37 genes reported here (Table 4.1). Hybridization was visualized using a histochemical AP-NBT/BCIP reaction





Table 4.1. Midline-expressed genes newly added to MidExDB.

Symbol	Function	Symbol	Function
α -Adaptin	Signaling	<i>Hsp27</i>	Chaperone
<i>ac</i>	Transcription factor	<i>KrT95D</i>	Metabolism
<i>CG11347</i>	Unknown	<i>Lis-1</i>	Cytoskeleton
<i>CG13248</i>	Transporter	<i>lola</i>	Transcription factor
<i>CG14968</i>	Unknown	<i>mid</i>	Transcription factor
<i>CG15117</i>	Metabolism	<i>nuf</i>	Cytoskeleton
<i>CG2893</i>	Neural function	<i>oc</i>	Transcription factor
<i>CG31088</i>	Unknown	<i>Oli</i>	Transcription factor
<i>CG6044</i>	Unknown	<i>Proct</i>	Neural function
<i>CG6847</i>	Metabolism	<i>Pvf2</i>	Signaling-receptor
<i>CG9336</i>	Unknown	<i>shal</i>	Neural function
<i>CG9743</i>	Metabolism	<i>slim</i>	Cytoskeleton
<i>ck</i>	Cytoskeleton	<i>spi</i>	Signaling
<i>cry</i>	Circadian rhythms	<i>sqz</i>	Transcription factor
<i>ct</i>	Transcription factor	<i>sty</i>	Signaling
<i>Gp150</i>	Signaling	<i>ush</i>	Transcription factor
<i>grim</i>	Apoptosis	<i>Vmat</i>	Neural function-transporter
<i>gsb</i>	Transcription factor	<i>W</i>	Apoptosis
<i>hbs</i>	Adhesion		

and examined by DIC microscopy (Kearney et al., 2004). For many genes, images are provided at each stage of development from stages 5 to 17. Midline expression in an individual embryo is often shown at multiple magnifications ranging from 12.5X to 100X. DIC imaging of AP histochemically-stained whole-mount embryos allows for analysis of midline gene expression in a large number of embryos at many stages. This is particularly useful for describing the temporal component of gene expression. However, they also provide insight into which midline cells express the gene, such as determining whether they are expressed in all midline cells or a subset of cells. In the mature CNS, it can often be determined whether the gene is expressed in MG or midline neurons based on their positions. However, it is difficult to assign with certainty exactly in which midline cell types the gene is expressed, particularly at earlier stages of development, such as stages 10-11. In this regard, confocal analysis (described under Confocal data) can determine exactly in which cell type a gene is expressed.

To categorize midline gene expression of AP data, a controlled vocabulary containing both temporal and cell-type terms was used, and is described in detail under the “Images” Help topic located on the Help page (the controlled vocabulary only applies to the AP data and not confocal data, since the confocal data determines gene expression precisely at the single-cell level). Temporally, midline cell development is subdivided into 3 major time periods: mesectoderm (stages 5-8), midline primordium (stages 9-12), and mature midline (stages 13-17). Regarding cell type, different terms were assigned for each developmental period. For the mesectoderm and midline primordium time periods, there are only two descriptors: all midline cells or a subset. As an example, several representative images corresponding to the *sim* gene are shown (Figure 4.3A). The

A *single-minded (sim)*

	stage 5	stage 6	stage 11	stage 17
				
AP data	mesectoderm: all	mesectoderm: all	midline primordium: all	mature midline: MG, neurons
confocal data	none	none	AMG, PMG, MPI neurons, H-cell, H-cell sib, all VUM neurons, MNB	AMG, PMG, H-cell sib, IVUM4, IVUM5, IVUM6, PNB, MNB progeny

B Dopamine transporter (*DAT*)

	stage 16	stage 17
		
AP data	mature midline: neurons	mature midline: neurons
confocal data	none	H-cell

C *CG11902*

	stage 12	stage 16
		
AP data	midline accessory: MM-CBG	midline accessory: CG
confocal data	none	none

D *CG6225*

Figure 4.3. Gene expression during midline cell development. Representative MidExDB images from multiple stage of embryonic development are shown for (A) *sim*, (B) *DAT*, (C) *CG11902*, and (D) *CG6225*. The *sim* and *DAT* genes are expressed in midline cells derived from *sim*⁺ mesectodermal cells, whereas *CG11902* and *CG6225* are expressed in midline accessory cells. *CG11902* is expressed in medial most-cell body glia (MM-CBG) and *CG6225* is expressed in channel glia (CG). Ventral and sagittal views are shown at either low (12.5X) or high (50X) magnification. Below each image is a description of its expression, both for AP data and for the confocal data. Stage 16 ventral views of *DAT* show its midline localization.

annotation indicates that *sim* is expressed in all midline cells during the mesectoderm and midline primordium periods. For the mature midline stages, gene expression was divided into three categories: midline cells, midline accessory cells, and apoptotic cells (Kearney et al., 2004). The midline cells include the midline neurons and MG that are derived from the *sim*⁺ mesectodermal cells. For example, both the *sim* gene and the *Dopamine transporter (DAT)* gene are expressed in midline neurons, while *sim* is also expressed in MG (Figure 4.3A, B). Midline accessory cells reside at the midline, but are not derived from the *sim*⁺ mesectodermal cells, and instead originate from either the lateral CNS or the mesoderm. These include the medial most-cell body glia (MM-CBG; Figure 4.3C), channel glia (CG; Figure 4.3D), and dorsal median cells. Apoptotic cells are dying cells that lie between the CNS and epidermis. Both temporal and cell type subcategories can be searched and compared in MidExDB.

Confocal data. Selecting “Confocal” from Gene Search (Figure 2A) returns a dataset (Figure 2B) derived from confocal imaging of fluorescence in situ hybridization and immunostaining data (Wheeler et al., 2006; Wheeler et al., 2008). These data have single-cell resolution, and gene expression was assigned to individual cell types by colocalization with cell type-specific markers. Five embryonic stages (9, 10, 11, 13, and 17) were selected for analysis because they correspond to periods of major midline developmental changes. The confocal data currently exists for 77 genes, and is represented by a text summary describing expression in each midline cell type at each stage examined (Figure 4.2B). QuickTime movies generated from the 3-dimensional stacks (Z-series) for each gene can be viewed by selecting the “Images available” link above the confocal text summary (Figure 4.2B). The confocal experiments page opens

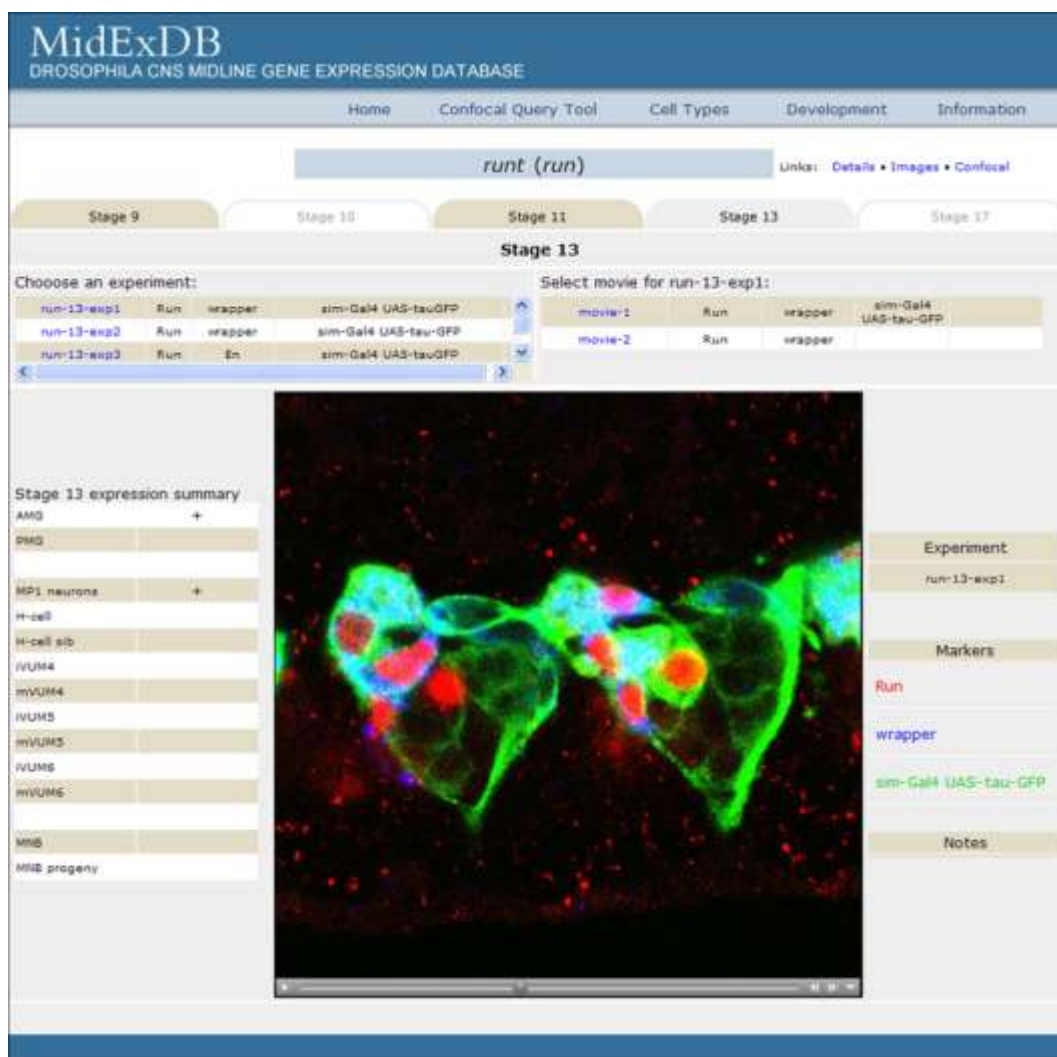


Figure 4.4. Movies of confocal data. Upon selecting the “Images available” link on the confocal data page (Figure 2B), a confocal experiments page opens. Selecting a tab matching a developmental stage reveals a list of experiments, each corresponding to a separate Z-series stack. The antibodies and probes employed in the confocal stack are indicated for each experiment. Selection of an experiment lists one or more movies derived from that stack with markers to the right. Selection of a movie link results in a QuickTime movie appearing in a window. The color-coded in situ probes or antibodies are listed to the right of the movie. The control bar underneath the movie allows the user to manually scroll through the movie. In the example shown, the *sim-Gal4 UAS-tau-GFP* embryo was stained for Run protein (red), *wrapper* RNA (blue), and GFP (green). The table to the left of the movie summarizes the data for each gene at the selected stage assembled from all experiments, not just the Z-series shown.

(Figure 4.4), and different experiments are listed for each stage of development. There are often multiple experiments (Z-series stacks) for each stage. Upon selecting a particular experiment, links to QuickTime movies appear and can be viewed. The in situ probes and antibodies are listed to the right of each movie. After a movie is selected and appears in the movie window, there is a control bar at the bottom of the movie that allows the choice of playing the movie or pausing on individual frames. Figure 4.4 shows an image that displays *run* (*run*) expression at stage 13. In this movie, the labels depict Run protein, *wrapper* RNA, and midline cells visualized by anti-GFP staining of a *sim-Gal4 UAS-tau-GFP* embryo (Wheeler et al., 2006). Anti-GFP staining of *sim-Gal4 UAS-tau-GFP* embryos allows specific visualization of all midline cells from stage 10-17, and greatly enhances midline cell identification (Wheeler et al., 2006). In this movie, Run was shown to colocalize with *wrapper*. Since *wrapper* is strongly expressed in AMG and weakly in PMG at stage 13, this indicated that *run* is expressed in AMG, as indicated to the left of the movie. Additional experiments with other markers indicated that *run* is also present in midline precursor 1 (MP1) neurons. These movies are intended to provide the original data that cell type-specific expression assignments for each gene were based, as well as assist other labs interested in studying the *Drosophila* midline cells.

Summary of midline gene expression data. The 286 midline-expressed genes can be grouped by expression and function. There are 44 genes expressed during the mesectodermal period, 162 at the midline primordium stage, and 198 in mature midline cells (these numbers do not include those genes with potential or uncertain midline expression). Of the genes expressed in mature midline cells, 54 are expressed in MG, 137 in midline neurons, 6 in both, and for 9 genes, the expression cannot be unambiguously

assigned. There are 34 genes expressed in midline accessory cells, and 4 present in apoptotic cells dying at the midline. Regarding function, the largest group of genes is concerned with transcription, including 83 members. There are 50 genes listed as cell signaling, and 26 are neural function genes, which encode neurotransmitter biosynthetic enzymes, neuropeptides, membrane transporters, vesicular transporters, and neurotransmitter receptors. The remaining genes are currently partitioned into an additional 21 classes. Previously, we estimated that the 286 midline-expressed genes in this database likely represented >50% of the genes expressed in midline cells (this does not generally include broadly-expressed genes also present in midline cells) (Kearney et al., 2004).

Utility and discussion

Search modes. MidExDB has two major search modes: basic data searches and the confocal query tool. The basic data searches return information from AP data and confocal data, while the confocal query tool returns information based on expression in specific cell types. For convenience, the basic data searches (Category, Gene, and Quick) are located on the MidExDB Home page, and the confocal query tool can be accessed on the navigation menu (Figure 4.2A). Under Category Search, the user can choose to list genes based on: (1) Gene Data (name, symbol or short name, CG#, protein type, or function), (2) Expression Data (AP data), and (3) Confocal Data. Each category is divided into subcategories. For example, the “Gene Data –Midline cell” category can be searched for expression in mesectoderm, midline primordium, mature midline, midline neurons, or MG. The Gene Data category selection results in a list of all genes that is

sorted based on selection of a subcategory entry, such as name, protein type, or function. If protein type or function is chosen, then another menu provides a list of proteins and functions to select. For example, selection of “Protein Type” and “bHLH-PAS transcription factor” returns two entries: *cycle* and *sim*. Once the list is present, it can be viewed in multiple ways to highlight different aspects of the gene’s features and expression. The data is also available in a printable format that can be copied into a database or spreadsheet.

Using Gene Search, the name of a gene is entered and three views are returned: Details, Images, and Confocal. It is also possible to analyze multiple genes together using the Batch Search. The Details view provides an overview of data for that gene. This includes protein type and function, midline cell and midline accessory cell expression data determined from AP data, and an indication if confocal data is available with a link to access that information. There are also links to the FlyBase (Tweedie et al., 2009) and the BDGP gene expression database (Tomancak et al., 2002) entries for the gene. The Images view displays AP histochemically-stained images of midline gene expression from embryonic stages 5 to 17. Below the row of images for each stage is a description of the expression pattern using the controlled vocabulary (Figure 4.3A-D). The descriptions for stages 9, 10, 11, 13, and 17 also include the results of confocal analysis for those genes analyzed. As an example, an entry for *sim* is shown for stage 17 in Figure 3A, and *DAT* at stage 17 in Figure 3B. They are both annotated as expressed in midline neurons based on the AP data, whereas the confocal data indicates that *DAT* is expressed in one neuron (H-cell), while *sim* is expressed in a larger set of midline neurons (H-cell sib, ventral unpaired median interneurons 4-6 (iVUMs4-6), median neuroblast progeny

(MNB progeny), as well as the median neuroblast (MNB) and AMG. The Confocal view (Figure 4.2B) provides a text-based summary of confocal expression data for the selected gene. The confocal data is divided into stages 9, 10, 11, 13, 17 with each corresponding cell type listed.

At the bottom of the MidExDB home page are 6 Quick Searches for AP data or confocal data (Figure 4.2A). The quick searches can be used to retrieve a list of all genes with either AP data or confocal data. There is also a quick search function for retrieving all genes expressed in MG or midline neurons. From the retrieved lists, clicking on the gene symbol will open the Details page for that gene.

The second major search mode, the Confocal Query Tool allows the user to customize a query to identify genes expressed in specific cell types at defined developmental stages (Figure 4.2C). Each cell type is listed for each of the 5 developmental stages in which confocal data is present. Complex queries using the Boolean operators AND, OR, and NOT are possible. As an example (Figure 4.2C), the database can be searched for genes expressed at: stage 13 in the MP1 neurons AND H-cell sib but NOT H-cell. Only 1 gene, *fork head (fkh)* appears. Its expression at each stage of development is listed in tabular form (Figure 4.2C). Lists of genes obtained using the Confocal Query Tool can be printed or exported to the Category Search to view additional data (for example, protein type) for each gene in the list.

Descriptive background information and protocols. Two types of background information on midline cells are provided in the navigation bar. The first, Cell Types, is a description of all of the midline cell types, including MG, midline neurons, and midline

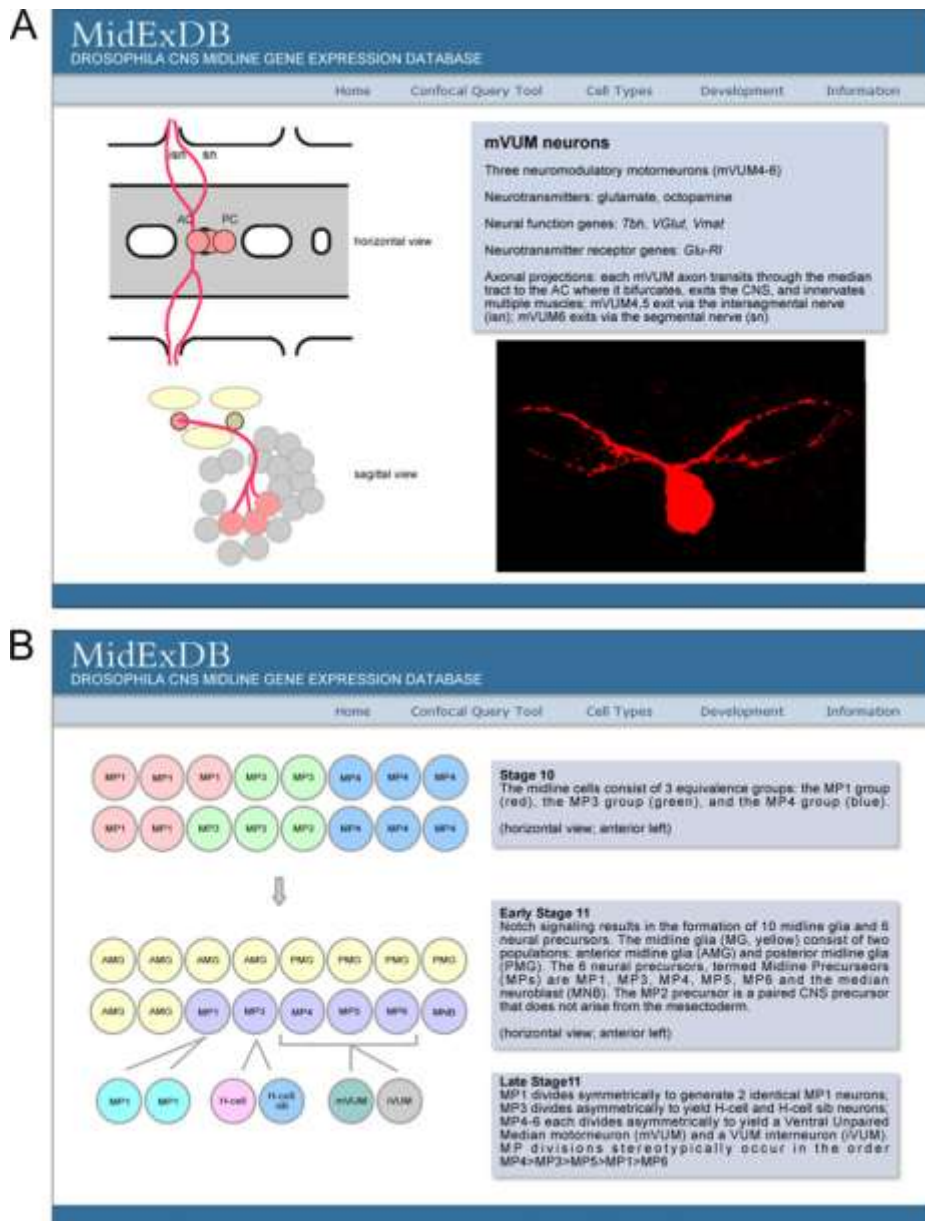


Figure 4.5. Descriptions of midline cell types and development. (A) The Cell Types menu allows selection of information regarding each midline cell type. Shown is a representative webpage summarizing the ventral unpaired median motoneurons (mVUM neurons). (B) The Development menu has a selection of different developmental stages. Shown are schematics and commentaries describing midline cell development at stages 10 and 11.

accessory cells (Figure 4.5A). The summary of each neuronal type includes schematic drawings illustrating cell position and axonal trajectories; in addition, a confocal image showing the axonal trajectories is included. The text description includes information regarding the neurotransmitters and neurotransmitter receptors present in the cell, as well as a list of genes expressed in the mature neurons that contribute to their neural properties. The second set of information is Development, in which midline cell development is presented as a series of schematics from stages 5-17 that are accompanied by commentary (Figure 4.5B). Key references to support this model are included in the References selection under the Information tab.

The Protocols section in the Information menu provides PDFs of detailed experimental protocols that were used to generate the data present in MidExDB. Antibody staining and in situ hybridization protocols are described for both fluorescence and AP detection, including the use of Tyramide Signal Amplification (TSA).

Conclusions

The goal of MidExDB is to disseminate information about the *Drosophila* CNS midline cells. MidExDB is able to search and integrate a large-scale midline gene expression dataset. The database provides a useful foundation for studying CNS midline development and function, particularly the underlying regulatory circuitry.

Availability and requirements

MidExDB is accessible at <http://www.unc.edu/~crews/MidExDB> or via the Crews Lab homepage at www.unc.edu/~crews. Any modern web browser including Mozilla Firefox, Safari, or Microsoft Internet Explorer is sufficient to access the database.

Acknowledgements

The authors would like to thank Joseph Kearney, Amaris Guardiola, and Joseph Pearson for data entry and useful advice. We are also grateful to Hínár Polczer for his help with software and server maintenance, and Bob Duronio for helpful comments on the manuscript. This work was supported by NIH grant R37 RD25251 to STC, an NRSA postdoctoral fellowship to SRW, and UNC Developmental Biology NIH training grant support to SBS.

References

- Jacobs, J. R.** (2000). The midline glia of drosophila: A molecular genetic model for the developmental functions of glia. *Prog. Neurobiol.* **62**, 475-508.
- Kearney, J. B., Wheeler, S. R., Estes, P., Parente, B. and Crews, S. T.** (2004). Gene expression profiling of the developing drosophila CNS midline cells. *Dev. Biol.* **275**, 473-92.
- Tomancak, P., Beaton, A., Weiszmamm, R., Kwan, E., Shu, S., Lewis, S. E., Richards, S., Ashburner, M., Hartenstein, V., Celniker, S. E. et al.** (2002). Systematic determination of patterns of gene expression during drosophila embryogenesis. *Genome Biol.* **3**, R88.1-R88.14.
- Tweedie, S., Ashburner, M., Falls, K., Leyland, P., McQuilton, P., Marygold, S., Millburn, G., Osumi-Sutherland, D., Schroeder, A., Seal, R. et al.** (2009). FlyBase: Enhancing drosophila gene ontology annotations. *Nucleic Acids Res.* **37**, D555-9.
- Wheeler, S. R., Kearney, J. B., Guardiola, A. R. and Crews, S. T.** (2006). Single-cell mapping of neural and glial gene expression in the developing *drosophila* CNS midline cells. *Dev. Biol.* **294**, 509-524.
- Wheeler, S. R., Stagg, S. B. and Crews, S. T.** (2008). Multiple notch signaling events control drosophila CNS midline neurogenesis, gliogenesis and neuronal identity. *Development* **135**, 3071-3079.

CHAPTER V

GENERAL DISCUSSION

The purpose of this work was to determine how individual neurons are generated from the same neural precursor. First, midline precursors needed to be identified and distinguished from each other. The timing and order of each MP division was also determined. Next, I investigated how cell type-specific gene expression in midline neurons was generated. This portion of the work focused on the regulatory events required for the cell type-specific gene expression of the dopaminergic H-cell. Finally, all of the gene expression that was determined over the course of this work and others was cataloged in a gene expression database.

Model of early midline development: identification of MPs and their divisions

The first chapter of this dissertation focused on identifying each of the MPs and when their divisions took place. Early midline cells were correlated with the identified neurons and glia of the mature midline using gene expression and morphology. In order to identify cells at earlier stages, a continuity of gene expression was established by correlating two sets of information: gene expression and cell location at stage 11, and gene expression and cell location at stage 10. Gene expression was linked between stages 10 and 11 by following gene expression of individual cells during early development.

There are 5 MPs: MP1, MP3, MP4, MP5 and MP6. The 5 MPs are arranged in a defined order, MP1→MP3→MP4→MP5→MP6 (anterior to posterior), within the segment. There is no variability in the anterior to posterior organization of the midline cells. We also determined that MP divisions take place during stage 11 and they divide in an ordered manner: MP4→MP3→MP5→MP1→MP6. It was previously thought that all MP divisions took place at stage 8 (Bossing and Technau, 1994; Jacobs, 2000; Klambt et al., 1991). There is a synchronous cell division at stage 8 where the midline cells go from 8 cells per segment to 16. But the MPs do not divide until later at stage 11. Several advances were made during this work that made the identification of MP divisions possible in both fixed tissue experiments and using time-lapse imaging. First, we used a midline-specific promoter to drive *tau-GFP* in all midline cells which resulted in each midline cell outlined with GFP. This allowed midline cells to be identified by both their morphology and location. The *tau-GFP* reporter also labels microtubules, so centrosomes and spindle fibers are visible and as a result divisions could be visualized during time-lapse imaging. This would not have been possible with another membrane marker such as *CD8-GFP*.

For fixed-tissue experiments, I used high resolution confocal microscopy with fluorescent markers to identify each MP and its neuronal progeny. I analyzed sagittal views and focused on a single segment to more easily identify and visualize individual cells. Sagittal views made it possible to distinguish between glia and MPs since glia reside more externally and MPs and their neuronal progeny reside more internally. Time-lapse imaging and fixed tissue experiments are complementary approaches, and together they give a detailed view of midline development.

One question that is raised by this work is: *What controls the timing of MP divisions?* The 5 MPs are arranged in a defined order, MP1→MP3→MP4→MP5→MP6 (anterior to posterior), within the segment. However, they divide in the order MP4→MP3→MP5→MP1→MP6. In addition, the MPs that express MP-specific genes first do not divide first. MP1, MP3 and MP4 express MP-specific genes such as *Elav* and *wor* before MP5 and MP6. But, MP5 divides before MP1. MP divisions occur after cell cycle 14 during embryogenesis. *cdc25* which is encoded by the gene *string* (*stg*) regulates mitosis by activating the Cdc2 kinase. The timing of cell cycles 14, 15, and 16 is regulated by the transcription of *stg* (Edgar et al., 1994). *stg* is most likely also controlling MP divisions. So, the factor or factors regulating *stg* expression in MPs are controlling the timing of MP divisions. In the developing wing, *ac* and *sc* repress *stg* to inhibit cell division (Johnston and Edgar, 1998). In the PNS, *sc* is extinguished before sensory organ precursors divide. It is thought that this is required to relieve repression of *stg* and *stg* then acts to trigger mitosis (Chang et al., 2008). *sc* is extinguished in each MP before division which would be consistent with *sc* having a role in regulating *stg* and MP division.

l(1)sc could also have a role in regulating MP divisions. At the midline in wild-type embryos, MPs become tau-dense during division. MP4 and MP3 divide in close temporal proximity so they could be observed to be tau-dense at the same time, but in general only single MPs are tau-dense. When *l(1)sc* is misexpressed in all midline cells, multiple MPs are tau-dense (Stagg and Crews, unpublished observations). This does not represent an increase in MPs because cell types are not duplicated. In wild-type, *l(1)sc* is expressed in MP1 after it is expressed in MP3 and MP4, and MP1 divides after MP3 and

MP4. When *l(1)sc* is misexpressed in all midline cells, *l(1)sc* is expressed in MP1 earlier than in wild-type. One hypothesis is that *l(1)sc* regulates the timing of MP divisions and that when *l(1)sc* is expressed earlier in MP1, this results in MP1 becoming tau-dense and dividing sooner. Time-lapse imaging of *sim-Gal4 UAS-l(1)sc* embryos could determine if MP1 divides earlier when *l(1)sc* is expressed earlier. It would also be interesting to see if all MP divisions occurred earlier.

AS-C genes are expressed in midline precursors and their neuronal progeny

After MPs were identified, we could determine how distinct neurons were generated from the same precursor cell. It was determined that *Notch* signaling regulates gene expression in iVUMs and H-cell sib, but it was unknown what regulates gene expression in mVUMs and H-cell. AS-C genes were good candidates to regulate midline neuronal cell fate because of their roles in regulating cell fate specification in the lateral CNS (Parras et al., 1996; Skeath and Doe, 1996). From AP in situ screens done in the lab, it was known that AS-C genes are expressed in midline cells (Kearney et al., 2004). One obstacle in determining the role of AS-C genes was analyzing their expression patterns. Antibodies did not exist for L(1)sc and Sc. Cell expression can be difficult to determine early in development with in situ hybridization because mRNA probe localization is cytoplasmic and cells overlap making it difficult to determine which cells are expressing each proneural gene. I generated polyclonal antibodies specific for L(1)sc and Sc in order to determine their expression patterns. The nuclear localization of each protein when immunostained was helpful in determining cell identity and in determining the relative levels of expression between two cells. L(1)sc is present in PMG and the MNB from stages 10-12. L(1)sc is present in all MPs (MP1, MP3, MP4, MP5, and MP6) and in the

newly divided neurons of MP3, MP5 and MP6 (H-cell, H-cell sib; mVUM5,6 and iVUM5,6). *L(1)sc* levels are different between H-cell and H-cell sib: *L(1)sc* is present in both H-cell and H-cell sib and then present at a higher level in H-cell than H-cell sib. *L(1)sc* is then extinguished in H-cell sib, but remains on in H-cell. Similar dynamics are seen for mVUM5 and iVUM5 with *L(1)sc* at higher levels in mVUM5 than iVUM5. Different expression levels of *L(1)sc* in sibling cells may be indicative of the mechanism for how proneural genes are regulated. Different expression levels of *L(1)sc* are also a way to identify specific neurons early in development. The expression pattern of *l(1)sc* is consistent with *l(1)sc* having a role in both neural precursor formation and establishing different daughter fates in the midline.

***l(1)sc* regulates gene expression in the Notch-independent cell**

Notch signaling is a way to generate two different sibling cells from an asymmetric division of a neural precursor. This has been shown for GMCs and their daughter cells in the lateral CNS (Spana et al., 1995). In the midline, MP3-6 undergo asymmetric cell divisions and *Notch* signaling is responsible for all gene expression in H-cell sib and iVUMs, but it is unknown what regulates gene expression in H-cell and mVUMs. To further determine the role of the *AS-C* genes in H-cell and mVUM development, *Df(1)sc^{B57}* mutants, which are deficient for the entire *AS-C*: *achaete*, *scute*, *lethal of scute* and *asense*, were screened for defects in H-cell and mVUM gene expression. There were defects in the expression of the H-cell genes: *BarH1*, *DAT*, *NPFR1*, *ple*, *SoxN* and *Vmat* and the mVUM genes: *Tbh*, *Vmat*, *dgk* and *zfh1*. The *Df(1)sc^{B57}* mutant strain provided strong evidence for defects in H-cell gene expression, but it is deficient for 4 genes (*ac*, *ase*, *l(1)sc*, *sc*). The analysis of additional mutations in

the AS-C locus indicated that only the *l(1)sc* gene was required for H-cell gene expression, since H-cell gene expression was unaltered in mutants for *ac*, *sc*, and *ase*. This showed a novel role for *l(1)sc* in regulating gene expression in the *Notch*-independent cell generated by an asymmetric cell division.

While we have shown that *l(1)sc* is a major regulator of H-cell gene expression, it is not the sole regulator of H-cell gene expression. When *l(1)sc* is misexpressed in all midline cells, H-cell-specific genes, such as *ple* and *NPFRI*, are only activated in H-cell and H-cell sib, and not throughout the midline. So, there are other factors present in the MP3 lineage that are required for H-cell specific gene expression that are absent in other midline neurons. Also, when *l(1)sc* is misexpressed in all midline cells, H-cell genes are expanded to 2 cells only ~20% of the time. One possible reason for this is that another factor along with *l(1)sc* is required for H-cell gene expression, and the small increase in H-cell gene expression occurs because only *l(1)sc* is increased and not the other factor. Both factors would need to be increased in order to see a bigger expansion in H-cell gene expression. Another possible reason is that *l(1)sc* is degraded from neurons quickly before it has a chance to activate downstream effectors. In *l(1)sc* misexpression embryos, *l(1)sc* is extinguished in neurons by stage 11, but remains on in glia longer to stage 14 (Stagg and Crews, unpublished observations).

One question that is raised is: *how is l(1)sc able to activate H-cell gene expression while sc cannot?* Misexpression of *l(1)sc* activates all known H-cell gene expression while misexpression of *sc* does not. Both *L(1)sc* and *Sc* bind E-box motifs (CANNTG). Residues that contact DNA are highly conserved between different proneural proteins while non-DNA-contacting residues are not. Non-DNA-contacting residues could be used

to interact with different cofactors (Powell and Jarman, 2008). The variability in non-DNA-contacting residues could result in each proneural protein interacting with different cofactors. One explanation while *L(1)sc* can activate H-cell gene expression and *Sc* can not is that H-cell-specific genes require input from another cofactor that interacts with *L(1)sc*, but not *Sc*.

l(1)sc and *tup* work in a combinatorial way to control H-cell gene expression. Expression of *ple* and *DAT* is reduced in both *l(1)sc* and *tup* mutants indicating that both *l(1)sc* and *tup* are required for *ple* and *DAT* expression in H-cell. *l(1)sc* can activate *tup* in misexpression experiments, but *l(1)sc* is not required for *tup* expression. This indicates that there is an unknown factor that also regulates *tup*. There are also unknown downstream targets of *l(1)sc* that control *ple*, *DAT*, and *Vmat* expression. *BarH1* is the one known candidate transcription factor that remains to be analyzed. An EMS screen could be performed to identify additional candidates that act to control H-cell gene expression.

It is unknown how *l(1)sc* controls H-cell gene expression. With the exception of *asense*, there are no known direct target genes of the *AS-C* genes that act to control cell fate (Jarman et al., 1993). The *SoxN* gene is a candidate target because it is expressed early in development at the time *l(1)sc* is expressed, and *SoxN* expression is reduced in an *AS-C* mutant. *NPFRI* is reduced in both *AS-C* and *SoxN* mutants. *l(1)sc* may be directly regulating *SoxN* to activate *NPFRI* in H-cell. Future experiments that identify midline enhancer regions of *SoxN* will determine how *l(1)sc* directly regulates cell fate specification. First, transgenic enhancer analysis will be used to identify a CNS midline enhancer region for *SoxN*. Then bioinformatic analysis will be used to identify putative

L(1)sc binding sites within the *SoxN* midline enhancer region. Next, site-directed mutagenesis will be used to determine which L(1)sc binding sites in the midline enhancer region are required for midline expression.

Another question that is raised is: *how is l(1)sc regulated in H-cell sib?* L(1)sc is expressed in MP3 and then in the newly divided H-cell and H-cell sib. L(1)sc is extinguished in H-cell sib, but remains present in H-cell. There are several possible mechanisms for how *l(1)sc* could be extinguished in H-cell sib. L(1)sc is degraded in H-cell sib. Ac and Sc were shown to be degraded by the 26S proteasome in larval wing discs, so a similar mechanism could be occurring in H-cell sib (Chang et al., 2008). This could be determined by misexpressing a dominant-negative temperature-sensitive form of the 26S proteasome in all midline cells (Schweisguth, 1999). If L(1)sc remains present in H-cell sib, this would suggest that the 26S proteasome functions to degrade L(1)sc in H-cell sib. A second possible mechanism is that *l(1)sc* is inhibited by the activation of a repressor. During neuroblast formation in the lateral CNS, *l(1)sc* is extinguished in the cells of the proneural cluster not selected to be the neuroblast. This is done by lateral inhibition mediated by *Notch* signaling (for review see Skeath and Thor, 2003). Suppressor of Hairless [Su(H)] is the transcriptional mediator of *Notch* signaling, and activates the *Enhancer of split* [*E(spl)*] genes (Jennings et al., 1994). There are 7 bHLH *E(spl)* genes that act as repressors (Delidakis et al., 1991). The *E(spl)* genes then act to inhibit AS-C genes (Giagtzoglou et al., 2003). A similar mechanism could be occurring in H-cell sib, since *Notch* signaling occurs in H-cell sib and not H-cell and *E(spl)* genes are expressed in the midline (Kearney et al., 2004).

The Tup protein is also present in both H-cell and H-cell sib early and then Tup is extinguished from H-cell sib and remains present in H-cell. In *Df(1)sc^{B57}* mutants, Tup is expanded to H-cell in 28% of segments indicating that *tup* is repressed by *l(1)sc*. AS-C genes have not been shown to act as repressors, so it is more likely that *l(1)sc* is activating a repressor that acts to inhibit *tup*. Since this repressor is not activated by *l(1)sc* in H-cell; this indicates that a co-activator present in H-cell sib and not H-cell is required to activate the repressor that inhibits *tup* in H-cell sib. Possible candidates for this are the repressor *E(spl)* genes (Jennings et al., 1994).

***l(1)sc* controls MNB formation and posterior MP formation**

Like its role in regulating neuroblast formation in the lateral CNS, *l(1)sc* controls the formation and fate of the MNB and MPs from the MP4 equivalence group. *wor* is expressed in the MNB and analysis of *wor* expression in *Df(1)sc^{B57}* mutants showed a complete absence from the midline and a reduction elsewhere in the CNS. The absence of *wor* and any MNB progeny in *Df(1)sc^{B57}* mutants suggests that the MNB does not form. Expression of *wor* was unaffected in *ase¹* mutant embryos, and in *Df(1)sc¹⁰⁻¹* mutant embryos no defects in cell number were seen, indicating that MNB formation was dependent on *l(1)sc* function. Analysis of MP6 lineage-specific gene expression and gene expression specific to the MP4 and MP5 lineages suggest that on average only 1 MP arises from the MP4 equivalence group in *Df(1)sc^{B57}* mutants and that this MP is either MP4, MP5, or MP6. The reduction of midline neurons observed in *Df(1)sc^{B57}* was not observed in *Df(1)sc¹⁰⁻¹* or *ase¹*, and, accordingly, is due to *l(1)sc*. Later in development, it is difficult to distinguish between MP4 and MP5 lineage neurons. So, it is not known whether it is a random choice deciding if MP4 or MP5 forms or whether only either MP4

or MP5 can form. It is easier to distinguish between MP4 and MP5 at stage 10 before they divide. The molecular map I generated for stage 10 and 11 can be used as a diagnostic tool to identify the MPs present in *Df(1)sc^{B57}* mutants.

L(1)sc is present in both MP3 and posterior MPs, but *l(1)sc* is required for posterior MP formation and not MP3 formation. This suggests that there is another factor upstream of *l(1)sc* that regulates MP3 formation. The role of this other factor or factors would be to regulate the formation of MP3 and activate *l(1)sc*, which then controls H-cell gene expression. Candidates of this factor are genes that are expressed early in development. *hedgehog* (*hh*) and *wingless* (*wg*) are expressed early in development and there is evidence that suggests that *hh* and *wg* may play a role in regulating *l(1)sc* expression at the midline (Bossing and Brand, 2006). The role of *hh* and *wg* in regulating *l(1)sc* expression and MP3 formation could be determined using misexpression experiments genetics and analysis of *hh* and *wg* mutants. These analyses would also help determine the regulatory networks occurring during early midline development.

One last question that remains is: *what is the role of ac and sc in midline cell development?* The *ac* gene is expressed in MP1, and transiently in MP5, MP6, and the MNB. *ac* is then expressed in the MP1 neurons from the time of their division through stage 17. Yet there are no defects in MP1 gene expression in *Df(1)sc^{B57}* mutants. This was somewhat surprising since it was shown that *ac* and *sc* are required for gene expression in the lateral CNS precursor, MP2 (Parras et al., 1996; Skeath and Doe, 1996), and MP2 give rises to the peptidergic dMP2 neuron which is closely related in gene expression to the MP1 neurons. While MP2 and MP1 share gene expression they do not express all of the same genes. Namely, MP2 expresses *ventral nervous system defective* (*vnd*), while

MP1 neurons express *single-minded* (*sim*). These genes have been shown to be important regulators and could account for the fact that *ac* is not required for MP1 neuron gene expression. *Ac* is also present in MP1 neurons at least until the end of embryogenesis so; it is possible that *ac* has a role in MP1s during larval stages. The *sc* gene is expressed in H-cell from stage 14 until stage 17. *Df(1)sc¹⁰⁻¹* mutants which are deficient for *ac* and *sc*, show no defects in H-cell gene expression. *sc* may also play a role late in H-cell development during larval stages. *ac* and *sc* may also be playing more subtle roles in MP1s and H-cell development such as regulating axon guidance and many other aspects of neuron function and gene expression not assayed. *Df(1)sc¹⁰⁻¹* mutants have not yet been analyzed for axon guidance defects.

Evolutionary Aspects of *Drosophila* Dopaminergic Cell Fate Specification

There is both anatomical homology and conservation of gene regulatory mechanisms between *Drosophila* and vertebrates. The midline cells are functionally similar to vertebrate floorplate cells because they both lie along the ventral midline of the embryo and they are both the source of guidance cues (Dickson, 2002; Ruiz i Altaba et al., 2003). The *Drosophila* midline and vertebrate floorplate also consist of similar cell types. Both consist of neuronal and glial cell types and *sim*⁺ interneurons. The vertebrate floorplate also contains precursors of dopaminergic neurons (Kittappa et al., 2007). In vertebrates there are dopaminergic neurons at the midline of the CNS including the dopaminergic neurons that comprise the ventral tegmental area, substantia nigra, and retrorubral region.

Similar to *l(1)sc* in *Drosophila*, the vertebrate the bHLH genes, *Mouse achaete-scute homolog* (*Mash1*; homolog of *l(1)sc*) and *Neurogenin 2* (*Ngn2*), can control both

neural precursor formation and cell fate specification (Bertrand et al., 2002). *Mash1* mutants and *Ngn2* mutants both show defects in neurogenesis. In addition, *Ngn2* directs the specification of excitatory pyramidal neurons in the cortex while *MASH1* promotes the specification of GABAergic interneurons. *Ngn2* and *Mash1* have both also been shown to play roles in midbrain dopaminergic neuron development (Kele et al., 2006).

Conclusion

This dissertation describes the identification of a neural precursor cell, its division, and the gene regulatory pathways occurring within the daughter cell that regulate neural function genes required for dopaminergic cell fate. While not all of the genes regulating H-cell dopaminergic fate have been identified, we have identified 286 midline expressed genes and these are cataloged in a searchable database. The midline is an ideal system to identify potential genes that could act to regulate H-cell dopaminergic cell fate.

Recently, reprogramming fibroblasts directly to neurons has been accomplished (Vierbuchen et al., 2010). The main transcription factor necessary for this transformation is *Mash1*. It is not yet known which downstream genes are activated by *Ascl1* that result in functional neurons. The majority of neurons produced expressed genes characteristic of excitatory cortical neurons. Factors necessary for transforming fibroblasts to dopaminergic neurons have not yet been identified. This is critical to determine since this will help provide the basis of cell based therapies for nervous system diseases. Parkinson's disease is caused by the selective loss of dopaminergic neurons in the

midbrain. One proposed treatment for Parkinson's disease is the replacement of dopaminergic neurons generated by stem cells or reprogrammed cells. The regulatory networks occurring during early midline development may be relevant to mammalian neurogenesis and regenerative medicine given the high degree of conservation between fly and vertebrate proneural genes.

References

- Bertrand, N., Castro, D. S. and Guillemot, F.** (2002). Proneural genes and the specification of neural cell types. *Nat. Rev. Neurosci.* **3**, 517-530.
- Bossing, T. and Brand, A. H.** (2006). Determination of cell fate along the anteroposterior axis of the drosophila ventral midline. *Development* **133**, 1001-1012.
- Bossing, T. and Technau, G. M.** (1994). The fate of the CNS midline progenitors in *drosophila* as revealed by a new method for single cell labelling. *Development* **120**, 1895-1906.
- Chang, P. J., Hsiao, Y. L., Tien, A. C., Li, Y. C. and Pi, H.** (2008). Negative-feedback regulation of proneural proteins controls the timing of neural precursor division. *Development* **135**, 3021-3030.
- Delidakis, C., Preiss, A., Hartley, D. A. and Artavanis-Tsakonas, S.** (1991). Two genetically and molecularly distinct functions involved in early neurogenesis reside within the enhancer of split locus of drosophila melanogaster. *Genetics* **129**, 803-823.
- Dickson, B. J.** (2002). Molecular mechanisms of axon guidance. *Science* **298**, 1959-1964.
- Dong, R. and Jacobs, J. R.** (1997). Origin and differentiation of supernumerary midline glia in *drosophila* embryos deficient for apoptosis. *Dev. Biol.* **190**, 165-177.
- Edgar, B. A., Sprenger, F., Duronio, R. J., Leopold, P. and O'Farrell, P. H.** (1994). Distinct molecular mechanism regulate cell cycle timing at successive stages of drosophila embryogenesis. *Genes Dev.* **8**, 440-452.
- Estes, P., Mosher, J. and Crews, S. T.** (2001). Drosophila single-minded represses gene transcription by activating the expression of repressive factors. *Dev. Biol.* **232**, 157-175.
- Giagtzoglou, N., Alifragis, P., Koumbanakis, K. A. and Delidakis, C.** (2003). Two modes of recruitment of E(spl) repressors onto target genes. *Development* **130**, 259-270.
- Jacobs, J. R.** (2000). The midline glia of drosophila: A molecular genetic model for the developmental functions of glia. *Prog. Neurobiol.* **62**, 475-508.
- Jarman, A. P., Brand, M., Jan, L. Y. and Jan, Y. N.** (1993). The regulation and function of the helix-loop-helix gene, asense, in drosophila neural precursors. *Development* **119**, 19-29.

- Jennings, B., Preiss, A., Delidakis, C. and Bray, S.** (1994). The notch signalling pathway is required for enhancer of split bHLH protein expression during neurogenesis in the drosophila embryo. *Development* **120**, 3537-3548.
- Johnston, L. A. and Edgar, B. A.** (1998). Wingless and notch regulate cell-cycle arrest in the developing drosophila wing. *Nature* **394**, 82-84.
- Kearney, J. B., Wheeler, S. R., Estes, P., Parente, B. and Crews, S. T.** (2004). Gene expression profiling of the developing drosophila CNS midline cells. *Dev. Biol.* **275**, 473-92.
- Kele, J., Simplicio, N., Ferri, A. L., Mira, H., Guillemot, F., Arenas, E. and Ang, S. L.** (2006). Neurogenin 2 is required for the development of ventral midbrain dopaminergic neurons. *Development* **133**, 495-505.
- Kittappa, R., Chang, W. W., Awatramani, R. B. and McKay, R. D.** (2007). The foxa2 gene controls the birth and spontaneous degeneration of dopamine neurons in old age. *PLoS Biol.* **5**, e325.
- Klambt, C., Jacobs, J. R. and Goodman, C. S.** (1991). The midline of the drosophila central nervous system: A model for the genetic analysis of cell fate, cell migration, and growth cone guidance. *Cell* **64**, 801-815.
- Parras, C., Garcia-Alonso, L. A., Rodriguez, I. and Jimenez, F.** (1996). Control of neural precursor specification by proneural proteins in the CNS of drosophila. *EMBO J.* **15**, 6394-6399.
- Powell, L. M. and Jarman, A. P.** (2008). Context dependence of proneural bHLH proteins. *Curr. Opin. Genet. Dev.* **18**, 411-417.
- Ruiz i Altaba, A., Nguyen, V. and Palma, V.** (2003). The emergent design of the neural tube: Prepattern, SHH morphogen and GLI code. *Curr. Opin. Genet. Dev.* **13**, 513-521.
- Skeath, J. B. and Doe, C. Q.** (1996). The achaete-scute complex proneural genes contribute to neural precursor specification in the drosophila CNS. *Curr. Biol.* **6**, 1146-1152.
- Spana, E. P., Kopczynski, C., Goodman, C. S. and Doe, C. Q.** (1995). Asymmetric localization of numb autonomously determines sibling neuron identity in the drosophila CNS. *Development* **121**, 3489-3494.
- Vierbuchen, T., Ostermeier, A., Pang, Z. P., Kokubu, Y., Sudhof, T. C. and Wernig, M.** (2010). Direct conversion of fibroblasts to functional neurons by defined factors. *Nature* **463**, 1035-1041.

Wheeler, S. R., Kearney, J. B., Guardiola, A. R. and Crews, S. T. (2006). Single-cell mapping of neural and glial gene expression in the developing *drosophila* CNS midline cells. *Dev. Biol.* **294**, 509-524.